

**Breaking tolerance to the natural  
human liver autoantigen cytochrome  
P450 2D6 by virus infection**

Dissertation  
zur Erlangung des Doktorgrades  
der Naturwissenschaften

Vorgelegt beim Fachbereich  
Chemische und Pharmazeutische Wissenschaften  
der Johann Wolfgang Goethe- Universität  
in Frankfurt am Main

von  
Martin Holdener  
aus Luzern

Frankfurt am Main, 2008

D30

vom Fachbereich

Chemische und Pharmazeutische Wissenschaften der

Johann Wolfgang Goethe-Universität als Dissertation angenommen.

Dekan: Prof. Dr. D. Steinhilber

1. Gutachter: Prof. Dr. Th. Dingermann

2. Gutachter: PD Dr. U. Christen

Datum der Disputation: 16.7.2009

**To my family**

# 1 Table of Contents

<b>1</b>	<b>TABLE OF CONTENTS</b> .....	<b>3</b>
<b>2</b>	<b>SUMMARY</b> .....	<b>5</b>
<b>3</b>	<b>ZUSAMMENFASSUNG</b> .....	<b>6</b>
<b>4</b>	<b>LIST OF ABBREVIATIONS</b> .....	<b>10</b>
<b>5</b>	<b>LIST OF FIGURES</b> .....	<b>12</b>
<b>6</b>	<b>LIST OF TABLES</b> .....	<b>12</b>
<b>7</b>	<b>INTRODUCTION</b> .....	<b>13</b>
7.1	OVERVIEW OF THE IMMUNE SYSTEM .....	13
7.1.1	<i>Innate Immune system</i> .....	13
7.1.2	<i>Adaptive Immune system</i> .....	14
7.2	TOLERANCE .....	17
7.2.1	<i>Generation of Tolerance</i> .....	18
7.2.2	<i>Breaking of tolerance – induction of autoimmune disease</i> .....	19
7.3	THE LIVER .....	25
7.3.1	<i>Anatomy and function of the liver</i> .....	25
7.3.2	<i>Liver immunology</i> .....	26
7.3.3	<i>Liver diseases</i> .....	28
7.3.4	<i>Autoimmune liver diseases</i> .....	28
<b>8</b>	<b>AIM OF THE STUDY</b> .....	<b>36</b>
8.1	STRATEGY .....	36
8.1.1	<i>The CYP2D6 humanized mice</i> .....	36
8.1.2	<i>Adenoviruses</i> .....	38
8.2	WORKING HYPOTHESIS.....	39
<b>9</b>	<b>RESULTS</b> .....	<b>41</b>
9.1	INTRODUCTION OF THE CYP2D6 MOUSE MODEL FOR AUTOIMMUNE HEPATITIS .....	41
9.1.1	<i>Route of infection</i> .....	41
9.1.2	<i>Protein expression in the liver</i> .....	42
9.1.3	<i>Infection of mice with adenovirus results in transient hepatic damage</i> .....	43
9.1.4	<i>Infection with Ad-2D6 results in severe and persistent liver damage</i> .....	45
9.2	PATHOGENIC MECHANISM IN THE CYP2D6 MOUSE MODEL FOR AUTOIMMUNE HEPATITIS .....	54
9.2.1	<i>B cell tolerance to liver-specific self antigen is broken after Ad-2D6 infection</i> ...54	
9.2.2	<i>Anti-CYP2D6 antibodies in Ad-2D6-infected mice and sera from AIH-2 patients recognize an identical immunodominant epitope</i> .....	58

9.2.3	<i>Virus infection is essential for persistent liver damage but not autoantibody production</i> .....	61
9.2.4	<i>T cell tolerance to liver-specific self antigen is broken after Ad-2D6 infection ...</i>	62
<b>10</b>	<b>DISCUSSION</b> .....	<b>67</b>
10.1	BREAKING TOLERANCE TO THE NATURAL HUMAN LIVER AUTOANTIGEN CYP2D6 BY VIRUS INFECTION .....	67
10.2	MOUSE MODELS FOR HUMAN AUTOIMMUNE HEPATITIS .....	67
10.3	LESSONS LEARNED FROM ANIMAL MODELS FOR AIH .....	69
10.4	THE CYP2D6 ANIMAL MODEL FOR AIH .....	71
10.5	ADVANTAGES OF THE CYP2D6 MOUSE MODEL.....	73
10.6	THE CYP2D6 MOUSE MODEL AND THE ETIOLOGY OF AIH .....	74
10.7	THE CYP2D6 MODEL AND PATHOGENIC MECHANISM OF AIH.....	77
10.8	POSSIBILITIES OF THE CYP2D6 MOUSE MODEL .....	81
<b>11</b>	<b>APPENDIX</b> .....	<b>84</b>
<b>12</b>	<b>MATERIAL AND METHODS</b> .....	<b>85</b>
12.1	SOURCE OF MATERIALS .....	85
12.1.1	<i>Plastic ware</i> .....	85
12.1.2	<i>Chemicals</i> .....	85
12.1.3	<i>Composition of buffers, solutions and culture media</i> .....	87
12.1.4	<i>Enzymes and proteins</i> .....	89
12.1.5	<i>Nucleotides and nucleic acids</i> .....	89
12.1.6	<i>Antibodies</i> .....	90
12.1.7	<i>Kits</i> .....	91
12.1.8	<i>Human Sera</i> .....	91
12.1.9	<i>Cell lines</i> .....	91
12.1.10	<i>Viruses</i> .....	91
12.1.11	<i>Mice strains</i> .....	92
12.2	METHODS .....	92
12.2.1	<i>Cell biological methods</i> .....	92
12.2.2	<i>Molecular biological methods</i> .....	102
12.2.3	<i>Experiments with mice</i> .....	107
<b>13</b>	<b>REFERENCES:</b> .....	<b>109</b>
<b>14</b>	<b>ACKNOWLEDGEMENTS</b> .....	<b>118</b>
<b>15</b>	<b>CURRICULUM VITAE</b> .....	<b>119</b>
<b>16</b>	<b>PUBLICATIONS</b> .....	<b>121</b>

## 2 Summary

Autoimmune hepatitis (AIH) is a chronic liver disease of unknown etiology, characterized by a loss of tolerance against hepatocytes leading to the progressive destruction of hepatic parenchyma and cirrhosis. Clinical signs for AIH are interface hepatitis and portal plasma cell infiltration, hypergammaglobulinemia, and autoantibodies. Based on serological markers AIH is defined in subtypes. The hallmark of AIH type 2 are type 1 liver/kidney microsomal autoantibodies (LKM-1), whereas AIH type 1 is characterized by the presence of anti-nuclear (ANA) and/or anti-smooth muscular (SMA) autoantibodies. The major autoantigen recognized specifically by LKM-1 autoantibodies was identified as the 2D6 isoform of the cytochrome P450 enzyme family (CYP2D6). Not much is known about the etiology and pathogenic mechanisms of AIH so far and most animal models available result in only transient hepatic liver damage after a rather complex initiation method. It was the aim of my project to generate a novel animal model for AIH that reflects the chronic and progressive destruction of the liver characteristic for the human disease while using a defined and feasible initiating event to further analyze the pathogenic mechanisms leading to the autoimmune-mediated destruction of the liver. Therefore, mice transgenically expressing the human CYP2D6 in the liver and wild-type mice were infected with a liver-tropic adenovirus expressing the human CYP2D6 (Ad-2D6). Self-tolerance to CYP2D6 was broken in Ad-2D6-infected mice, resulting in persistent autoimmune liver damage, apparent by cellular infiltration, hepatic fibrosis and necrosis. Similar to type 2 AIH patients, Ad-2D6-infected mice generated LKM-1-like antibodies recognizing the same immunodominant epitope of CYP2D6. Taken together, we could introduce a new animal model that reflects the persistent autoimmune-mediated liver damage as well as the serological marker characteristic for AIH type 2 and we could demonstrate that chronic autoimmune diseases targeting the liver can be triggered by molecular mimicry occurring in the context of a hepatotropic viral infection.

### 3 Zusammenfassung

Jeder Organismus wird täglich mit vielen verschiedenen Antigenen und Pathogenen konfrontiert. Um den Organismus gegen diese Fremdkörper zu schützen hat das Immunsystem verschiedene Schutzfunktionen entwickelt. Eine der wichtigsten Voraussetzungen des Immunsystems ist es körpereigene und körperfremde Antigene unterscheiden zu können, da es sonst zu folgeschweren Komplikationen wie Autoimmunerkrankungen kommen kann. Komplexe Selektionsmechanismen während der Reifung von Immunzellen als auch während dem Zusammentreffen von Immunzellen und Antigenen führen dazu, dass körpereigene Antigene toleriert und körperfremde Antigene eliminiert werden. Diese Selektionsmechanismen sind jedoch nicht immer komplett gewährleistet oder können beeinflusst werden, so dass es unter gewissen Umständen zu Autoimmunerkrankungen kommen kann. Zum Beispiel kann ein Pathogen, das sehr ähnliche molekulare Strukturen wie körpereigene Antigene aufweist, eine Immunantwort auslösen, welche nicht zwischen körpereigen und körperfremd unterscheiden kann. Dieser Vorgang wird auch als molekulare Mimikry bezeichnet und es wird vermutet dass dies eine Ursache für Autoimmunerkrankungen, wie zum Beispiel rheumatisches Fieber und das Guillain-Barré-Syndrom, sein kann.

Die Leber ist das grösste innere Organ des Menschen und dient neben lebenswichtigen Funktionen wie Entgiftung und Stoffwechsel auch als Speicher- und Ausscheidungsorgan und produziert Gallensaft zur Unterstützung der Fettverdauung. Wegen der einzigartigen Funktion der Leber, lebensnotwendige nicht-körpereigene Substanzen wie Nahrung als auch gefährliche giftige Stoffe aus der Verdauung abzubauen, ist es besonders wichtig, dass Immunreaktionen in der Leber sorgfältig reguliert werden. Generell tendieren in der Leber aktivierte Immunzellen eher dazu Antigene zu tolerieren, auch wenn dies nicht immer der Fall ist, wie zum Beispiel bei der potenten Immunreaktion gegen den Hepatitis B Virus.

Die Autoimmune Hepatitis (AIH) ist eine seltene chronische Lebererkrankung, bei der als Folge des Toleranzverlustes gegen hepatozelluläre Proteine eine

durch das körpereigene Immunsystem ausgelöste Zerstörung der Hepatozyten mit Übergang in eine Zirrhose zugrunde liegt. Klinisch ist die AIH charakterisiert durch lymphozytäre und plasmazelluläre Infiltrate im Periportalfeld, Hypergammaglobulinämie und Autoantikörper. Serologisch lässt sich die AIH in Subtypen klassifizieren. Typisch für AIH vom Typ 1 sind Antikörper gegen Zellkerne (ANA) und Antikörper gegen glatte Muskulatur (SMA). LKM-1 Autoantikörper sind die serologischen Marker für AIH vom Typ 2 und reagieren mit immundominanten Regionen des Isomers 2D6 der Enzymfamilie Zytochrom P450 (CYP2D6). Bis jetzt ist sehr wenig über die Krankheitsursachen und die, der Krankheit zugrunde liegenden Mechanismen bekannt. Zudem fehlen repräsentative Tiermodelle. Die meisten Tiermodelle für AIH konnten nur eine vorübergehende Hepatitis auslösen und benötigten dazu meistens komplexe krankheitsauslösende Mechanismen.

Es war das Ziel meines Projekts ein neues Maus-Modell für AIH zu entwickeln welches die chronische Zerstörung der Leber bei menschlicher AIH möglichst genau reflektiert. Zusätzlich sollte ein klar definierter und möglichst plausibler Auslöser für die Krankheit gewählt werden, um die Mechanismen, die zur autoimmunen Zerstörung der Leber führen, genauer untersuchen zu können. Dafür wurden wild-typ Mäuse (FVB/N Mäuse) und Mäuse, die das menschliche CYP2D6 als Transgen in der Leber exprimieren (CYP2D6 Mäuse) mit einem lebertropen Adenovirus, das das menschliche CYP2D6 exprimiert (Ad-2D6), infiziert. Als Kontrollvirus, das keine Autoimmunerkrankung zur Folge haben sollte, wurde ein Adenovirus, das das grün fluoreszierende Protein (Ad-GFP) exprimiert, gewählt. Der Gebrauch eines Adenoviralen Vektors gewährleistet sowohl eine hohe als auch spezifische Expression des Transgenen CYP2D6 in der Leber der Mäuse. Das humane CYP2D6 wurde gewählt da Autoantikörper spezifisch für CYP2D6 das Hauptmerkmal zur Diagnose von AIH vom Typ 2 im Patienten sind und wild-typ Mäuse Zytochrom P450 mit hoher Homologie zum humanen CYP2D6 besitzen.

Durch Infektion von wild-typ FVB/N und CYP2D6 Mäusen mit dem Kontrollvirus Ad-GFP konnte gezeigt werden, dass die virale Proteinexpression in der Leber nur vorübergehend war und dass schon nach zwei Wochen fast kein GFP mehr in der Leber exprimiert wurde.

Infektion von wild-typ FVB/N sowie CYP2D6 Mäusen mit Adenovirus führte zu einer akuten virus-vermittelten Hepatitis mit vorübergehender Erhöhung der Leberwerte. Die Selbsttoleranz gegenüber CYP2D6 konnte jedoch nur in Ad-2D6-infizierten Mäusen durchbrochen werden und nicht in Ad-GFP-infizierten Mäusen. Das Durchbrechen der Toleranz führte zu lymphozytären und plasmazellulären Infiltraten, Leberfibrose und Nekrose. Dies konnte durch histologische Analysen gezeigt werden. Die Mehrzahl der infiltrierenden Zellen waren B-Zellen, CD4<sup>+</sup> T-Zellen und Makrophagen, wobei weniger CD8<sup>+</sup> T-Zellen gefunden wurden.

Die B-Zell Toleranz wurde nur nach Ad-2D6 Infektion durchbrochen und führte zur Aktivierung von CYP2D6-spezifischen B-Zellen und zur Produktion und Sekretion von CYP2D6-spezifischen Antikörpern. Diese CYP2D6-spezifischen Antikörper erkannten die gleiche immundominante Region des menschlichen CYP2D6 wie LKM-1 Antikörper von Patienten mit AIH vom Typ 2.

Interessanterweise zeigten die transgenen CYP2D6 Mäuse im Vergleich zu den wild-typ FVB/N Mäusen einen abgeschwächten autoimmunen Leberschaden, verspätete Immunzellinfiltrationen, weniger Leberfibrose und einen tieferen anti-CYP2D6 Antikörpertiter. Dies lässt die Vermutung zu, dass molekulare Ähnlichkeit (Maus Zytochrom P450 gegenüber humanen CYP2D6 vom Ad-2D6), eine stärkere Autoimmunantwort auslösen kann als molekulare Gleichheit (CYP2D6 Mäusen gegenüber Ad-2D6).

Injektion des humanen CYP2D6 Proteins in Kombination mit verschiedenen Adjuvantien führte zur Produktion von CYP2D6-spezifischen Antikörpern, aber nicht zu autoimmuner Hepatitis. Dadurch konnte gezeigt werden, dass in unserem System die virus-vermittelte Expression von CYP2D6 nötig war um autoimmunen Leberschaden auszulösen.

Die T-Zell Toleranz wurde ebenfalls nur nach Ad-2D6 Infektion durchbrochen. Dies konnte durch *ex-vivo* Stimulation von T-Zellen mit CYP2D6 Peptiden und der darauf folgenden Produktion von Zytokinen gezeigt werden. Interessanterweise konnte eine viel höhere Frequenz an Zytokinproduzierenden und daher CYP2D6 spezifischen T Zellen aus der Leber isoliert werden als aus der Milz. Wie schon bei der Durchbrechung der B Zell Toleranz konnte in wild-typ FVB/N verglichen mit transgenen CYP2D6 Mäusen eine stärkere Autoimmunantwort nachgewiesen werden.

Zusammengefasst ist es uns gelungen ein neues Maus-Model zu etablieren, welches den chronischen autoimmunen Leberschaden und die serologischen Marker von AIH vom Typ 2 widerspiegelt. Zum ersten Mal konnte in einem Maus-Model die Produktion von Autoantikörpern mit derselben Spezifität wie menschliche LKM-1 Antikörper in AIH vom Typ 2 in Kombination mit einem chronischen autoimmunen Leberschaden gezeigt werden. Zusätzlich konnten wir zeigen, dass eine lebertrope Virusinfektion via molekulare Mimikry eine chronische autoimmune Lebererkrankung auslösen kann.

Dieses Maus-Model sollte durch die Ähnlichkeit zum menschlichen Krankheitsbild der AIH vom Typ 2 und dem klar definierten und plausiblen Auslöser der Krankheit noch viel zu dem Verständnis der Mechanismen die zu AIH führen, beitragen können.

## 4 List of abbreviations

aa	Amino acid
Ad-2D6	Adenovirus expressing CYP2D6
Ad-C	Empty adenovirus vector
Ad-GFP	Adenovirus expressing GFP
AIH	Autoimmune hepatitis
AIRE	Autoimmune regulator
ALD	Autoimmune liver disease
ALT	Alanine aminotransferase
AMA	Antimitochondrial autoantibodies
ANA	Antinuclear antibodies
ANCA	Anti-neutrophil cytoplasmic antibodies
Anti-SLA/LP	Autoantibodies against soluble liver antigen and liver-pancreas antigen
AP	Alkaline phosphatase
APC	Antigen presenting cells
APECED	Autoimmune polyendocrinopathy-candidiasis-ectodermal dystrophy
AST	Aspartate aminotransferase
B cells	B lymphocytes
BCR	B cell antigen receptor
CFA	Complete Freud adjuvant
CTL	CD8 <sup>+</sup> cytotoxic T lymphocyte
CYP2D6	Isoform 2D6 of the cytochrome mono-oxygenase P450 enzyme family
CYP2Ds	Mouse homologues of the human cytochrome mono-oxygenase P450 enzyme family
DC	Dendritic cell
E1/3	Early region 1/3 genes
ECM	Extracellular matrix
FTCD	Frominminotransferase cyclodeaminase
GFP	Green fluorescent protein
GGT	Gamma glutamyl transpeptidase
GP	Glycoprotein
HBsAg	HBV surface antigen
HBV	Hepatitis B virus
HCV	Hepatitis C virus
HIS	Histological infiltration score
HSC	Hepatic stellate cells
HSV-1	Herpes simplex virus 1
ICCS	Intracellular cytokine stain

IFA	Incomplete Freud adjuvant
IFN- $\gamma$	Interferon $\gamma$
Ig	Immunoglobulin
IL-	Interleukin-
LC1	Antibodies to liver-cytosol type 1
LCMV	Lymphocytic choriomeningitis virus
LDS	Liver damage score
LKM-1	Autoantibodies to liver-kidney microsomal type 1 antigens
LSEC	Liver sinusoidal endothelial cells
MHC	Major histocompatibility complex
MS	Multiple sclerosis
NOD	Nonobese diabetic mouse
NP	Nucleoprotein
PBC	Primary biliary cirrhosis
PDC-E2	Subunit E2 of the pyruvate dehydrogenase complex
pfu	Plaque forming units
PSC	Primary sclerosing cholangitis
RIP	Rat insulin promoter
SLE	Systemic lupus erythematosus
SMA	Smooth muscle antibodies
T cells	T lymphocytes
T1D	Type 1 diabetes mellitus
TCR	T cell antigen receptor
TFA	Trifluoroacetyl
TGF- $\beta$	Tumor growth factor $\beta$
T <sub>H</sub> cells	CD4 <sup>+</sup> T helper cells
TNF- $\beta$	Tumor necrosis factor
T <sub>reg</sub>	Regulatory T cells

## 5 List of figures

Figure 1: Mechanism that can lead to broken self-tolerance.....	22
Figure 2: The liver and its microenvironment.....	26
Figure 3: Generation and analysis of the CYP2D6 humanized mouse.....	37
Figure 4: Working hypothesis for breaking self-tolerance to liver autoantigens by viral infection .....	40
Figure 5: GFP expression in the liver after different route of Ad-GFP infection.....	42
Figure 6: Expression of GFP after AD-GFP infection.....	42
Figure 7: Serum enzyme activity tests related to liver damage after adenovirus infection..	44
Figure 8: Morphology of the livers after adenovirus infection .....	46
Figure 9: LDS at several time points after infection with adenovirus.....	47
Figure 10: Hepatic necrosis and massive cellular infiltrations after Ad-2D6 infection .....	49
Figure 11: HIS at several time points after infection with adenovirus.....	50
Figure 12: Immunohistochemical analysis of liver sections after infection with Ad-2D6 .....	51
Figure 13: Subcapsular fibrosis after infection of mice with Ad-2D6 but not Ad-GFP.....	53
Figure 14: Generation of anti-CYP2D6-specific antibodies after Ad-2D6 infection .....	55
Figure 15: Activation of CYP2D6-specific B cells after Ad-2D6 infection .....	57
Figure 16: Staining pattern of anti-CYP2D6 antibodies after Ad-2D6 infection.....	58
Figure 17: Mouse anti-CYP2D6 and sera of AIH-2 patients recognize the identical immunodominant CYP2D6 epitope.....	60
Figure 18: Antibody titer after different immunization strategies .....	61
Figure 19: Intracellular IFN- $\gamma$ staining after peptide pool stimulation .....	63
Figure 20: Intracellular IFN- $\gamma$ staining after single peptide stimulation .....	64
Figure 21: Possible mechanism for induction of AIH .....	76
Figure 22: Possible pathogenic mechanism in the CYP2D6 model .....	80
Figure 23: 61 20mer sequences spanning the entire human CYP2D6.....	84

## 6 List of tables

Table 1: LDS definition to assess morphological liver alterations by visual examination...	46
Table 2: HIS definition to assess liver infiltration.....	49

# **7 Introduction**

## **7.1 Overview of the Immune system**

To protect an organism from infectious agents and the damage they cause a variety of mechanisms have evolved which have led to the complex immune system of vertebrates. In order to be effective, the immune system must protect the individual against disease while limiting the damage made to the individual itself.

The immune system can functionally be divided into two distinct parts that act in a cooperative way. The initial non-specific defenses mechanisms against infections that are called the innate immune system and the adaptive immune system that displays a high degree of antigen-specificity.

### **7.1.1 Innate Immune system**

Innate immunity provides the first line of defense against a wide range of invading pathogens. It includes anatomic, physiologic, phagocytic or endocytic and inflammatory barriers. The skin and the surface of mucous membranes act as anatomic barriers by preventing entry of most microorganisms and the low pH inhibits growth of most bacteria. Saliva, tears and mucous secretion act to wash away potential invaders and contain antibacterial or antiviral substances. Physiological barriers include body temperature and fever responses, which inhibit growth of some pathogens, gastric acidity that kills most ingested microorganisms and a variety of soluble factors like lysozymes that cleave bacterial cell walls, interferons, which induce an antiviral state in uninfected cells and the complement that lyses microorganisms. The phagocytic or endocytic barrier is provided by white blood cells, such as blood monocytes, neutrophils, natural killer cells and tissue macrophages which are able to ingest and kill microorganisms by producing a variety of toxic chemicals and degradative enzymes. The inflammatory response is a complex sequence of events that is caused by tissue damage or invading pathogenic microorganism and leads to

vasodilatation, increased capillary permeability and influx of phagocytic active cells from capillaries into the tissue. The innate immune system is also responsible for the initial release of cytokines and chemokines that activate the adaptive immune system (1, 2).

### **7.1.2 Adaptive Immune system**

Adaptive, or specific, immunity is capable of recognizing and selectively eliminating specific foreign microorganisms and molecules. The four major characteristics of adaptive immunity are the antigen-specificity which permits the immune system to distinguish subtle differences among antigens, the enormous diversity of recognition molecules that can be generated, the immunologic memory that enables the immune system to respond to previously encountered antigens with a higher reactivity and the self and non-self recognition which enables the immune system to distinguish self from non-self. The ability of the immune system to distinguish self from non-self and respond only to non-self molecules is essential since an inappropriate response to self molecules leads to autoimmune diseases and can be fatal. Adaptive immune responses can be divided into humoral and cell-mediated responses. The two major groups of cells of the adaptive immune system are the lymphocytes and the antigen presenting cells (APC), whereas the lymphocytes can be divided into B lymphocytes (B cells) and T lymphocytes (T cells) (1, 2).

#### **7.1.2.1 Lymphocytes**

T and B lymphocytes confer specific immunity and possess specific receptors, the T and B cell antigen receptors, which are responsible for the enormous diversity of T and B cells and are able to discriminate between self and non-self.

##### *T Lymphocytes*

T lymphocytes express a T cell antigen receptor (TCR) that recognizes processed antigen peptides bound to cell-membrane proteins called major

histocompatibility complex (MHC). T lymphocyte progenitors arise from hematopoietic stem cells in the bone marrow and migrate to the thymus to mature. During maturation TCR with too low or too high affinity for MHC molecules are deleted in a two-step selection process in the thymus. Positive selection of T cells ensures that mature TCRs bind to self-MHC molecules which confers MHC restriction (3). T cells with high affinity TCR for self-MHC molecules or self-MHC plus self-antigen undergo negative selection which ensures self-tolerance. T cells that fail positive selection or get negative selected during maturation die by apoptosis. As a result of this two-step selection process about 99% of T cells die within the thymus during the maturation and only T cells that are self-MHC restricted and self-tolerant survive thymic selection. After maturation T cells can be divided into two distinct populations depending on their functional phenotype and expression of the CD4 or CD8 co-receptor.

CD4<sup>+</sup> T helper cells (T<sub>H</sub> cells) are specific for antigenic peptides presented by MHC class II molecules and upon activation, proliferate and secrete various cytokines which in turn activate B cells, T cells, macrophages and other cells involved in the immune response. T<sub>H</sub> cells can be classified into T<sub>H</sub>1 and T<sub>H</sub>2 cells based on their cytokine profile. The T<sub>H</sub>1 subset supports inflammation by secreting interleukin-2 (IL-2), interferon  $\gamma$  (IFN- $\gamma$ ) and tumor necrosis factor  $\beta$  (TNF- $\beta$ ) and is responsible for classical cell-mediated functions involving CD8<sup>+</sup> T cells. The T<sub>H</sub>2 subset supports mostly humoral immune responses involving B cell proliferation and differentiation into antibody-secreting plasma cells and memory cells. Other groups of T<sub>H</sub> cells include the regulatory T (T<sub>reg</sub>) and T<sub>H</sub>-17 cell populations. Reductions in T<sub>reg</sub> cells may contribute to autoimmunity, chronic viral infection, tumor immunity and allergy while the role of the pro-inflammatory interleukin 17 (IL-17) secreting subgroup pertains probably to host defense and autoimmunity (4, 5).

Activated CD8<sup>+</sup> cytotoxic T lymphocytes (CTL) recognize and lyse specifically own cells, which present foreign antigenic peptides on MHC class I molecules. CTL are able to produce IFN- $\gamma$ , which inhibits viral replication,

increases expression of MHC molecules and enhances the activity of macrophages (1, 2).

### *B Lymphocytes*

B lymphocytes express a B cell antigen receptor (BCR) that recognizes the native form of an antigen. Once a B cell is activated it secretes the BCR in a soluble form, referred to as an antibody. The basic unit of an antibody, or immunoglobulin (Ig) molecule is composed of two identical light and two identical heavy chains that are stabilized by non-covalent forces and covalent disulfide bonds. The N terminal domains of the heavy as well as the light chains of different antibodies are extremely diverse and are responsible for the antigen binding site that recognize one specific B cell epitope, that consists typically of up to 22 amino acids on the surface of a foreign protein. B lymphocyte progenitors arise from hematopoietic stem cells and mature to B lymphocytes in the bone marrow. During maturation B cells go through several stages which are characterized by changes in the rearrangement of immunoglobulin heavy and light chain genes and intracellular as well as surface marker expression. Mature B cells leave the bone marrow and traffic to the B cell zone in secondary lymphoid organs, such as the spleen and lymph nodes. When a naïve B cell gets activated by encountering antigen in the presence of cytokines secreted by  $T_H$  cells, the B cell starts to proliferate and differentiate into effector B cells called plasma cells that secrete large amounts of antibodies and into memory cells. Differentiating B cells produce IgM isotype antibodies and can upon activation, depending on the cytokines present, switch to different antibody classes (IgG, IgA and IgE) with different effector functions without changing the antigen-specificity (1, 2).

#### **7.1.2.2 Antigen processing and presentation on MHC molecules**

Every cell is capable of presenting endogenous antigens on class I MHC complexes whereas only APC display endogenous as well as exogenous antigens on class I and class II MHC molecules. The best studied APC are macrophages, dendritic cells (DC) and B cells but it could be shown that

other cells such as liver sinusoidal endothelial cells are able to present exogenous antigens on class II MHC molecules as well (6).

Complexes between antigenic peptides and MHC molecules are formed by degradation of a protein antigen by two different antigen-processing pathways. MHC class I presentation is associated with the processing of endogenous antigens and MHC class II presentation with that of exogenous antigens.

Endogenous proteins derived from normal cells, tumors, viruses or intracellular bacteria are degraded by the proteasome into peptides and transported into the rough endoplasmic reticulum where they are loaded onto MHC class I molecules. MHC class I molecules preferentially bind peptides of 8 – 13 amino acids. The peptide-loaded MHC class I molecules are transported through the Golgi complex to the cell surface, where they present the endogenous peptide to CD8<sup>+</sup> cytotoxic T cells

Exogenous antigens are internalized by APC by receptor-mediated endocytosis in all APC and by phagocytosis and macropinocytosis in dendritic cells and macrophages. The internalized antigens are degraded into peptides of 13 – 18 residues within the acidic compartments in the cytoplasm. Within the endocytic compartments the degraded endogenous peptides associate with the MHC class II molecules transported from the rough endoplasmic reticulum and the MHC class II-peptide complex is transported to the cell surface membrane, where the exogenous peptide is presented to CD4<sup>+</sup> T cells (1, 2)

## **7.2 Tolerance**

Upon encountering an antigen, the immune system can either develop an immune response or enter a state of unresponsiveness called tolerance. The development of immunity or tolerance needs to be carefully regulated since an inappropriate response can have life-threatening consequences caused by immunity against self-antigens (autoimmunity) or tolerance to a potential pathogen.

## 7.2.1 Generation of Tolerance

The first regulatory mechanism of the immune system to distinguish between self and non-self is called central tolerance. It occurs during lymphocyte maturation in the thymus and bone marrow when newly formed lymphocytes are especially sensitive to inactivation by strong signals through their antigen receptors, whereas the same signals would activate a mature lymphocyte. Since central tolerance requires the presence of self-antigens during the maturation process of lymphocytes in the thymus and bone marrow and not all self-proteins can be present during that time, another regulatory mechanism becomes necessary that controls matured lymphocytes. This mechanism is called peripheral tolerance. Peripheral tolerance ensures that mature lymphocytes can distinguish between self and non-self even if they haven't seen the antigen during their maturation. Peripheral tolerance often depends on how the mature lymphocytes encounter the not yet seen antigen. High and constant antigen concentrations from self-proteins can provide strong signals that tolerize mature lymphocytes. On the other hand suddenly introduced and rapidly increasing foreign antigens as during the early stages of an infection activate mature lymphocytes. The innate immune system contributes to peripheral tolerance by providing signals such as cytokines and upregulation of co-stimulatory molecules on APC that are crucial in enabling the activation of an adaptive immune response to infections. In the absence of infection these signals are not generated and the encounter of a naïve lymphocyte with a self antigen tends to lead to a negative, inactivating signal that leads to anergic (functional unresponsive) lymphocytes rather than no signal at all (7). The route of how an antigen is introduced to the immune system can have effects on the lymphocytes specific for that antigen as well. It is known for example that orally administered antigens tend to lead to oral tolerance. Oral tolerance induction is believed to be achieved by the induction of antigen-specific  $T_{reg}$  cells that emerge after activation in the gut-associated lymphatic tissues under physiological conditions in the absence of inflammation. It has been shown that these weakly self-reactive  $T_{reg}$  cells can be immunosuppressive and

dampen other classes of immune responses in their immediate vicinity by secreting non-inflammatory  $T_H2$  cytokines such as interleukin 4 (IL-4), interleukin 10 (IL-10) and tumor growth factor  $\beta$  (TGF- $\beta$ ) (1, 2, 8).

## **7.2.2 Breaking of tolerance – induction of autoimmune disease**

Despite all tolerance mechanism the discrimination between self and non-self by the immune system is imperfect and self-reactive lymphocytes exist in the natural immune repertoire but are not often activated. In autoimmune disease, however, these cells become activated and lead to tissue damage.

### **7.2.2.1 Autoimmune diseases**

For a disease to be defined as autoimmune, the tissue damage must be shown to be caused by the adaptive immune response to self-antigens. Autoimmune diseases are generally classified into organ-specific autoimmune diseases that affect a specific organ and systemic autoimmune diseases that affect tissues throughout the body. Organ-specific autoimmune diseases such as type 1 diabetes mellitus (T1D), multiple sclerosis (MS), Graves' disease, autoimmune hepatitis (AIH) or primary biliary cirrhosis (PBC) have in common that the effector functions target autoantigens that are restricted to particular organs: insulin-producing  $\beta$  cells of the pancreas in T1D, the myelin sheathing axons in the central nervous system in MS, the thyroid-stimulating hormone receptor in Graves' disease, the cytochrome P450 2D6 in hepatocytes in type 2 AIH or the bile ducts in the liver in PBC. Systemic autoimmune diseases, such as systemic lupus erythematosus (SLE) or rheumatoid arthritis, cause inflammation in multiple tissues because their autoantigens like chromatin in SLE are not restricted to a specific organ but rather can be found in every cell of the body. For many autoimmune diseases it is still unknown what part of the immunesystem mediates the disease and in most cases it is likely to be a combination of several factors such as autoreactive lymphocytes and/or their soluble products, pro-inflammatory cytokines and autoantibodies. The etiology of most

autoimmune diseases is still largely unknown. However, it could be shown that autoimmune diseases are the result of multiple factors, including genetic predisposition and environmental triggers (1, 2).

### *Genetic predisposition*

First evidence that there are genetically predispositions in humans for autoimmune diseases came from the fact that some autoimmune diseases like T1D run in families. Further evidence was given by certain inbred mouse strains that are prone to various types of autoimmune disease like the non-obese diabetic mouse line (NOD) for T1D (9). During the last decade new methodologies were able to link genetic factors to several autoimmune disease. It could be shown that the MHC haplotype and polymorphisms in genes involved in establishing self-tolerance and immune regulation can influence the development of autoimmune diseases. The MHC haplotype for example can influence the susceptibility to a given autoimmune disease in two ways. It can either ineffectively present self-antigens in the thymus, which leads to more aggressive T cells in the periphery or enhance the presentation of peptide epitopes in the periphery which leads to increased T cell activation. Many human autoimmune diseases could already be associated with MHC haplotypes so for example T1D with HLA-DQ2/DQ8 heterozygote (10), Graves' disease with HLA-DRB3 (11) and AIH type 2 with HLA-DRB1 and HLA-DQB1 (12) to only name a few. Genetic polymorphism in genes like CTLA-4 or TIM proteins have been found that could be linked to autoimmune diseases in humans (Graves' disease in case of CTLA-4) or in animal models (experimental allergic encephalomyelitis, an animal model for MS, in case of TIM proteins) further proving that genetic susceptibility factors can influence the development of autoimmune diseases (reviewed in (13)). Patients with a defect in a single transcription factor called autoimmune regulator (AIRE) that is responsible for turning on many peripheral genes in the thymus during central tolerance induction develop a rare inherited form of autoimmunity called autoimmune polyendocrinopathy-candidiasis-

ectodermal dystrophy (APECED) that leads to the destruction of multiple endocrine tissues (14).

### *Environmental factors*

Genetic variations alone are not always sufficient to cause autoimmune diseases, as it is the case for the very rare APECED disease. One prove that environmental factors must play a role in the etiology of autoimmune disease is the fact that there is a considerable discordance in the incidence of autoimmune diseases in human monozygotic twins as well as in genetically identical mice. There is also a decrease in incidence of autoimmunity from north to south in the northern hemisphere independent of ethnic background and a reduced incidence of autoimmunity in developing countries with poor sanitary conditions compared with industrial countries which further substantiates the involvement of environmental factors in the manifestation of autoimmune diseases (15).

However, how environmental factors influence the incidence of autoimmunity is still largely unknown. There are several theories how self-tolerance in an individual can be broken by environmental triggers leading to activation of auto-reactive lymphocytes and initiation of autoimmune disease. The most common theories that could be confirmed to induce autoimmune diseases in animal models are bystander activation, molecular mimicry and drug metabolism (see figure: Figure 1) (reviewed in (13)). It is likely however, that those theories alone can't explain the induction of autoimmunity in humans by itself. It has become clear that the initiation of autoimmunity is a multifactorial and complex process that requires genetic components to synergize with environmental events (reviewed in (13)). Taken together, it is believed that microbial infection can induce a temporary immunological state that can, depending on other environmental and genetic factors yield in a pathological outcome of an infection leading to autoimmune diseases. This temporary immunological state is referred to as a 'fertile field' (16).

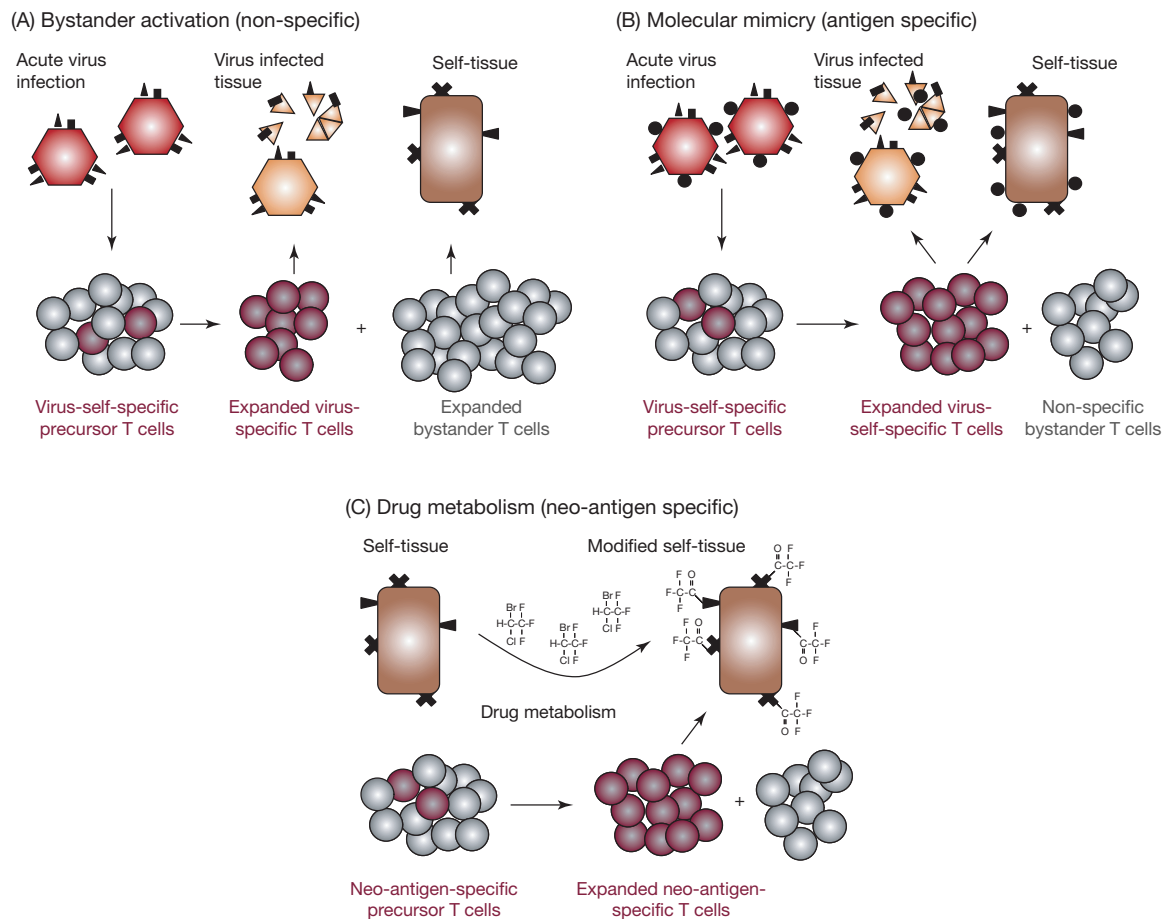


**Figure 1: Mechanism that can lead to broken self-tolerance**

(A) Infections lead to antigen-specific activation of the adaptive immune response. During that process however, there is always a proportion of non-specifically activated bystander-lymphocytes at the site of infection. The sum of all non-specifically activated cells can cause damage to self-tissue. (B) An infection with a pathogen that resembles host molecules can lead to a pathogen-specific immune response that not only attacks the pathogen but also the self-tissue. (C) Drug metabolism can lead to the formation of protein adducts against which the immunesystem could not induce tolerance against leading to a neo-antigen-specific response against self-tissue (adapted from (13)).

### *Bystander activation*

Despite all the tolerance mechanisms (see chapter: Generation of Tolerance) autoreactive B and T cells are present in all healthy subjects. However, these autoreactive lymphocytes alone are not enough to initiate autoimmune disease despite the presence of their autoantigen. Any infection leads to the release of pro-inflammatory cytokines that help the adaptive immune system to accumulate and activate pathogen-specific lymphocytes at the site of

infection. However, since cytokines are soluble small proteins that can act in a paracrine as well as endocrine fashion on all cells that express the complementary cytokine receptors there will always be some antigen-independent, non-specific lymphocyte attraction. In this context pathogen-specific lymphocyte activation can lead to polyclonal activation of non-specific as well as pre-existing autoreactive lymphocytes. This antigen-independent lymphocyte attraction and polyclonal activation of potentially autoreactive lymphocytes is referred to as bystander activation (see Figure 1: (A)) (reviewed in (13)). As an example it has been shown that infection with Coxsackie virus during the pre-diabetic phase in NOD mice can accelerate T1D when their autoreactive T cells have reached a critical mass (17).

### *Molecular mimicry*

Molecular mimicry has been defined as a structural similarity between host and pathogen (18, 19). An infection with a pathogen that confers molecular mimicry to host molecules can therefore lead to pathogen-specific antibodies that cross-react with 'self' or to the activation of autoreactive T cells (see Figure 1: (B)). One of the best studied animal model system for molecular mimicry has been generated using transgenic mice that express the glycoprotein (GP) or nucleoprotein (NP) of lymphocytic choriomeningitis virus (LCMV) under the control of the rat insulin promoter (RIP) which directs transcription in the  $\beta$ -cells of the islets of Langerhans. The transgenically expressed LCMV proteins in these mice are considered self-proteins. However, upon infection of RIP-LCMV mice with LCMV these mice develop diabetes (20, 21). Several other animal models have been introduced that link infections with autoimmune diseases via molecular mimicry (22-24) making this hypothesis very popular. However, so far there is very little direct evidence for the relevance of this theory for human autoimmune disease (19, 25, 26). Several circumstances make it difficult to identify a single microorganism as the cause of a human autoimmune disease. First, it is very likely that an acute infection that can induce autoreactive cells has already been cleared by the time these cells become auto-aggressive or at diagnosis

of the resulting autoimmune disease, making a causative association very hard to prove (also referred to as 'Hit-and-run events'). Second, it is likely that in many cases a simple infection by one single infectious agent is not enough to initiate autoimmune diseases. It is possible that more than one subsequent infection is needed to amplify the number and/or activation status of autoreactive cells and that the timing of those infections in relation to each other plays an important role, which in retrospect are probably impossible to correlate between individuals of interest. Third, some virus infections are extremely common and traces of these infections can be found in almost every individual and not only in those that develop autoimmune disease, making it extremely hard to associate those infections with autoimmune disease (16). The two best documented cases for molecular mimicry in human autoimmune diseases are rheumatic fever and Guillain-Barré syndrome. In rheumatic fever antibodies that appear after *Streptococcal pyogenes* infections cross-react with heart autoantigens and it is postulated that this can lead to antibody-mediated and possibly T cell-mediated anti-heart autoimmunity (27). In case of Guillain-Barré syndrome it could be shown that antibodies specific for *Campylobacter jejuni* appearing after intestinal infections with *C. jejuni* cross-react with peripheral nerve gangliosides (28).

#### *Drug metabolism*

Another evidence of external causative agents in human autoimmunity comes from the effects of certain drugs, which elicit autoimmune reactions as side effects in a small proportion of patients. Those drugs are believed to initiate the autoimmune reaction by formation of neo-antigens to which no previous tolerance could have been established in the host (see Figure 1: (C)). One example for this would be the highly reactive intermediate trifluoroacetyl (TFA) that can covalently bind to self-proteins, resulting in the formation of protein adducts. TFA is generated during the oxidative metabolism of 2-bromo-2-chloro-1,1,1-trifluoroethane, an anesthetic agent called halothane that is metabolized in the liver by cytochrome P450 2E1.

The formation of TFA protein adducts can in susceptible individuals lead to a specific immune response against these newly formed antigens and result in fulminant autoimmune-mediated hepatitis with a frequently fatal outcome (29). Interestingly, although the formation of TFA protein adducts can be observed in all individuals, only very few suffer from halothane hepatitis suggesting the role of other factors in disease development. Indeed, the susceptibility to disease is suggested to be linked to the pyruvate dehydrogenase complex that shares a structural similarity to TFA protein adducts and is aberrantly expressed in individuals with halothane hepatitis (29). Another well documented case is procainamide, a drug used to treat heart arrhythmias, and its metabolite procainamide-hydroxylamine that is responsible for the induction of autoantibodies similar to those in SLE (13, 30, 31).

## **7.3 The liver**

### **7.3.1 Anatomy and function of the liver**

The liver is the largest internal organ in the human body and can be divided into four lobes based on surface features. The liver is essential for survival, plays a major role in metabolism and detoxification and has numerous functions including glycogen storage, decomposition of red blood cells, plasma protein and bile synthesis. The liver is the only organ receiving a dual blood supply, one from the hepatic arteries and the other from the portal veins draining the intestines, pancreas and spleen (see Figure 2: (A)). The liver tissue is organized around vascular bundles, which are known as portal tracts. From the portal tracts, blood flows through a sponge-like meshwork of sinusoids that exists between plates of hepatocytes allowing the liver to carry out its physiologic functions of digestion, detoxification and plasma protein synthesis (see Figure 2: (B)). The sinusoids are lined by liver sinusoidal endothelial cells (LSEC) and contain liver resident macrophages, known as Kupffer cells, hepatic stellate cells, lymphocytes and immature DC. The unique blood circulation in the liver allows molecules absorbed by the

intestine to transit through the liver where they are metabolized or degraded if toxic. Because the liver is the major primary site of detoxification for the body and acts as a first line of defense against infectious, toxic, or carcinogenic agents arriving from the gut, the liver has evolved mechanisms that allow it to regenerate very quickly if injured (32, 33).

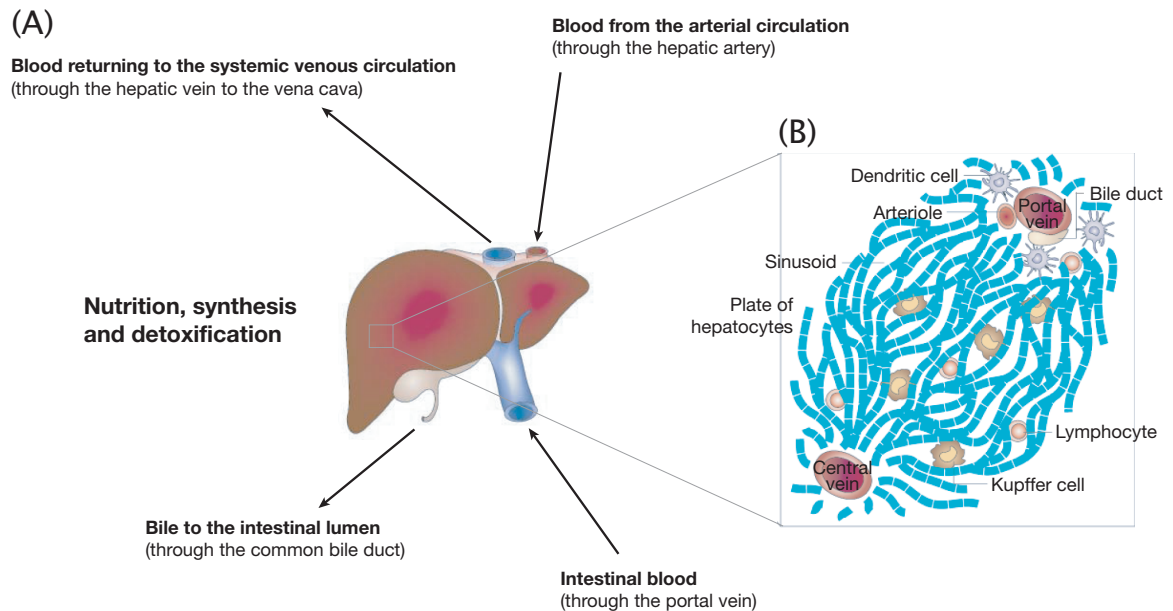


**Figure 2: The liver and its microenvironment**

(A) The inputs and outputs of the liver showing the liver's uniqueness by receiving blood from the hepatic arteries as well as from the portal veins draining the intestines, pancreas and spleen. (B) Diagram showing the structure of a liver lobule. The tissue is organized around portal tracts and the blood flows from them to the central veins, passing between plates of hepatocytes through spaces called sinusoids. This organization maximizes the exchange of molecules between the sinusoidal space and hepatocytes, allowing the liver to carry out its function (adapted from (33)).

### 7.3.2 Liver immunology

Already from the unique function of the liver to metabolize and detoxicate non-self molecules arriving from the intestine, a special role of the liver in controlling these mechanisms locally can be assumed. Pathogenic microorganisms must be efficiently eliminated while the large number of antigens derived from harmless food-derivates must be tolerized to avoid damage to hepatocytes. From experimental observations, initially demonstrated by spontaneous acceptance of liver allografts in many species

(34) it is evident that the liver favors the induction of tolerance rather than the induction of immunity. Nevertheless, bacterial as well as viral infections occur within the liver and have to be cleared by the immunessystem. It could be shown that immunization with an attenuated sporozoite can protect mice from experimental plasmodium infection and that this protection is mediated primarily by CD8<sup>+</sup> cytotoxic lymphocytes that persist in the liver for up to four months (35). It is also known that individuals are able to completely clear hepatitis viruses such as the hepatitis B virus (HBV), which is cleared in more than 95% of immunocompetent adults (36). On the other hand it could be shown *in vitro* that LSEC or Kupffer cells are able to endocytose, process and present antigen to T cells leading to local activation of T cells, however the most common outcome of T cell priming by LSEC is tolerance either by failure of CD8<sup>+</sup> T cells to differentiate into cytotoxic effector cells or by induction of a regulator phenotype in CD4<sup>+</sup> T cells by the lack of co-stimulatory signals of LSEC (37). It could also be shown that induction of peripheral tolerance to allograft antigens could be achieved by injection of donor-specific leukocytes prior to organ transplantation and that this tolerance depends on Kupffer cells, because it is impaired if the Kupffer cells are depleted (38, 39). In addition, induction of T cell apoptosis and accumulation in the liver occurring as a function of insufficient antigen presentation, defective T cell activation and deprivation of survival signals could be shown after T cell activation by hepatocytes suggesting a role for apoptosis in the immune regulation of the liver (40). In a recently published article it could be demonstrated that targeted expression of autoantigens in liver cells could induce autoantigen-specific T<sub>reg</sub> cells that were able to suppress subsequent induction of experimental allergic encephalomyelitis (EAE), a murine autoimmune disease that models human MS (41). Taken together there is an overall bias of intrahepatic T cell responses towards tolerance. The underlying mechanisms that lead to reversal of this default state of tolerance induction in the liver to allow priming of an effector response are not completely understood yet. But the cytokine profile present during antigen presentation, the site of primary activation as well as the

activation status of presenting APC are thought to play an important role (33, 37).

### **7.3.3 Liver diseases**

Liver disease is a broad term describing any number of diseases affecting the liver. Most often it is accompanied by hepatitis, the presence of inflammatory cells in the liver. The condition can be self-limiting, healing on its own within a month, or progress to a more severe chronic form. Several viruses such as Hepatitis virus A through E, Herpes simplex virus, Cytomegalovirus, Adenoviruses and Epstein-Barr virus can cause acute forms of hepatitis whereas only hepatitis B with or without hepatitis D and hepatitis C can cause chronic hepatitis. Several toxins, drugs and also alcohol can lead to acute phase hepatitis and in some cases to chronic forms. The breakdown of tolerance to self-antigens leads to autoimmunity (see chapter: Breaking of tolerance – induction of autoimmune disease) and can result in chronic inflammation of the liver as it is the case in several autoimmune liver diseases described in the following chapter. Extensive and long-lasting liver damage can lead to development of fibrosis and cirrhosis, a consequence of chronic liver diseases that is characterized by extensive deposition of extracellular matrix (ECM) proteins such as collagen types I, III, IV and V, laminin and elastin by hepatic stellate cells (HSC). While fibrosis, the less severe form of cirrhosis is generally still reversible, cirrhosis is irreversible and in advanced stages it leads to a complete loss of liver functions (42).

### **7.3.4 Autoimmune liver diseases**

Autoimmune liver diseases (ALD) include a spectrum of diseases which comprises both cholestatic and hepatitic forms like primary biliary cirrhosis (PBC), primary sclerosing cholangitis (PSC), autoimmune hepatitis (AIH) and the so called overlap syndromes where hepatitic and cholestatic damage coexists. The respective syndromes of those ALD partially overlap and sometimes a definite diagnosis is difficult, because clinical signs and

symptoms are often inconsistent and variable. However, all of those diseases can be severe, progressive and can lead to cirrhosis and death from end-stage liver disease. The precise etiology as well as the exact pathogenic mechanism of those autoimmune diseases are still unknown and the diagnostic approach is mainly based on the detection and characterization of non organ-specific autoantibodies and the responsiveness to immunosuppressive therapy in case of AIH and to ursodeoxycholic acid in cholestatic conditions (43-45).

#### **7.3.4.1 Primary biliary cirrhosis**

PBC is a chronic cholestatic liver disease characterized by the slow progressive destruction of intrahepatic bile duct leading to fibrosis and cirrhosis. It affects predominantly the female gender and is more common in first-degree relatives suggesting a genetic predisposition of patients. However, no strict association with major histocompatibility complex alleles could be found. PBC is characterized by the presence of detectable antimitochondrial autoantibodies (AMA) in approximately 90 – 95% of affected individuals. The observation that patients lacking AMA have disease characteristics and progression similar to those of AMA-positive subjects appears to argue against a pathogenic role for these autoantibodies. The most frequent antigen reactivity of AMA is against the subunit E2 of the pyruvate dehydrogenase complex (PDC-E2). The fact that this target antigen can be found on all cells of an organism but autoimmune attacks in PBC are organ-specific further suggests that AMA are not involved in the pathogenic mechanisms of PBC. About the etiology and pathogenesis of PBC is very little known so far but the main proposed hypothesis includes microbial-mediated molecular mimicry as trigger in genetically susceptible individuals by *Escherichia coli*, *Sphingomonas* species or *Helicobacter* species (45-48).

#### **7.3.4.2 Primary sclerosing cholangitis**

PSC is a progressive cholestatic liver disease characterized by the destruction of intra- and extra-hepatic bile ducts larger than those affected

by PBC also leading to fibrosis and cirrhosis. It occurs in children and young adults and is more common in men than women. The etiology of PSC is unknown and despite the association with autoantibodies and inflammatory bowel disease its autoimmune origin is controversial. Diagnosis of PSC is most specifically achieved by the detection of structures of intra- or extra-hepatic bile ducts via endoscopic retrograde cholangiopancreatography. The autoantibodies found in about 90% of PSC patients are anti-neutrophil cytoplasmic antibodies (ANCA). However, the presence of these autoantibodies is not specific for PSC since they can be detected in other autoimmune diseases such as AIH type 1 as well. Furthermore, their presence does not appear to have a pathological role (43, 45, 49).

#### **7.3.4.3 Autoimmune hepatitis**

AIH is a non-resolving inflammation of the liver of unknown cause that is characterized by the presence of interface hepatitis and portal plasma cell infiltration on histologic examination, hypergammaglobulinemia and autoantibodies and leads to a loss of tolerance against hepatocytes and the destruction of hepatic parenchyma followed by cirrhosis and liver failure in almost all cases. There are no features that are absolutely diagnostic and the existence of the condition can be established by recognition of various compatible features and the exclusion of other diseases. Therefore the international autoimmune hepatitis group standardized and published a list of criteria for the diagnosis of autoimmune hepatitis (50). Those criteria involve the gender, biochemical evaluations, various serum parameters, changes in the liver histology, genetic parameters, the exclusion of other liver diseases such as viral markers and drug or alcohol abuse/misuse as well as the outcome of immunosuppressive therapy. Liver biopsy examination as well as the presence of autoantibodies is essential to establish the diagnosis. Based on the autoantibodies present in the serum of patients AIH can be subdivided into two major types, type 1 and type 2 AIH (51, 52).

### *Autoimmune hepatitis type 1*

The main serologic markers of type 1 AIH are antinuclear antibodies (ANA) and/or smooth muscle antibodies (SMA). ANA are a largely non-specific marker of AIH and can also be found in other autoimmune liver disease, liver diseases in general and even in up to 15% of the general healthy population predominantly among older age groups. ANA have been found to be reactive with centromeres, ribonucleoproteins, cyclin A, histones and many other antigens and so far no liver-specific or liver-disease-specific ANA has been discovered. SMA are directed against actin and non-actin components of the cytoskeleton such as tubulin, vimentin, desmin and skeletin. Actin-associated SMA are found in a large majority of SMA-positive AIH patients but are rare in other chronic liver diseases. Positivity for actin-associated SMA is more frequently seen in patients with the HLA B8, DR3 and DR4 haplotypes and is associated with early disease onset and worse prognosis. Autoantibodies against soluble liver antigen and liver-pancreas antigen (Anti-SLA/LP) are the most specific autoantibody identified in type 1 AIH however, it is only found in 10 – 30% of cases (44, 51-54).

### *Autoimmune hepatitis type 2*

Autoantibodies to liver-kidney microsomal type 1 antigens (LKM-1) have been found to be the hallmark of AIH type 2 and the target antigen was identified as the isoform 2D6 of the large cytochrome mono-oxygenase P450 enzyme family (CYP2D6). LKM-1 antibodies in AIH type 2 recognize the linear CYP2D6<sub>254-271</sub> sequence as immunodominant but not exclusive epitope in almost all patients with AIH type 2 (55-58). However, LKM-1 antibodies also occur in up to 10% of sera from patients chronically infected by hepatitis C virus (56). Antibodies to liver-cytosol type 1 (LC1), another autoantibody that is found in up to 50% of patients with AIH type 2, recognize formiminotransferase cyclodeaminase (FTCD), a liver-specific metabolic enzyme. Susceptibility factors for AIH type 2 are associated primarily with HLA-DRB1 and HLA-DQB1 (59).

The pathogenic mechanism underlying AIH type 2 are still unknown. It could be shown that CYP2D6, the target recognized by LKM-1 antibodies is not exposed on the surface of hepatocytes excluding antibody-mediated cell lysis directed against membrane CYP2D6 (58). On the other hand more recent data could show that LKM-1 autoantibodies do recognize and bind to CYP2D6 exposed on the plasma membrane of hepatocytes (60) and that anti-LC1 antibodies seem to correlate with disease activity suggesting a pathogenic role of autoreactive B cells in AIH type 2 (61). Very recently it could also be shown that MHC class I as well as class II restricted immune responses seem to influence autoimmunity in patients with AIH type 2 (59, 62, 63). However, the exact mechanisms of the pathogenesis remain unclear.

Another unsolved problem of AIH is its etiology. A common hypothesis to explain the etiology of autoimmune diseases is genetic predisposition of the host paired with environmental triggers (see chapter: Autoimmune diseases). As previously explained (see chapter: Environmental factors) infections are the prime candidates for initiating autoimmunity in predisposed individuals since they frequently induce strong inflammatory responses in various organs and can therefore attract a multitude of potentially autoaggressive lymphocytes to the site of infection (13). Although a direct link between AIH and viral or bacterial infections has not been proven to date, there are several experimental findings that add credence to a hypothesis of virally triggered AIH. First, it is known that a significant number of AIH type 2 patients carry antibodies to HCV (64). Second, it could be shown that sera of 38% of chronic HCV-infected patients reacted specifically with CYP2D6, whereas none of the sera from patients with chronic hepatitis B showed CYP2D6 reactivity (65). In addition, it was found that HCV has the potential to induce autoreactive CD8<sup>+</sup> T cells, which cross-reactively recognize the cytochrome P450 isoforms 2A6 and 2A7 that contain sequence homology to HCV (66). Furthermore, it could be shown that antibodies against CYP2D6 in HCV and LKM-1 positive patients can cross-react with the HCV proteins NS3 and NS5a (56) and that CYP2D6-specific antibodies could be found in HCV-infected patients (67). In addition, other sequence homologies like between

the immunodominant CYP2D6 epitope and a protein of herpes simplex virus 1 (HSV-1) have been reported (57). Such a phenomenon of cross-reactivity on the level of T cell or antibody recognition is commonly referred to as 'molecular mimicry' (see chapter: Environmental factors) and remains a favored hypothesis for the initiation of autoimmunity in general or autoimmune liver diseases as PBC or AIH type 2 although the definite proof remains elusive.

#### **7.3.4.4 Overlap syndromes**

Overlap syndromes are diagnoses made by clinicians who felt that a single designation is inadequate to convey the mix of clinical, laboratory and histological features of a disease process. For example, the classical description of AIH does not involve the presence of AMA, high serum levels of alkaline phosphatase or the histological features of destructive cholangitis. In addition, the classical diagnosis of PBC does not involve the presence of increased serum levels of aminotransferase and IgG and the histological findings of moderate to severe interface hepatitis. However, those diagnoses exist and are commonly referred to as overlap syndromes or more precisely as hepatic PBC or cholestatic AIH (68).

#### **7.3.4.5 Animal models for AIH**

Animal disease models are an invaluable resource in elucidating the pathogenic mechanisms underlying complex conditions such as autoimmune diseases and are widely studied by immunologists (see chapter: Environmental factors). However, animal models for AIH have proven difficult to generate and none of them have covered all the attributes that are linked to the autoimmune destruction of hepatocytes occurring in human AIH, perhaps at least in part because of the overall bias of intrahepatic immune responses towards tolerance (see chapter: Liver immunology). Breaches of tolerance leading to autoimmunity and hepatitis have been demonstrated but often depend on a rather complex disease induction protocol and hepatitis was in most cases only transient. In most animal models for AIH a transgenic

target antigen expressed specifically in the liver is used to target the autoaggressive immune response to the liver (69, 70).

In the early 1990s a HBV surface antigen (HBsAg) transgenic mouse was developed that expressed the HBsAg under the mouse albumin promoter and therefore specifically in the liver. Upon adoptive transfer of activated T cells from HBsAg-primed donor mice they found liver infiltrating HBsAg-specific CTL targeting HBsAg expressing hepatocytes. However, only a transient form of hepatic injury could be observed (71).

In another model, the MHC class I molecule H-2K<sup>b</sup> was transgenically expressed in the liver of mice that were carrying in addition T cells with a transgenic TCR specific for H-2K<sup>b</sup>. Those mice displayed peripheral tolerance to H-2K<sup>b</sup> that could only be broken by transferring cells expressing the H-2K<sup>b</sup> target antigen and IL-2 or by infecting the mice with a liver-specific pathogen, indicating that bystander activation within the liver microenvironment is necessary to break tolerance and cause autoimmune tissue damage (72).

Further, a model similar to the RIP-LCMV mouse model for type 1 diabetes (see chapter: Environmental factors) was described with the difference that the GP was expressed under the control of the albumin promoter exclusively in the liver. As in the RIP-LCMV model these mice did not show any signs of autoimmunity under normal conditions and similar to the H-2K<sup>b</sup> transgenic mice, adoptive transfer of TCR transgenic T cells specific for the LCMV-GP expressed in the liver alone was not sufficient to induce disease. However, when these mice were infected with LCMV after adoptive transfer a transient form of hepatitis developed (73).

In another study, mice expressing the LCMV-NP under the control of the transthyretin promoter specifically in the liver were vaccinated with plasmids expressing the LCMV-NP. Liver injury characterized by cellular infiltration and elevated serum aminotransferase levels could only be detected after plasmid vaccination in combination with the T<sub>H</sub>1 stimulating cytokine interleukin-12 (IL-12) (74).

A related approach was used in another study in which wild-type mice were xenoimmunized with a plasmid containing the human antigenic region of CYP2D6 (the target of LKM-1 antibodies) and FTCD (the target of LC1 antibodies). However, minor elevations in serum aminotransferase levels, a transient generation of anti-CYP2D6 and anti-LC1 antibodies and significant inflammation in the liver could only be found after co-expression of IL-12 (75).

## **8 Aim of the study**

**It was the aim of my project to generate a novel animal model for autoimmune hepatitis that reflects the chronic inflammation and the progressive destruction of the liver characteristic for the human disease. In addition, we were interested in the mechanism underlying this autoimmune liver damage and the potential contributions of humoral and cellular immunity to hepatic autoimmunity.**

### **8.1 Strategy**

A common hypothesis to explain the etiology of autoimmune diseases is genetic predisposition of the host paired with environmental triggers, whereas infections remain the prime candidates for initiating autoimmunity since they frequently induce strong organ-specific inflammatory responses. In addition, it could be shown that viruses can induce, accelerate and even prevent autoimmune processes in animal mouse models most likely via a process called molecular mimicry (see chapter: Environmental factors) (76). Nevertheless, no direct link between autoimmune hepatitis and viral infections could be found yet even though several studies implicate viruses in its initiation. In animal models for autoimmune liver diseases an often only transient form of autoimmune-mediated liver damage could only be achieved with rather complex ways of induction. Our strategy was therefore to build an animal model on the initial concept of molecular mimicry by virus infection and see if viral inflammation caused by liver-tropic adenovirus can facilitate the breaking of tolerance to a naturally occurring autoantigen in the liver (CYP2D6) resulting in a chronic form of severe, autoimmune liver damage.

#### **8.1.1 The CYP2D6 humanized mice**

The CYP2D6 humanized mouse line was generated by Frank J. Gonzalez (National Cancer Institute, U.S. National Institutes of Health, Bethesda, MD) to overcome the species differences between animal models and human in preclinical studies on the pharmacology, toxicology, and physiology of

CYP2D6-mediated metabolism. Therefore the complete CYP2D6 gene (GenBank accession number M33388), including its promoter and regulatory elements, was microinjected into a fertilized FVB/N mouse egg to produce a transgenic mouse line. Successful incorporation of the CYP2D6 DNA within the mouse genome was determined by both PCR and southern blot analysis (see Figure: Figure 3 (A) and (B)). The transgene was present at  $5 \pm 1$  copies per haploid genome. Expression of the transgenic protein was assessed by western blotting and CYP2D6 expression was found in liver, intestine and kidney microsomes only (see Figure: Figure 3 (C)). Debrisoquine hydroxylase activity was enhanced in CYP2D6 transgenic mice compared with wild-type mice, indicating that CYP2D6 in humanized mice is functional (77).

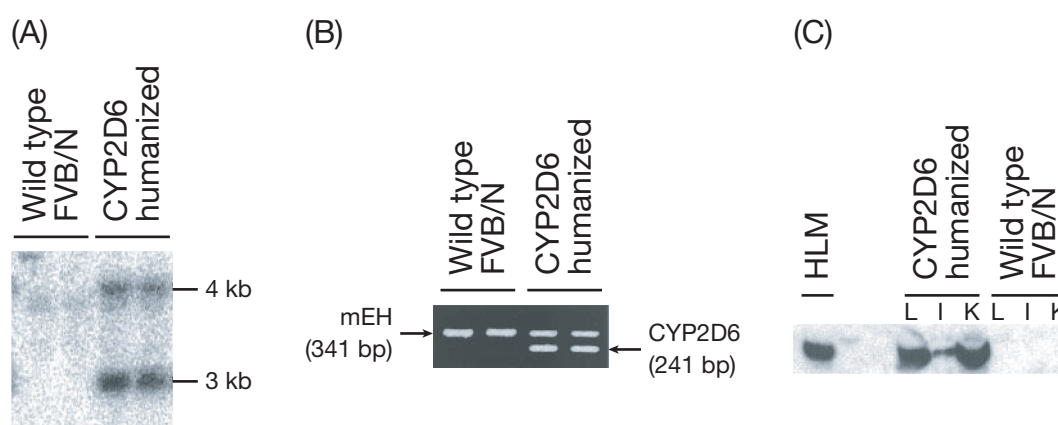


**Figure 3: Generation and analysis of the CYP2D6 humanized mouse**

(A) Southern blot genotyping of wild-type FVB/N and CYP2D6 humanized mice. Tail DNA was digested and probed with CYP2D6 cDNA. (B) PCR genotyping of wild-type FVB/N and CYP2D6 humanized mice. Tail DNA was amplified with mouse epoxide hydrolase (mEH) and CYP2D6 gene-specific primers. (C) Western blot analysis of CYP2D6 protein expression in wild-type FVB/N and CYP2D6 humanized mice. Liver (L), intestine (I) and kidney (K) microsomal proteins were separated and stained with a human CYP2D6-specific monoclonal antibody. Human liver microsomes (HLM) were used as a control (adapted from (77)).

The cell-specific expression of human CYP2D6 in liver, kidney and intestine in humanized mice was similar to that reported in humans. In addition, the orthologous mouse cytochrome P450 isoenzymes (CYP2Ds) that are expressed in wild-type FVB/N mice as well as in humanized CYP2D6 mice showed a similar expression pattern to those in humans in liver and kidney

(78). There are at least nine different mouse CYP2Ds genes and one isoenzyme, CYP2D22, has been suggested to be the functional ortholog of CYP2D6 (79). Mouse CYP2Ds genes display high sequence homology of the human CYP2D6 and other human CYP isoenzymes and by screening of the National Center for Biotechnology Information databank we could show that the mouse CYP2Ds isoenzymes CYP2D9, CYP2D11, CYP2D22 and CYP2D26 display up to 75% aa sequence homology to human CYP2D6 (80).

### **8.1.2 Adenoviruses**

Adenoviruses are medium-sized (90 – 100 nm), nonenveloped icosahedral viruses composed of a nucleocapsid and a double-stranded linear DNA genome that are generally associated with benign pathologies in humans. Since adenoviruses deliver their genome to the nucleus of cells and can replicate with high efficiency using the host's replication machinery they are prime candidates for the expression and delivery of genes. The adenovirus infectious cycle can be clearly divided into two phases. The first or early phase covers the entry of the virus into the host cell and the passage of viral genome to the nucleus followed by the selective transcription and translation of the early genes. Those early events modulate the function of the cell to initiate the transcription and translation of the late genes in the second or late phase of the adenoviral infection cycle. Adenoviral vectors are based on the adenovirus type five backbone in which an expression cassette containing up to 6.5 kb foreign DNA can be introduced in place of the early region 1 (E1) and/or early region 3 (E3) genes. Viruses in which E1 has been deleted are defective for replication and have to be propagated in the human 293 complementation cells, providing the E1 products in *trans*. Viruses defective in E3 lose their E3 gene-mediated defense mechanisms against host immune responses (81). The Adenovirus 2D6 (Ad-2D6) used in our study, obtained via Prof. Eric F. Johnson (The Scripps Research Institute, La Jolla, CA) was created by homologous recombination in *Escherichia coli* BJ5183 between a shuttle vector containing the cDNA for CYP2D6 and pAdE1-E3 and was therefore defective in both, its replication via deletion of E1 and its

immunosuppressive functions by deletion of E3 (82). One of the adenoviruses used as control (Ad-C) was the empty Adenovirus vector used for the production of Ad-2D6 whereas the other control adenovirus (Ad-GFP) that expresses the green fluorescent protein (GFP) instead of CYP2D6 was kindly provided by D.J. von Seggern (The Scripps Research Institute, La Jolla, CA).

## **8.2 Working hypothesis**

By the use of a newly designed animal model we wanted to see if viral inflammation caused by a liver-tropic adenovirus conferring molecular mimicry to a naturally occurring autoantigen in the liver can break tolerance and induce autoimmunity. Therefore we used the naturally occurring human CYP2D6 autoantigen as target antigen. The wild-type FVB/N mice, expressing only the mouse CYP2D6 homologues and the humanized CYP2D6 mice, expressing the mouse homologues as well as the human CYP2D6 under the control of its own promoter as a self-antigen in the liver were chosen as model system. Those mice are under normal conditions tolerant/ignorant to the transgenic/self CYP2D6 antigens. In order to break natural tolerance to the transgenic/self CYP2D6 antigen by viral infection we choose an adenovirus vector expressing the human CYP2D6 gene that is replication deficient and stripped from its immunosuppressive functions due to a deletion of the adenoviral E1 and E3 genes. The use of a liver-tropic adenovirus ensured a high expression rate of the triggering antigen in the liver as well as potent activation of the immune system by viral infection. Thus, infection with Ad-2D6 causes local non-specific activation of the innate immune system and possibly direct damage to hepatocytes leading to chemokine and cytokine release that attract and activate lymphocytes via bystander activation. In parallel, infection with Ad-2D6 leads to high expression of viral CYP2D6 in the liver that activate the antigen-specific adaptive immune response and leads to expansion of both viral and self CYP2D6-specific lymphocytes via molecular identity in case of the human CYP2D6 or molecular mimicry in case of the mouse CYP2Ds isoenzymes. Activated and expanded antigen-specific effector cells cause destruction of

virus-infected altered self cells as well as self cells. After all virus and viral-infected cells are deleted activated lymphocytes migrate deeper into the liver parenchyma and cause further damage to hepatocytes expressing self CYP2D6 (CYP2D6 mice) as well as CYP2Ds (FVB/N) resulting in clinically overt liver damage (see figure: Figure 4).

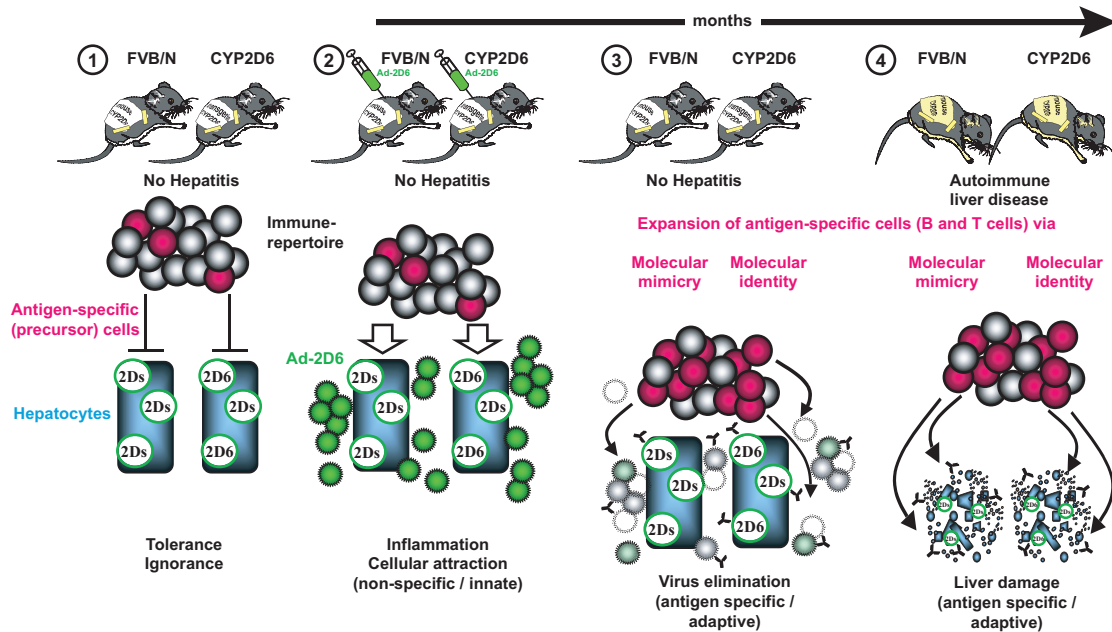


**Figure 4: Working hypothesis for breaking self-tolerance to liver autoantigens by viral infection**

(1) Wild-type FVB/N as well as CYP2D6 mice are tolerant/ignorant to their self CYP2D antigens. (2) Ad-2D6 infection causes local non-specific inflammation and possibly direct damage to hepatocytes. Chemokines and cytokines attract and activate lymphocytes in a non-specific manner (bystander activation). In parallel, infection with Ad-2D6 leads to high expression of viral CYP2D6. (3) Specific anti-viral CYP2D6 lymphocytes (B and T cells) are activated and expanded reacting against both human CYP2D6 (molecular identity) and self CYP2Ds (molecular mimicry). Effector lymphocytes destroy viral-infected altered self cells as well as self cells. (4) Later, activated lymphocytes migrate deeper into the liver parenchyma and cause further damage to hepatocytes expressing self CYP2D6 as well as CYP2Ds resulting in clinically overt liver damage.

## 9 Results

### 9.1 Introduction of the CYP2D6 mouse model for autoimmune hepatitis

As described previously the wild-type FVB/N mice, expressing the mouse CYP2D6 and the humanized CYP2D6 mice (see chapter The CYP2D6 humanized mice), expressing the mouse homologues as well as the human CYP2D6 under the control of its own promoter as a self-antigen in the liver were chosen as animal models. An adenovirus expressing the human CYP2D6 (see chapter Adenoviruses) was used to break self-tolerance to the transgenic CYP2D6 (via molecular identity) and potentially to the mouse CYP2D6 (via molecular mimicry) by viral infection (see chapter: Working hypothesis). Infection with Ad-2D6 resulted in two distinct phases of liver damage, an acute, antiviral phase characterized by transient elevation of serum values related to liver damage and minor cellular infiltrations, followed by a persistent, autoimmune-mediated phase characterized by massive hepatocellular damage, strong cellular infiltration and the development of subcapsular fibrosis. Infection with Ad-GFP resulted in only acute phase hepatitis but no long-lasting liver damage.

#### 9.1.1 Route of infection

To assess the difference between intra-peritoneal (*i.p.*) and intra venous (*i.v.*) infections CYP2D6 mice were infected with  $1 \times 10^{10}$  particles of Ad-GFP. The livers were removed at day seven post-infection and examined under a fluorescence microscope. After *i.p.* infection with Ad-GFP most GFP expressing cells in the liver were found in subcapsular areas, whereas *i.v.* infection led to GFP expressing cells located within the liver (Figure 5). Since the purpose of our model was to break tolerance to a self-antigen, we were interested in having as many cells expressing the adenoviral delivered proteins as possible. Hence, we decided to choose a combination of *i.p.* and *i.v.* infections for further analysis.

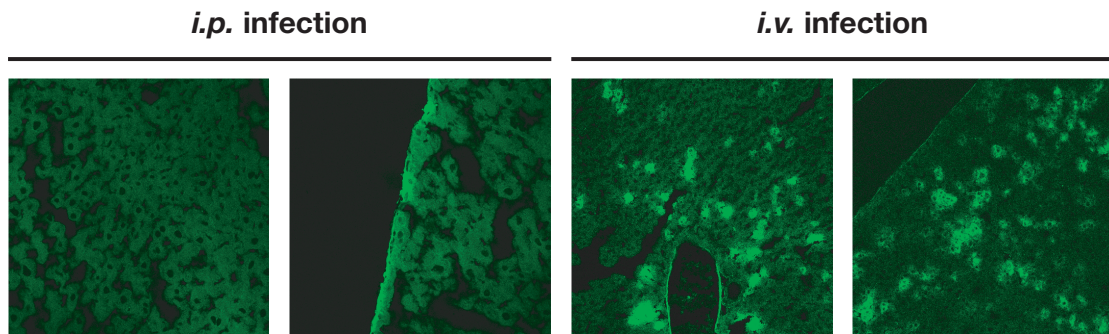


**Figure 5: GFP expression in the liver after different route of Ad-GFP infection**

Expression of GFP in liver sections of CYP2D6 mice at day seven after *i.p.* or *i.v.* infection with Ad-GFP.

### 9.1.2 Protein expression in the liver

To assess the kinetics of protein expression in the liver after adenovirus infection wild-type FVB/N and transgenic CYP2D6 mice were infected with  $2 \times 10^{10}$  particles ( $1 \times 10^{10}$  particles *i.p.* and *i.v.*) of adenovirus expressing GFP. The mice were sacrificed and the liver removed at different days after infection. Examination under a fluorescence microscope revealed GFP-expressing cells in the liver as early as one day after infection. Strongest expression of GFP was detected at day seven post-infection and after 14 days only very few remaining cells still produced low levels of the adenovirus delivered GFP protein (see Figure 6). Similar expression kinetics for GFP were detected in Ad-GFP-infected wild-type FVB/N mice (not depicted).

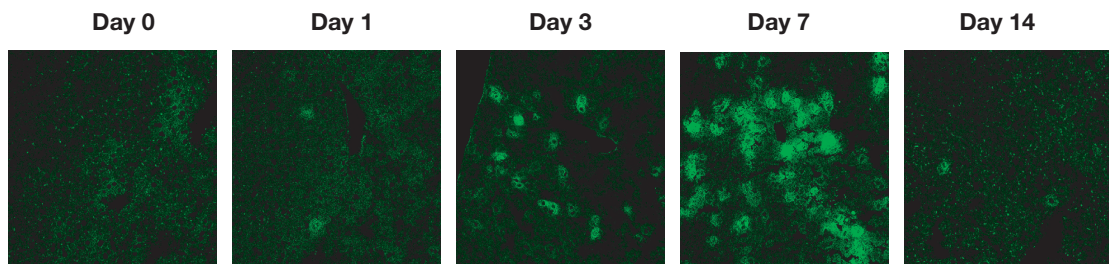


**Figure 6: Expression of GFP after AD-GFP infection**

Expression of GFP in liver sections at several times after infection of CYP2D6 mice with Ad-GFP.

### **9.1.3 Infection of mice with adenovirus results in transient hepatic damage**

In patients, abnormal serum values related to liver damage are often the first clinical signs for ALD. However, abnormal serum values related to liver damage are not exclusive to ALD but can be seen in a wide range of acute and chronic diseases targeting the liver as well as after intake of several drugs. On the other hand, patients with chronic ALD not always show increased serum values. Depending on the enzyme activity measured, it can be distinguished if the disease causing the abnormal values is more related to hepatocyte injury or biliary obstruction. Increased alanine aminotransferase (ALT) and aspartate aminotransferase (AST) activities are more related to hepatocyte injury, whereas increased alkaline phosphatase (AP) and gamma glutamyl transpeptidase (GGT) activities indicate biliary obstruction.

To find out more about the direct effect of adenovirus infection on the liver, FVB/N and CYP2D6 mice were infected with either Ad-GFP or Ad-2D6, serum was collected at time points indicated and serum values related to liver damage were measured (Figure 7). All mice developed transient hepatic damage characterized by an elevation of ALT and AST serum levels. Values reached up to 250 U/liter of serum for ALT and up to 150 U/liter of serum for AST. However, this elevation appeared only transiently from week one to five after infection and serum aminotransferase levels regressed to normal, preinfection levels around week six after Ad-2D6 or Ad-GFP infection (Figure 7 (A)). Mice that have been infected with Ad-2D6 showed a nonsignificant tendency toward an earlier increase in ALT and AST compared to mice infected with Ad-GFP. However, statistical evaluation of the augmentation over time after infection revealed that there was no significant difference between mice that have been infected with Ad-2D6 and Ad-GFP and between FVB/N and CYP2D6 mice. In addition to the hepatic damage marker ALT and AST, we measured AP and GGT in order to see if adenovirus infection caused biliary obstruction in our mice. We found a minor increase in AP at weeks one and two after infection with Ad-2D6 but not with Ad-GFP

and no acute or persistent elevation of GGT levels (Figure 7 (B)). As observed for ALT and AST, the elevation in AP was only transient and no significant increase was found at week four or later, indicating that no persistent biliary obstruction occurred after infection of mice with either Ad-2D6 or Ad-GFP. In summary, these data indicate that adenovirus infection by itself results in acute but transient hepatocellular damage.

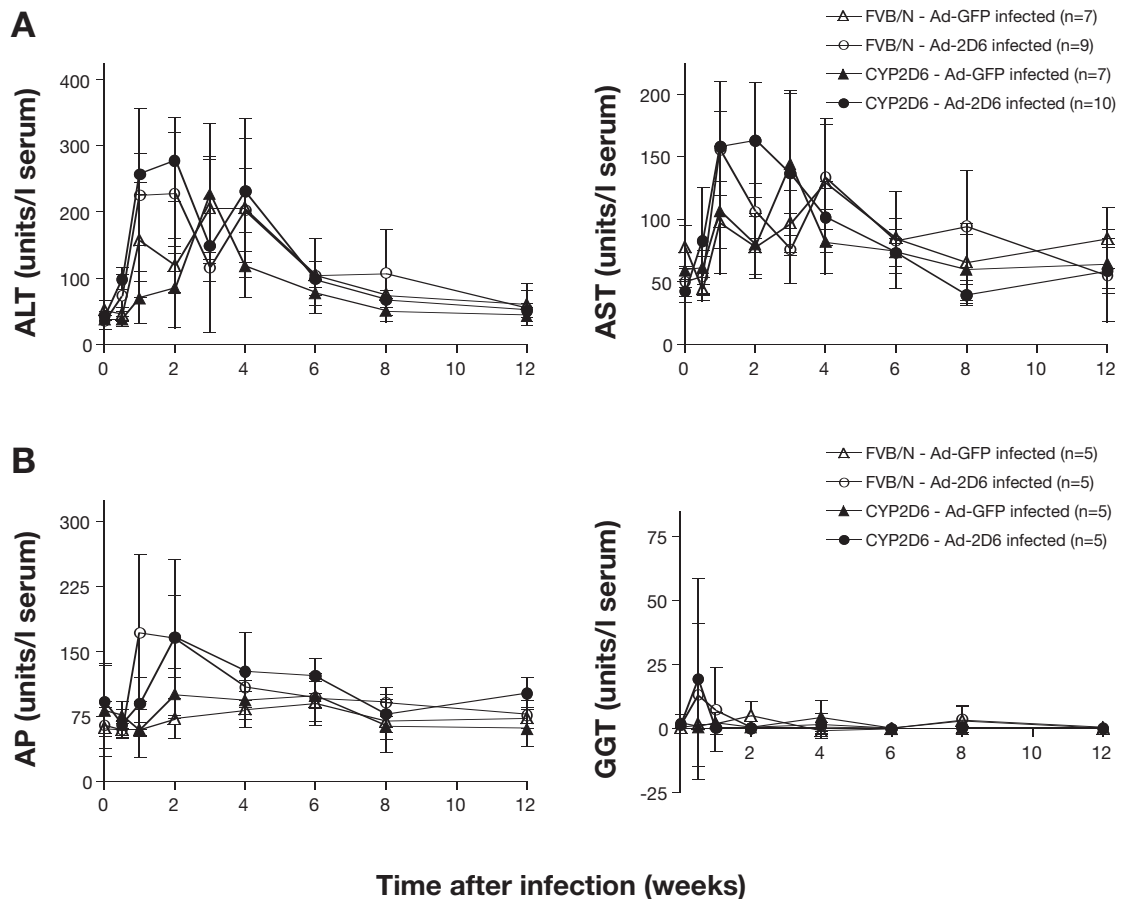


**Figure 7: Serum enzyme activity tests related to liver damage after adenovirus infection**

(A) Serum levels of ALT and AST in wild-type FVB/N (open symbols) and humanized CYP2D6 (closed symbols) mice at time points indicated after infection with Ad-GFP (triangle) or Ad-2D6 (circle). Statistical evaluation (*t* test) revealed no significant differences in AST and ALT augmentation curves over time between Ad-GFP- and Ad-2D6-infected mice and between FVB/N and CYP2D6 mice (*n* = mice per group). (B) Serum levels of AP and GGT in wild-type FVB/N (open symbols) and humanized CYP2D6 (closed symbols) mice infected with Ad-GFP (triangle) or Ad-2D6 (circle) at time points indicated post-infection (*n* = mice per group). Statistical evaluation (*t* test) revealed only at week one and two significant differences in serum AP compared with preinfection levels and between Ad-2D6- and Ad-GFP-infected mice. Data are mean  $\pm$  SD.

## **9.1.4 Infection with Ad-2D6 results in severe and persistent liver damage**

To evaluate if autoimmune-mediated liver damage can be triggered by viral infections, we infected wild-type FVB/N and humanized CYP2D6 mice either with  $2 \times 10^{10}$  particles of Ad-2D6 or with  $2 \times 10^{10}$  particles of Ad-GFP. Mice were sacrificed and livers removed and analyzed at several times after infection. In contrast to the infection of mice with the control virus Ad-GFP, Ad-2D6 infection resulted in severe and long-lasting liver damage characterized by morphological alterations of the liver, massive infiltration and fibrosis.

### **9.1.4.1 Morphological signs of liver damage after Ad-2D6 infection**

Morphologically, livers of Ad-2D6-infected mice showed several features characteristic for liver damage associated with autoimmune-mediated liver disease and/or chronic viral hepatitis that could already be assessed while the liver was removed. The most obvious morphological changes included aberrancies in size and shape of the liver, fusion of the individual liver lobes, hyperplastic nodules and capsular fibrosis. Importantly, these morphological alterations only occurred after Ad-2D6 infection and not after Ad-GFP control virus infection (Figure 8).

To semiquantitatively evaluate the morphological appearance we defined a liver damage score (LDS) based on liver alterations found after adenovirus infections (Table 1). Evaluation of LDS was determined by visual examination of the freshly harvested liver after sacrificing the mice. Pictures of representative livers of LDS 0 (Ad-GFP-infected) and LDS 5 (Ad-2D6-infected) are depicted in Figure 8 (B).

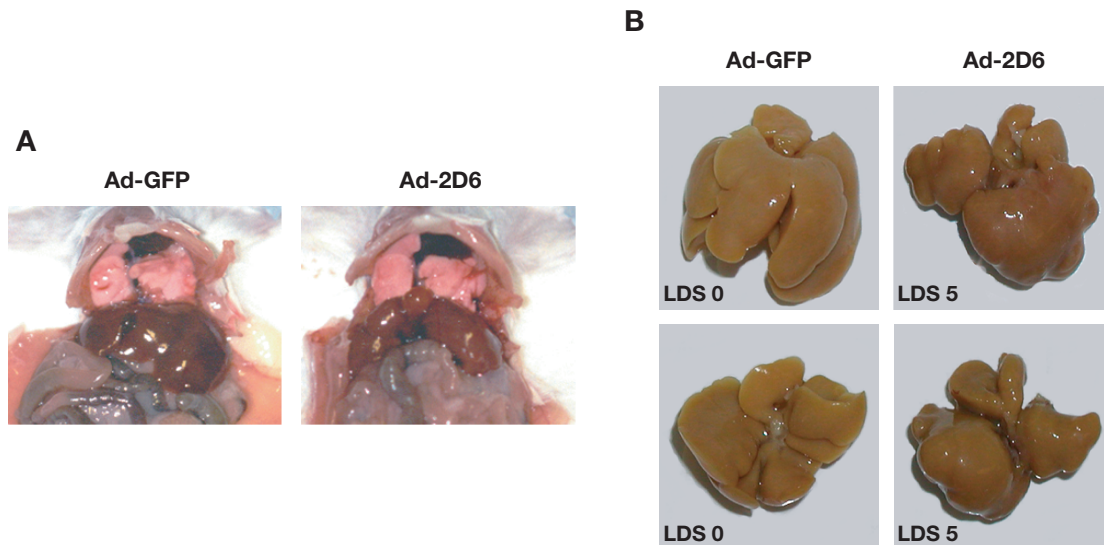


**Figure 8: Morphology of the livers after adenovirus infection**

(A) Exposed livers in the abdomen of CYP2D6 mice infected with either Ad-GFP (left side) or Ad-2D6 (right side) at week eight after infection. (B) Paraformaldehyde-fixed livers of CYP2D6 mice infected with either Ad-GFP (left side) or Ad-2D6 (right side) at week eight after infection. Livers are either shown from the anterior side (upper panel) or the visceral side (lower panel). The Liver damage score for these representative livers are shown as LDS 0 (Ad-GFP-infected liver) and LDS 5 (Ad-2D6-infected liver).

<b>Liver damage score (LDS)</b>	<b>Fused liver lobes</b>	<b>Size/shape</b>	<b>Cirrhosis</b>	<b>Hyperplastic nodules</b>	<b>Capsular fibrosis</b>
0	No	Regular	No	No	No
1	Partial	Regular	No	No	No
2	Partial	Swollen	No	No	No
3	Complete	Swollen	Starting	Some	Visible
4	Complete	Clump	Strong	Many	Visible
5	Complete	Clump	Strong	Many	Strong

**Table 1: LDS definition to assess morphological liver alterations by visual examination**

LDS was used to determine the morphological liver alterations of FVB/N and CYP2D6 mice infected with either Ad-GFP or Ad-2D6 over a time period of 45 weeks (Figure 9). Importantly, LDS was persistently elevated in both FVB/N and CYP2D6 mice after infection with Ad-2D6 only and almost no

morphological signs of liver damage were detected in mice infected with Ad-GFP. Statistical evaluation revealed that the LDS was significantly different between Ad-2D6- and Ad-GFP-infected FVB/N as well as CYP2D6 mice.

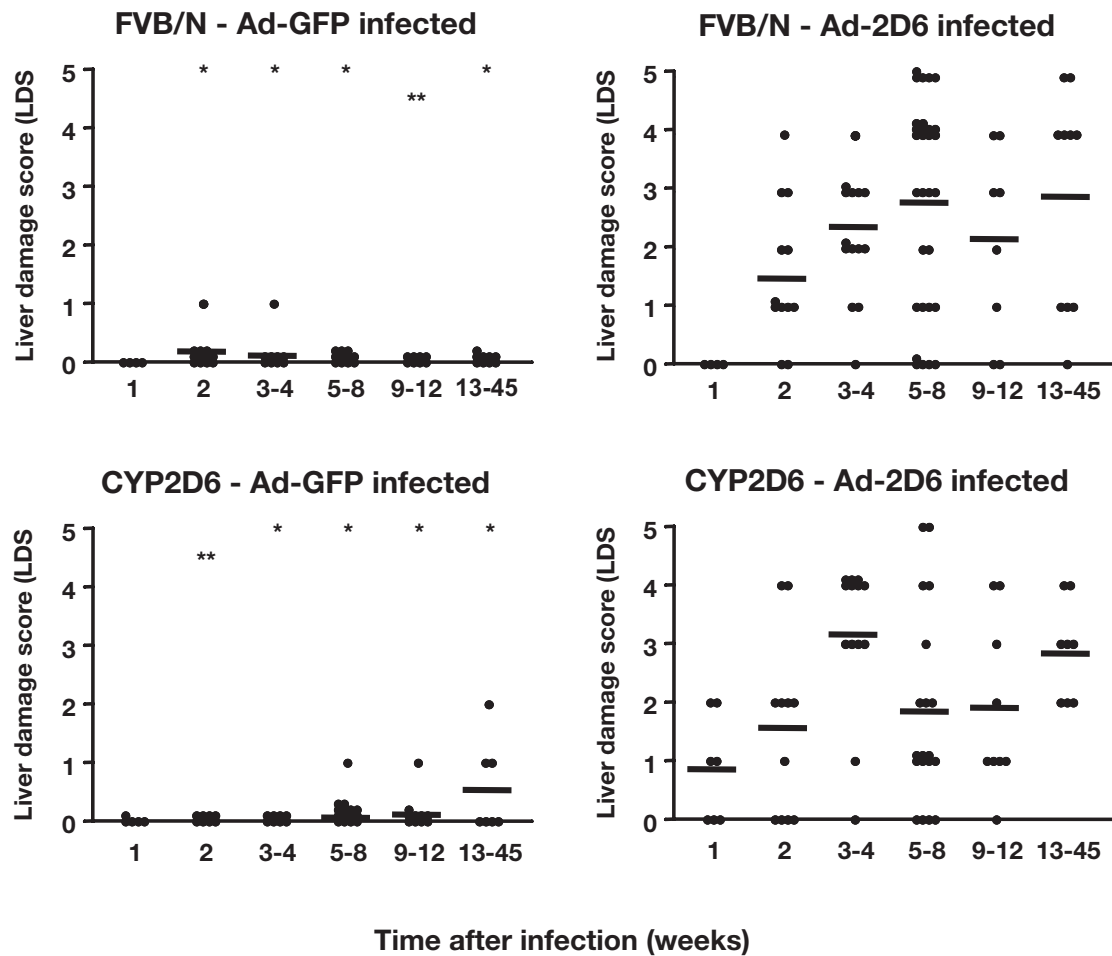


**Figure 9: LDS at several time points after infection with adenovirus**

Livers of FVB/N (upper panel) and CYP2D6 (lower panel) mice were harvested at time points indicated after infection with either Ad-GFP (left side) or Ad-2D6 (right side) and LDS was determined by morphological examination. The mean LDS for each group is indicated by horizontal lines. Statistical analysis (Mann-Whitney test) revealed significant differences between Ad-2D6- and Ad-GFP-infected mice at the indicated time points: \* = P < 0.01; \*\* = P < 0.05.

Interestingly, >50% of wild-type FVB/N mice showed the first morphological signs of liver damage already one week after infection with Ad-2D6 whereas in transgenic CYP2D6 mice obvious signs of liver damage was first detectable after two weeks of infection with Ad-2D6. However, no significant difference in the overall LDS between wild-type and transgenic mice was detected at later times. These data demonstrate that the viral expression of

CYP2D6 resulted in persistent liver damage although only a transient elevation of serum markers related to liver damage could be found after adenovirus infection of FVB/N and CYP2D6 mice.

#### **9.1.4.2 Ad-2D6-infected mice show massive infiltration**

An important diagnostic feature in human ALD is histological examinations of liver biopsies. To evaluate the infiltrations after adenovirus infection, FVB/N and CYP2D6 mouse livers were harvested at various time points after infection with Ad-GFP or Ad-2D6 and liver sections were stained for histological analysis. An early inflammatory phenotype was seen in FVB/N and CYP2D6 mice after infection with both, Ad-GFP and Ad-2D6 virus (Figure 10 (top row)). However, this initial acute hepatitis was only transient and likely caused by the direct antiviral immune response. Importantly, only infection with Ad-2D6, but not Ad-GFP, resulted in a massive increase in inflammation and liver cell destruction in both FVB/N and CYP2D6 mice at later time points after infection. Already at week four after infection Ad-GFP-infected mice showed a reduced amount of cellular infiltrates compared to Ad-2D6-infected mice and no focal necrosis, whereas in Ad-2D6-infected mice the areas of focal necrosis and cellular infiltrations were becoming larger and increased in numbers (Figure 10 (middle row)). After eight weeks FVB/N and CYP2D6 mice infected with Ad-GFP showed nearly no focal points of lymphocyte accumulation and only some scattered lymphocytes were still detectable. Mice infected with Ad-2D6 however, showed a massive increase in inflammation and liver cell destruction. Interface hepatitis with extensive infiltrates in the periportal and parenchymal regions could be detected and the areas of focal necrosis were growing larger and confluent (Figure 10 (bottom row)).

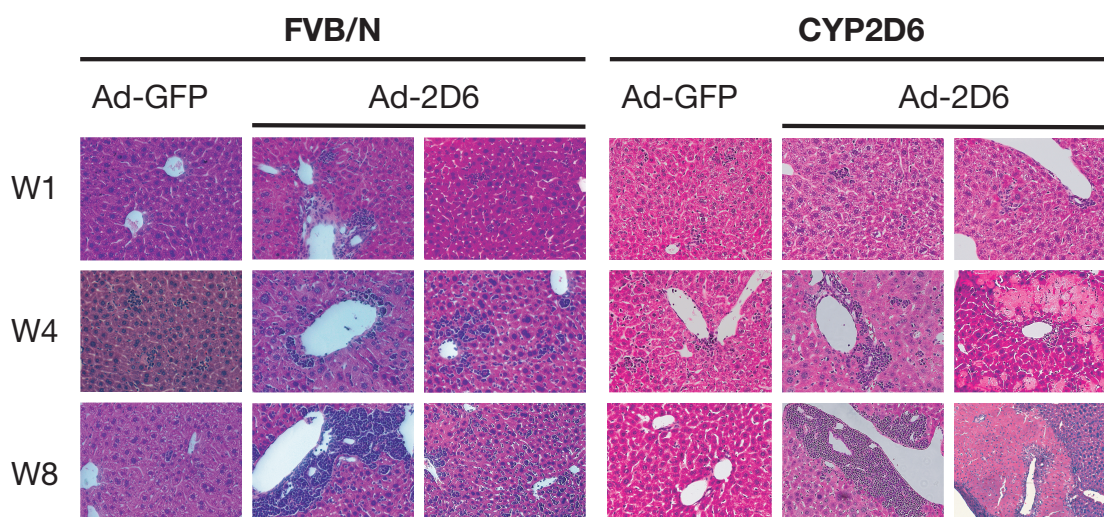


**Figure 10: Hepatic necrosis and massive cellular infiltrations after Ad-2D6 infection**

Hematoxylin and eosin staining of liver sections obtained from FVB/N (left side) and CYP2D6 (right side) mice one, four and eight weeks after infection with Ad-GFP or Ad-2D6.

Similar to the LDS we defined a histological infiltration score (HIS) based on liver infiltrations found after adenovirus infections to semiquantitatively evaluate the infiltration in our mice (Table 2). Evaluation of HIS was determined by blinded analysis of complete liver sections obtained from mice infected with either Ad-GFP or Ad-2D6.

<b>Histological infiltration score (HIS)</b>	<b>Description of found infiltration</b>
0	No visible infiltration
1	Few focal infiltrates
2	Numerous scattered focal infiltrates
3	Few large clusters of infiltrating cells (perivascular or subcapsular)
4	Numerous large clusters of infiltrating cells occupying >50% of portal tracts or central veins
5	Confluent periportal infiltrates

**Table 2: HIS for blinded evaluation of infiltrations in mouse livers after adenovirus infection**

HIS was used to determine liver infiltrations of FVB/N and CYP2D6 mice infected with either Ad-GFP or Ad-2D6 at week one, four and eight post-infection (Figure 11). Importantly, persistently high HIS in FVB/N and CYP2D6 mice was only detected after Ad-2D6 infection, whereas the acute elevated HIS one week after Ad-GFP infection reverted to almost pre-infection scores after eight weeks of infection. Interestingly, in FVB/N mice, a significant difference in HIS after Ad-GFP and Ad-2D6 infection was already detectable from week four after infection, suggesting an accelerated liver damage in wild-type FVB/N mice compared to humanized CYP2D6 mice.

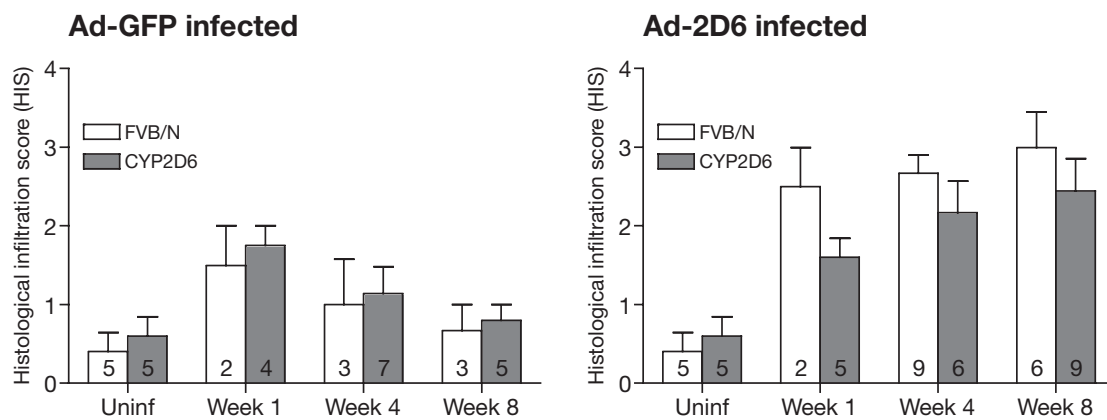


**Figure 11: HIS at several time points after infection with adenovirus**

Liver sections of FVB/N (open bars) and CYP2D6 (filled bars) mice infected with Ad-GFP (left side) or Ad-2D6 (right side) were analyzed in a blinded fashion at time points indicated using HIS. The presented data are mean HIS  $\pm$  SEM. Statistical analysis (Mann-Whitney test) revealed significant differences between mice infected with Ad-GFP and Ad-2D6 at the indicated times after infection: \* =  $P < 0.05$ . The number of individual mouse livers analyzed per experimental group is indicated at the bottom of each bar.

To determine what cell types are infiltrating the livers of FVB/N and CYP2D6 mice after Ad-2D6 infection immunohistochemical analysis of liver sections obtained from mice two weeks after Ad-2D6 infection were performed (Figure 12). Cellular infiltrates consisted predominantly of B cells (B220<sup>+</sup> cells), CD4<sup>+</sup> T cells and macrophages (F4/80<sup>+</sup> cells) whereas only a few CD8<sup>+</sup> T cells were found. In keeping with our initial observation that wild-type FVB/N mice showed higher HIS compared to humanized CYP2D6 mice four weeks after Ad-2D6 infection (Figure 11), we found that FVB/N had more rapid cellular infiltration compared to CYP2D6 mice. Liver sections of Ad-2D6-infected

FVB/N mice two weeks post-infection showed already cellular infiltrations similar to liver sections of CYP2D6 mice four and eight weeks after Ad-2D6 infection, whereas liver sections of Ad-2D6-infected CYP2D6 mice two weeks after infection showed only minor infiltrates.

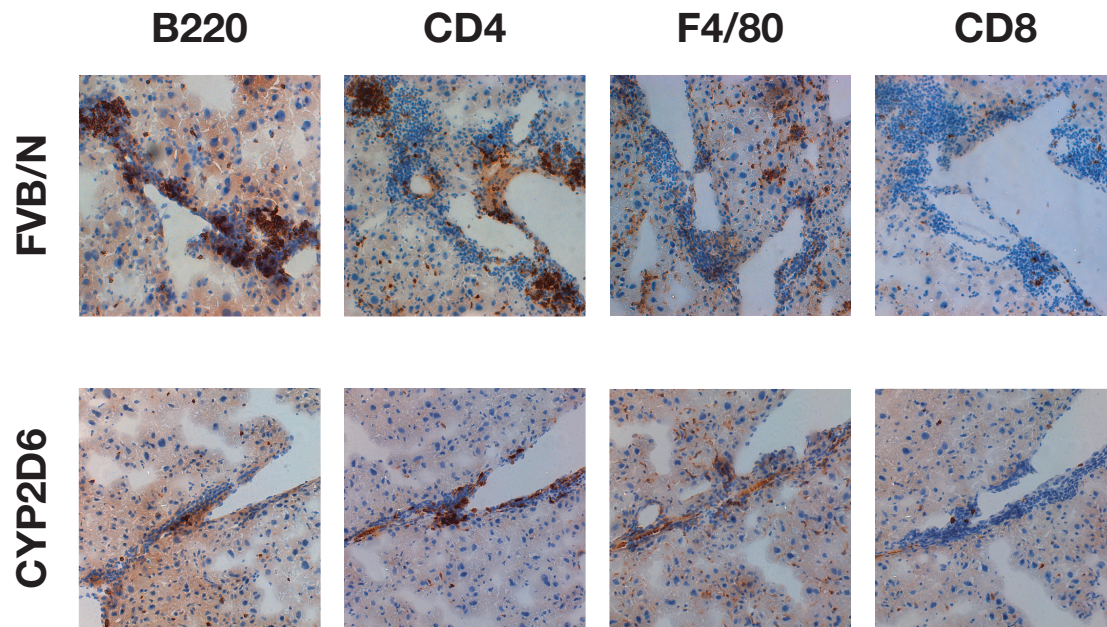


**Figure 12: Immunohistochemical analysis of liver sections after infection with Ad-2D6**

Liver sections obtained from FVB/N (upper panel) and CYP2D6 (lower panel) two weeks after Ad-2D6 infection stained for B cells (B220), CD4<sup>+</sup> T cells (CD4), macrophages (F4/80) and CD8<sup>+</sup> T cells (CD8).

#### **9.1.4.3 Ad-2D6-infected mice show development of subcapsular fibrosis**

Extensive and long-lasting liver damage as in human ALD or chronic hepatitis in general leads to the development of fibrosis and often to progression from fibrosis to cirrhosis, a more severe and mostly irreversible form of fibrosis in the liver. Fibrosis is characterized by an increase in extracellular matrix protein production and a shift to collagen I as major component of it. To evaluate liver fibrosis after adenovirus infection, FVB/N and CYP2D6 mice were infected with Ad-GFP or Ad-2D6 and liver sections obtained at various time points after infection were stained for collagen fibers by Sirius red or fluorescence immunohistochemistry staining for collagen I (Figure 13). Tissue sections covering the entire liver from FVB/N and CYP2D6 mice after Ad-

GFP and Ad-2D6 infection were analyzed by Sirius red staining at several time points after infection (Figure 13 (A)). Importantly, an increase in subcapsular liver fibrosis over time was detected exclusively after Ad-2D6 infection in FVB/N and CYP2D6 mice, whereas no difference in collagen I deposition over time could be found after Ad-GFP control virus infection. Interestingly, the development of subcapsular fibrosis was accelerated and more pronounced in wild-type FVB/N mice compared to transgenic CYP2D6 mice supporting our previous findings of an accelerated liver damage in wild-type FVB/N mice. For a better visualization of the predominantly subcapsular and interlobular fibrosis, we performed a reconstruction of a liver section stained by fluorescence immunohistochemistry for collagen I covering the entire liver of a representative CYP2D6 mouse eight weeks after infection with Ad-2D6 (Figure 13 (B) (left side)). The figure shows the massive subcapsular fibrosis and the interlobular collagen I deposits that glue the individual lobes (including the left and right medial as well as the left lateral lobes) together. Confirming our results obtained by Sirius red staining no significant collagen I deposits were found in Ad-GFP-infected mice. Costaining for B cells (B220<sup>+</sup> cells) showed that many cellular infiltrates are located in close proximity to the subcapsular collagen I deposits (Figure 13 (B) (right side)). In summary, these data indicate that infection with Ad-2D6 but not with Ad-GFP can induce a persistent liver damage in both, the wild-type FVB/N as well as the humanized CYP2D6 mice. Additionally, the findings that wild-type FVB/N mice showed accelerated liver damage, more rapid cellular infiltration and an accelerated and more pronounced development of subcapsular fibrosis than humanized CYP2D6 mice indicates the existence of partial tolerance in CYP2D6 mice.

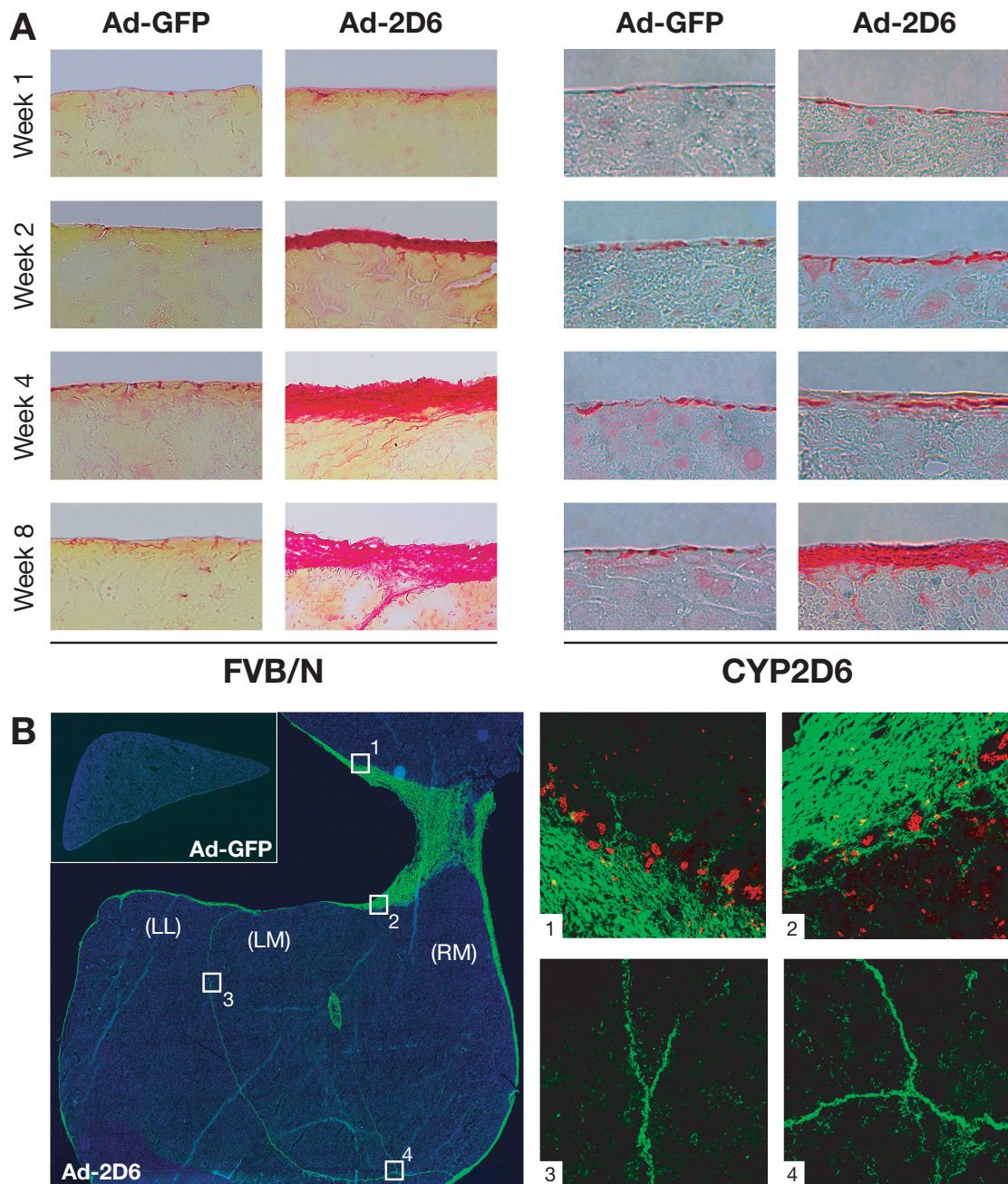


**Figure 13: Subcapsular fibrosis after infection of mice with Ad-2D6 but not Ad-GFP**

(A) Sirius red staining of collagen fibers in the subcapsular region of the liver of FVB/N (left side) and CYP2D6 (right side) mice at time points indicated after Ad-GFP or Ad-2D6 infection. Tissue sections covering the entire liver from three to five mice per experimental group were analyzed and a representative picture of the subcapsular region is displayed for each time point. (B) Reconstruction of a large section of a CYP2D6 mouse liver eight weeks after infection with Ad-2D6 including the left medial (LM) and right medial (RM) lobes and the left lateral (LL) lobe, stained for collagen I (green) by fluorescence immunohistochemistry. (Inset) Reconstruction of the left lateral lobe of a CYP2D6 mouse liver eight weeks after infection with Ad-GFP. Regions 1 – 4 are shown at a higher magnification. In addition to staining for collagen I (green), staining for B cells (B220<sup>+</sup>, red) was overlaid. Region 1 and 2 show B cells entrapped in pockets within the collagen I deposits in the subcapsular region of the liver. Region 3 and 4 show areas where two or three individual liver lobes are joined by collagen I fibers.

## **9.2 Pathogenic mechanism in the CYP2D6 mouse model for autoimmune hepatitis**

Since we could show that virally delivered CYP2D6 protein can induce long-lasting liver damage characterized by persistent hepatic infiltrates and necrosis as well as the development of subcapsular fibrosis in wild-type FVB/N and humanized CYP2D6 mice, we were interested on the immunological mechanisms responsible for the observed liver damage. Because infection with a control virus (Ad-GFP) resulted in only transient hepatitis but no long-lasting liver damage, we could assume that the virally delivered human CYP2D6 protein was responsible for the persistent liver damage found in our mice and that this damage was likely to be autoimmune-mediated. However, in order to prove that the persistent liver damage found in our mice was autoimmune-mediated we intended to demonstrate breaking of tolerance to liver-specific self-antigens by Ad-2D6 infection. Since the hallmark of human AIH type 2 are LKM-1 autoantibodies targeting the CYP2D6 protein we first investigated if the B cell tolerance in our mice is broken after Ad-2D6 infection. Infection with Ad-2D6 but not with Ad-GFP resulted in breaking of B cell tolerance and generation of LKM-1 like antibodies in wild-type FVB/N as well as humanized CYP2D6 mice. In addition, viral infection was essential for persistent liver damage but not for breaking of B cell tolerance and autoantibody production. Lastly, infection with Ad-2D6 but not with Ad-GFP resulted in breaking of T cell tolerance and CYP2D6-specific IFN- $\gamma$  production from CD4<sup>+</sup> and CD8<sup>+</sup> T cells.

### **9.2.1 B cell tolerance to liver-specific self antigen is broken after Ad-2D6 infection**

Breaking of B cell tolerance leads to activation and differentiation of self-reactive B cells that then will produce and secrete autoantibodies specific for the self-antigen. In order to investigate if Ad-2D6 infection leads to a loss of B cell tolerance and production of autoantibodies in wild-type FVB/N and humanized CYP2D6 mice we collected serum of Ad-GFP- or Ad-2D6-

infected mice at various times after infection and determined the serum titer of anti-human CYP2D6 antibodies by ELISA. Anti-CYP2D6 antibodies of the IgM isotype were found to a similar extent in FVB/N and CYP2D6 mice after infection with Ad-2D6 and reached a maximum titer of 500-900 between weeks two and four after infection. No detectable anti-CYP2D6 IgM antibodies could be found after Ad-GFP infection in FVB/N or CYP2D6 mice (Figure 14 (left side)). Importantly, anti-CYP2D6 IgG antibodies could be detected at high titers in FVB/N and CYP2D6 mice after Ad-2D6 infection. In contrast, only very low titers of CYP2D6-specific IgG antibodies could be detected after Ad-GFP infection (Figure 14 (right side)). Interestingly, anti-CYP2D6 IgG antibodies reached higher titers in Ad-2D6-infected wild-type FVB/N mice than in humanized CYP2D6 mice.

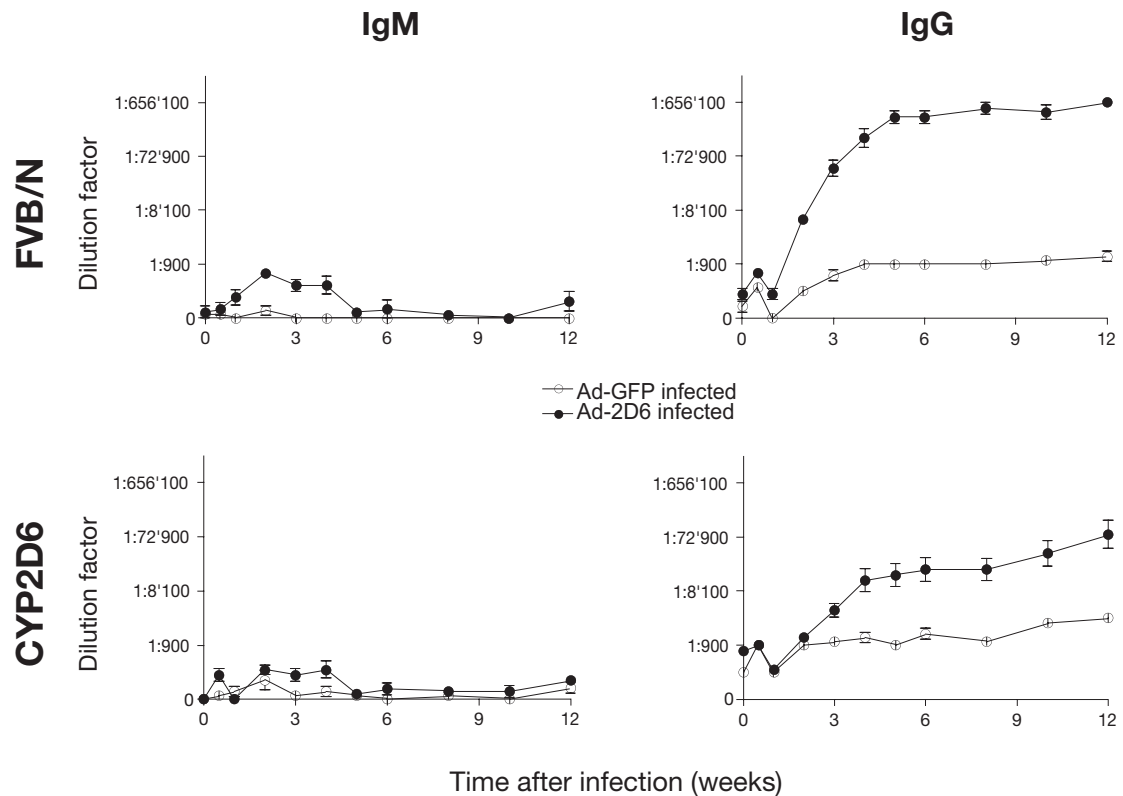


**Figure 14: Generation of anti-CYP2D6-specific antibodies after Ad-2D6 infection**

Serum titers of IgM (left side) and IgG (right side) anti-CYP2D6 antibodies in FVB/N (upper panel) and CYP2D6 (lower panel) mice at time points indicated after Ad-GFP (open symbols) or Ad-2D6 (closed symbols) infection. Sera dilutions with values of three standard deviations above the mean value of negative controls were considered positive. Data are mean  $\pm$  SEM.

Anti-CYP2D6 antibodies of the IgE isotype have not been detected after infection with Ad-GFP or Ad-2D6 in both FVB/N and CYP2D6 mice (not depicted).

The anti-CYP2D6-specific antibody titer detected after Ad-2D6 infection could either be produced by very potent antibody producing plasmacells or by a large number of CYP2D6-specific B cells. To investigate how many B cells produced the anti-CYP2D6-specific antibodies and analyze if there was a polyclonal activation of antibody producing plasmacells after Ad-GFP or Ad-2D6 infection in general, FVB/N and CYP2D6 mice were infected and spleens were removed at various time points after infection. Splenocytes were then used to determine the number of total Ig and anti-CYP2D6 antibody producing plasmacells in a B cell ELISPOT assay (Figure 15 (A)). Analysis of the ELISPOT data revealed no striking differences in the frequency of Ig-producing cells of FVB/N or CYP2D6 mice infected either with Ad-GFP or Ad-2D6 (Figure 15 (B) (upper panel)). Importantly, B cells secreting anti-CYP2D6-specific antibodies were exclusively found in Ad-2D6-infected mice (Figure 15 (B) (lower panel)). The highest frequency of anti-CYP2D6-specific antibody-secreting cells was found at week four after infection in both FVB/N and CYP2D6 mice, whereas wild-type mice showed a higher number of anti-CYP2D6-specific antibody-secreting cells than CYP2D6 mice. These data confirm our previous finding that humanized CYP2D6 mice did not reach as high anti-CYP2D6 IgG antibody titers as FVB/N mice. In addition, it further supports our previous findings indicating the existence of partial tolerance to human CYP2D6 in humanized CYP2D6 mice, which is characterized by attenuated hepatocellular damage, less rapid cellular infiltration and less severe fibrosis when compared with less tolerant wild-type FVB/N mice

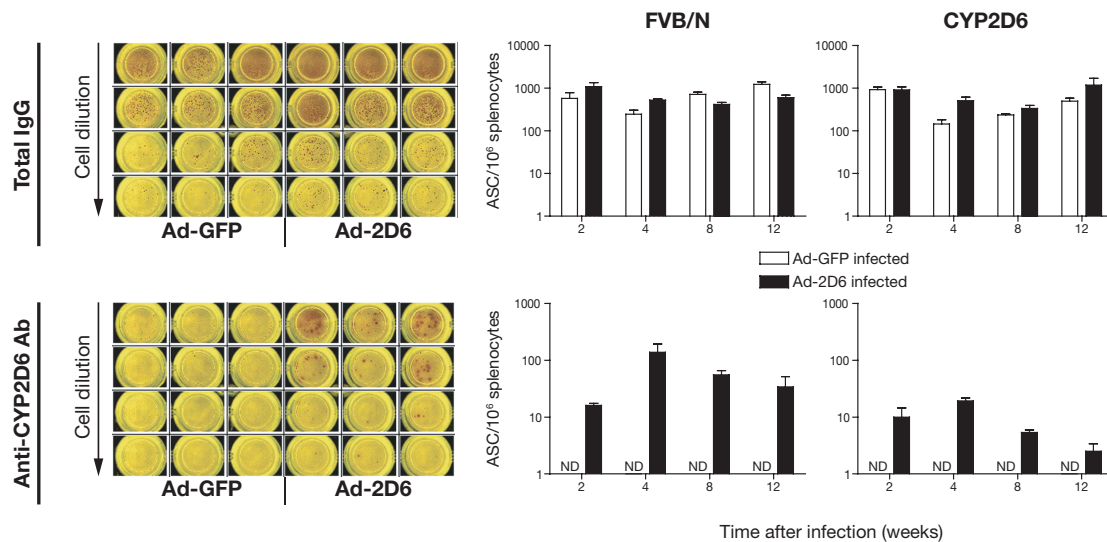


**Figure 15: Activation of CYP2D6-specific B cells after Ad-2D6 infection**

(A) Picture of representative end-results of total IgG (upper panel) or CYP2D6-specific (lower panel) spot-forming assays. Brownish spots indicate the reaction of enzyme-labeled secondary antibodies against secreted IgG and represent one antibody-secreting cell. (B) Quantification of total IgG (upper panel) and CYP2D6-specific IgG (lower panel) secreting cells per  $10^6$  splenocytes in FVB/N (left) and CYP2D6 (right) mice at time points indicated after infection with Ad-GFP (open bars) or Ad-2D6 (closed bars). ND = not detectable.

One of the most reliable diagnostic tests for the characterization of ALD in humans is the characterization of non-organ-specific autoantibodies in human patients. This characterization is usually performed by indirect immunofluorescence staining of autoantibodies on rat tissue sections. Therefore we compared the staining pattern of anti-CYP2D6 antibodies found in the sera of mice after Ad-2D6 infection with the staining pattern of sera from patients with various autoimmune liver diseases on rat liver sections (Figure 16). Sera from Ad-2D6-infected mice recognized a typical microsomal (ER/Golgi) pattern, characteristic for LKM-1 type autoantibodies present in sera from AIH type 2 patients. In contrast, sera from PBC or AIH type 1 patients showed a clearly distinguishable mitochondrial or nuclear staining pattern typical for AMA autoantibodies found in PBC or ANA autoantibodies found in type 1 AIH patients.

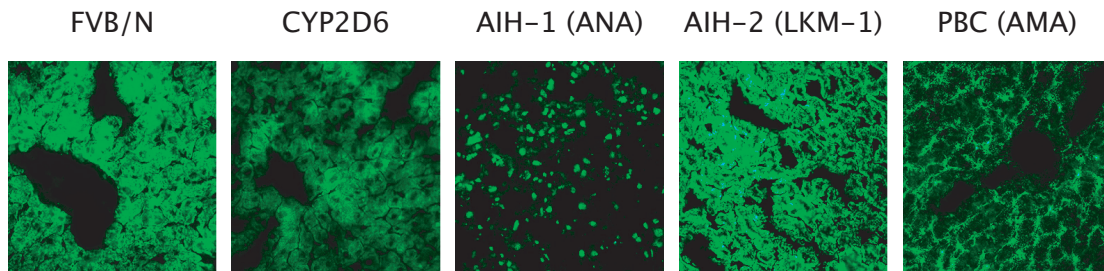


**Figure 16: Staining pattern of anti-CYP2D6 antibodies after Ad-2D6 infection**

Representative pictures of rat liver sections stained with sera from Ad-2D6-infected FVB/N and CYP2D6 mice, AIH type 1, AIH type 2 and PBC patients followed by appropriate staining with a fluorescence-conjugated secondary antibody.

In summary, we could show that infection with Ad-2D6 resulted in a loss of B cell tolerance to the virally delivered self-protein CYP2D6 and that Ad-2D6-infected FVB/N as well as CYP2D6 mice produced LKM-1 like antibodies. In addition, we could confirm our previous results that indicated a partial tolerance in humanized CYP2D6 resulting in a lower number anti-CYP2D6-specific antibody-secreting cells and lower anti-CYP2D6 IgG antibody titers compared to wild-type FVB/N mice.

### **9.2.2 Anti-CYP2D6 antibodies in Ad-2D6-infected mice and sera from AIH-2 patients recognize an identical immunodominant epitope**

LKM-1 autoantibodies are the hallmark of AIH type 2. It could be shown that such autoantibodies recognize an immunodominant epitope of CYP2D6 in most patients with AIH type 2. To further analyze the antibodies found in Ad-2D6-infected mice we mapped the dominant B cell epitopes using the SPOTs technology. To this end, staggered peptides covering the entire human CYP2D6 sequence were covalently linked to a nylon membrane. The SPOTs membranes have been incubated with sera obtained from Ad-2D6-infected mice overnight and reactivity was visualized by the incubation with enzyme-labeled secondary antibodies against mouse IgG (Figure 17 (A)). Linear epitopes reacting with the sera were clearly visible and could easily be quantified. To compare the recognized B cell epitopes of Ad-2D6-infected mice, AIH type 1 and AIH type 2 patients the serum reactivity profile to

SPOTs peptides was quantified and illustrated in a consecutive way (Figure 17 (B) and (C)). Interestingly, sera from all Ad-2D6-infected FVB/N and CYP2D6 mice predominantly reacted to a cluster of overlapping peptides within the core amino acid (aa) sequence WDPAQPPRD (CYP2D6 aa 262-270). It has been shown that LKM-1 autoantibodies of AIH-2 patients predominantly recognize the immunodominant linear CYP2D6<sub>254-271</sub> sequence and indeed, all of the AIH-2 patient sera we tested reacted to the same core aa sequence as the sera of Ad-2D6-infected mice. In contrast, sera from patients with other ALD, like AIH type 1 or PBC, did not recognize the immunodominant CYP2D6 B cell epitope. As for AIH-2 patients other epitopes were recognized by the sera of Ad-2D6-infected mice, however, to a much lesser extent and with some variation between individual mice. We found that the pattern of epitope recognition was mostly overlapping between sera from Ad-2D6-infected mice and patients with AIH type 2, but not with the sera of patients with other ALD. In summary, we found that the Ad-2D6-induced breakdown of B cell tolerance to human CYP2D6 in wild-type FVB/N and humanized CYP2D6 mice resulted in an autoimmune reactivity that is very similar to that found in AIH type 2 patients. In addition, we could demonstrate that the autoimmune reactivity after Ad-2D6 infection is characterized by the presence of autoantibodies recognizing an immunodominant epitope identical to that recognized by sera from patients with type 2 AIH.

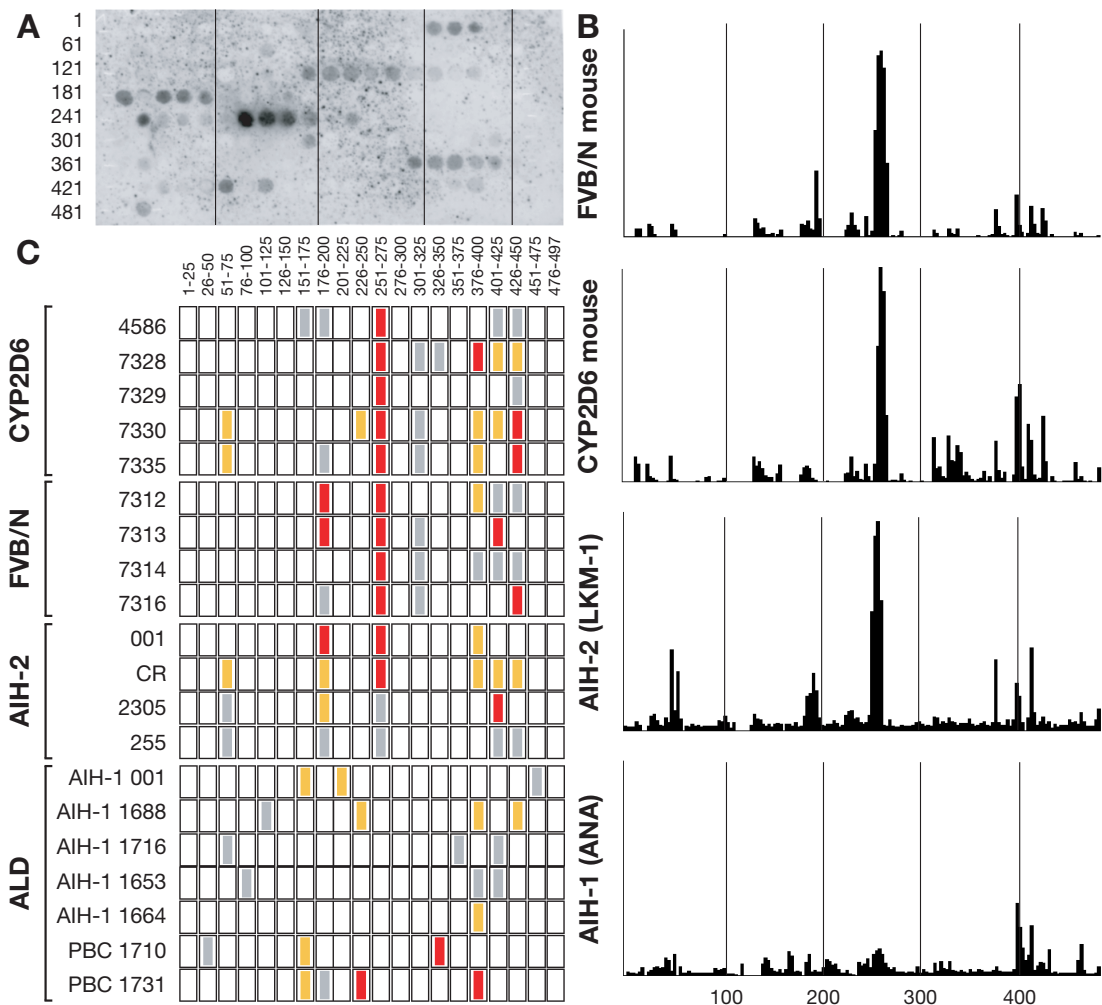


**Figure 17: Mouse anti-CYP2D6 and sera of AIH-2 patients recognize the identical immunodominant CYP2D6 epitope**

(A) SPOTs membrane containing staggered peptides of 12 aa in length covering the entire 497 aa of the human CYP2D6 molecule. This representing membrane was developed with serum of an Ad-2D6-infected CYP2D6 mouse. Numbers indicate the position within the CYP2D6 sequence of the first aa of the first peptide spot in each horizontal lane. (B) Quantification of the serum reactivity profile to SPOTs peptides. Representative quantification of serum samples of an Ad-2D6-infected FVB/N mouse, an Ad-2D6-infected CYP2D6 mouse, an AIH-2 patient and an AIH-1 patient are depicted. Numbers indicate the aa position within the human CYP2D6 sequence. (C) For an overview of the epitope profile, the human CYP2D6 sequence was divided into 20 25-aa long sections, as indicated at the top of each column. Signal intensities of sera from Ad-2D6-infected CYP2D6 and FVB/N mice, patients with AIH-2, and patients with other ALD such as AIH-1 or PBC are indicated in red (strong), orange (medium), gray (low) and white (no reactivity).

### 9.2.3 Virus infection is essential for persistent liver damage but not autoantibody production

To analyze the importance of viral delivery of the human CYP2D6 to the liver and the resulting acute inflammation mice were infected with Ad-2D6 or immunized with human recombinant CYP2D6 alone or in combination with Poly-IC (*i.v.*), CpG (*i.v.*), IFA (*s.c.*) or CFA (*s.c.*). Anti-CYP2D6 antibody titers as well as LDS as marker for persistent liver damage were analyzed. Interestingly, although all immunization strategies resulted in low anti-CYP2D6 antibody titers (Figure 18) only mice infected with Ad-2D6 showed persistent liver damage reflected by increased LDS at 12 weeks after infection.

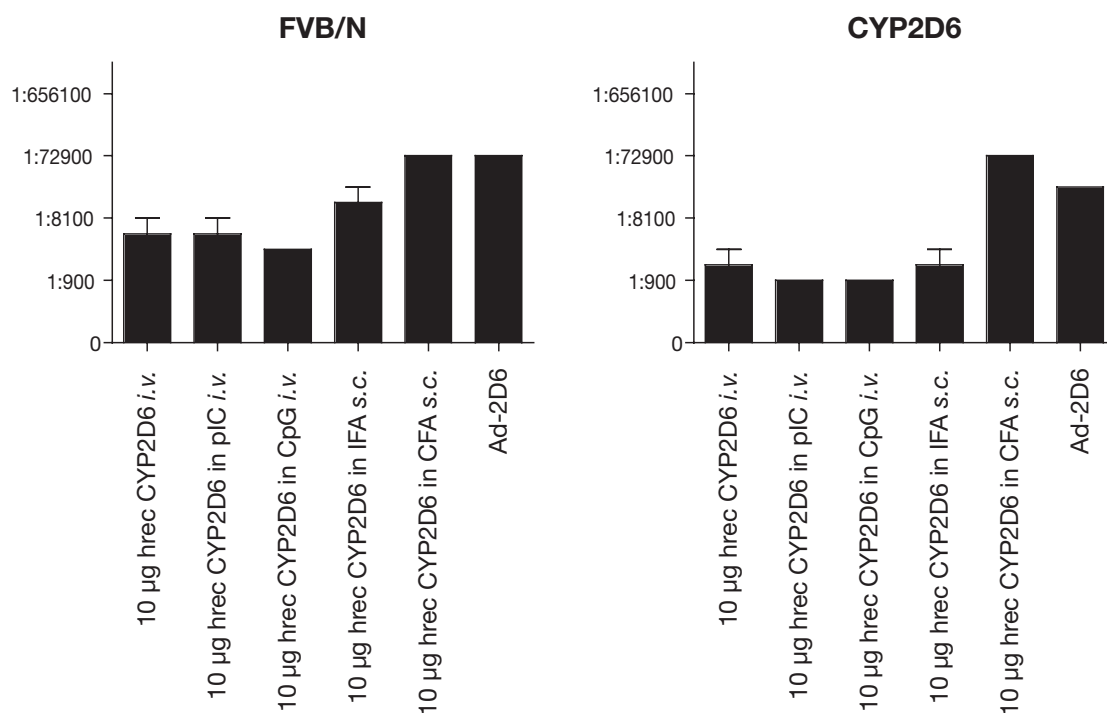


**Figure 18: Antibody titer after different immunization strategies**

Serum titers of IgG anti-CYP2D6 antibodies in FVB/N (left side) and CYP2D6 (right side) mice at 12 weeks post-treatment with 10 µg human recombinant CYP2D6 (hrec CYP2D6) alone, in combination with pIC, CpG, IFA or CFA or 12 weeks post-infection with Ad-2D6. Sera dilutions with values of three standard deviations above the mean value of negative controls were considered positive. Data are mean ± SEM. *i.v.* = *intra venous*; *s.c.* = *sub cutan*

In particular, immunization with recombinant human CYP2D6 in combination with CFA (*s.c.*) resulted in a antibody titer similar to that found after Ad-2D6

infection but did not result in autoimmune liver disease. These data indicate that the generation of anti-CYP2D6 antibodies alone is not sufficient to induce autoimmune liver damage in our mice. In addition, these data underline the importance of the liver-tropic viral infection in initiating autoimmune-mediated liver damage in our mouse model and suggest an important role for environmental factors like viral inflammation as trigger mechanism for autoimmunity.

#### **9.2.4 T cell tolerance to liver-specific self antigen is broken after Ad-2D6 infection**

Since we could show that infection of FVB/N and CYP2D6 mice with Ad-2D6 leads to a loss of B cell tolerance as well as the production of anti-CYP2D6 antibodies of the IgG isotype and antibody class switching requires specific CD4<sup>+</sup> T cell help we could assume that the T cell tolerance in our mice had to be broken as well. Breaking of T cell tolerance leads to activation and differentiation of self-reactive T cells. Upon activation T cells produce and release cytokines and chemokines that attract and activate other immune cells and lead to differentiation and immunoglobulin class switch of activated B cells. Most importantly, they have direct pathogenic functions depending on the cytokines released and on the T cell subset activated. Through collaboration with D. Bogdanos we received 61 20-aa long peptides overlapping by 12 aa and spanning the entire human CYP2D6 sequence (63) (see chapter Appendix, Figure 25). These peptides have been previously used to demonstrate that MHC class I as well as MHC class II restricted T cell responses influence autoimmunity in AIH type 2 patients. We used those 61 20mer peptides to analyze if the T cell tolerance to the liver-specific CYP2D6 self antigen was broken in FVB/N mice after infection with Ad-GFP or Ad-2D6 by staining for intracellular cytokines (ICCS) produced by T cell subsets after *ex vivo* stimulation with those peptides. Therefore, FVB/N mice were infected with Ad-GFP or Ad-2D6 and splenocytes as well as liver lymphocytes were isolated and stained for surface marker to distinguish between the T cell subsets as well as for intracellular IFN- $\gamma$  production to

analyze the activation status after overnight incubation with a pool of five 20mer peptides. IFN- $\gamma$  production was measured by FACS analysis (Figure 19). Only one peptide pool (peptides six to ten) was able to induce IFN- $\gamma$  production in CD4<sup>+</sup> T cells whereas CD8<sup>+</sup> T cells were found to produce IFN- $\gamma$  after stimulation with several peptide pools spanning the peptides 16 to 30 of the human CYP2D6. Importantly, IFN- $\gamma$  producing T cells were only found after Ad-2D6 infection, but not after Ad-GFP infection.

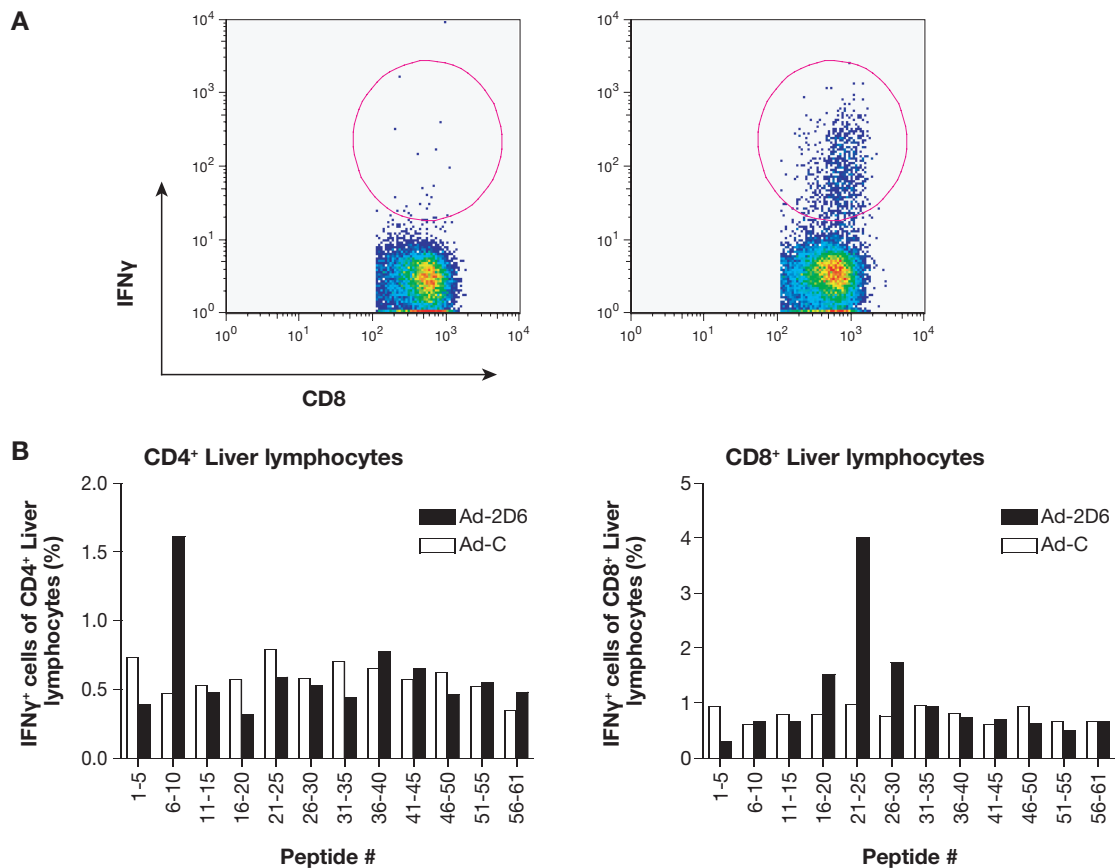


**Figure 19: Intracellular IFN- $\gamma$  staining after peptide pool stimulation in FVB/N mice**

(A) Representative dot plots of liver lymphocytes of an Ad-GFP- (left side) and Ad-2D6-infected (right side) FVB/N mouse five weeks post-infection stained for surface CD8 and intracellular IFN- $\gamma$ . (B) Surface CD4 (left side) and surface CD8 (right side) staining in combination with intracellular IFN $\gamma$  staining of liver lymphocytes of control virus (open bars) and Ad-2D6 (closed bars) FVB/N mice at week four post-infection after overnight stimulation with the corresponding peptide pool.

To further evaluate the CYP2D6-specific T cell response in Ad-2D6-infected FVB/N mice those peptide pools that resulted in CYP2D6-specific T cell stimulation were split up and used for further ICCS (Figure 20). Interestingly,

CD4<sup>+</sup> T cells producing IFN- $\gamma$  were found only after stimulation with a single peptide spanning the aa 41 to 60 of the human CYP2D6, whereas five peptide clusters were found to induce IFN- $\gamma$  production in CD8<sup>+</sup> T cells. Importantly, none of these peptides induced IFN- $\gamma$  production in CD4<sup>+</sup> or CD8<sup>+</sup> T cells if the mice have been infected with Ad-GFP. Interestingly, lymphocytes isolated from the liver showed an approximately three times higher frequency of IFN- $\gamma$  producing T cells of both, the CD4<sup>+</sup> and CD8<sup>+</sup> T cell subsets compared to lymphocytes isolated from the spleen. This indicates that CYP2D6-specific CD4<sup>+</sup> and CD8<sup>+</sup> T cells either migrate and remain in the liver or that they extensively proliferate within the target organ.

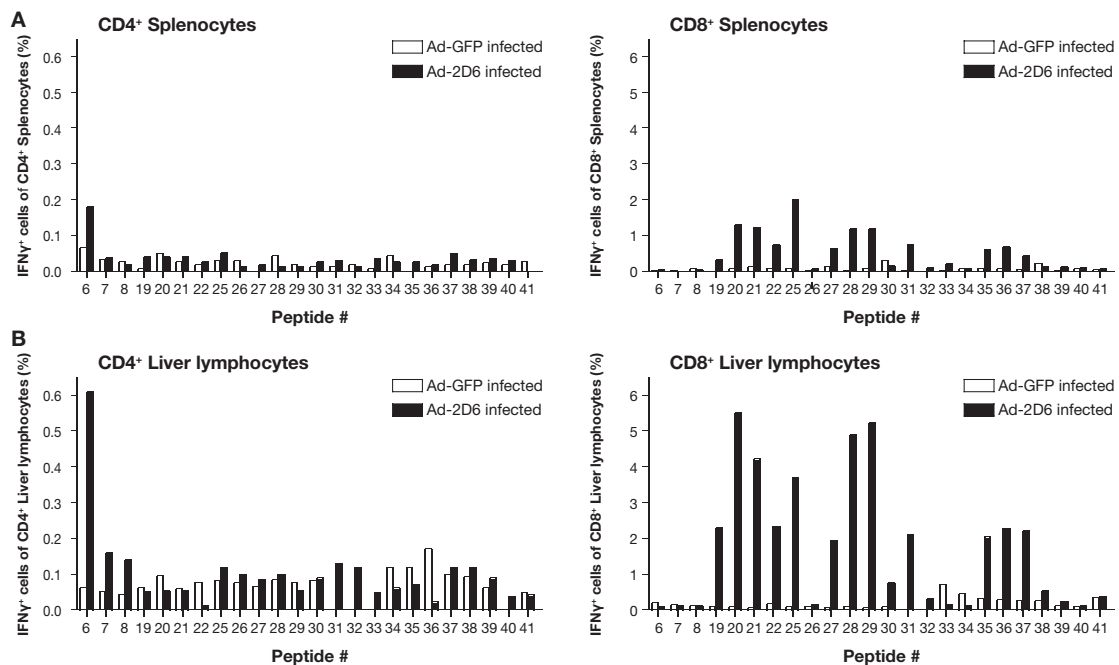


**Figure 20: Intracellular IFN- $\gamma$  staining after single peptide stimulation in FVB/N mice**

(A) Surface CD4 (left side) or surface CD8 (right side) and intracellular IFN $\gamma$  staining of splenocytes of Ad-GFP (open bars) and Ad-2D6-infected (closed bars) FVB/N mice at week six post-infection after overnight stimulation with the corresponding peptide. (B) Surface CD4 (left side) or surface CD8 (right side) and intracellular IFN $\gamma$  staining of liver lymphocytes of Ad-GFP (open bars) and Ad-2D6-infected (closed bars) FVB/N mice at week six post-infection after overnight stimulation with the corresponding peptide.

To evaluate if T cell tolerance in CYP2D6 mice after infection with Ad-2D6 was broken as it could be shown in FVB/N mice, CYP2D6 mice were infected with Ad-GFP or Ad-2D6 and splenocytes as well as liver lymphocytes were isolated and used for ICCS after overnight stimulation with the 61 20mer

peptides (Figure 21). Interestingly, no IFN- $\gamma$  producing T cells could be detected after peptide pool stimulation of splenocytes isolated from CYP2D6 mice. CYP2D6-specific CD8 T cells could only be found in liver lymphocytes (peptide pool 21-25). However, CD8<sup>+</sup> liver lymphocytes of Ad-2D6-infected CYP2D6 mice showed an approximately ten times lower frequency of IFN- $\gamma$  producing T cells compared to CD8<sup>+</sup> liver lymphocytes of FVB/N mice.

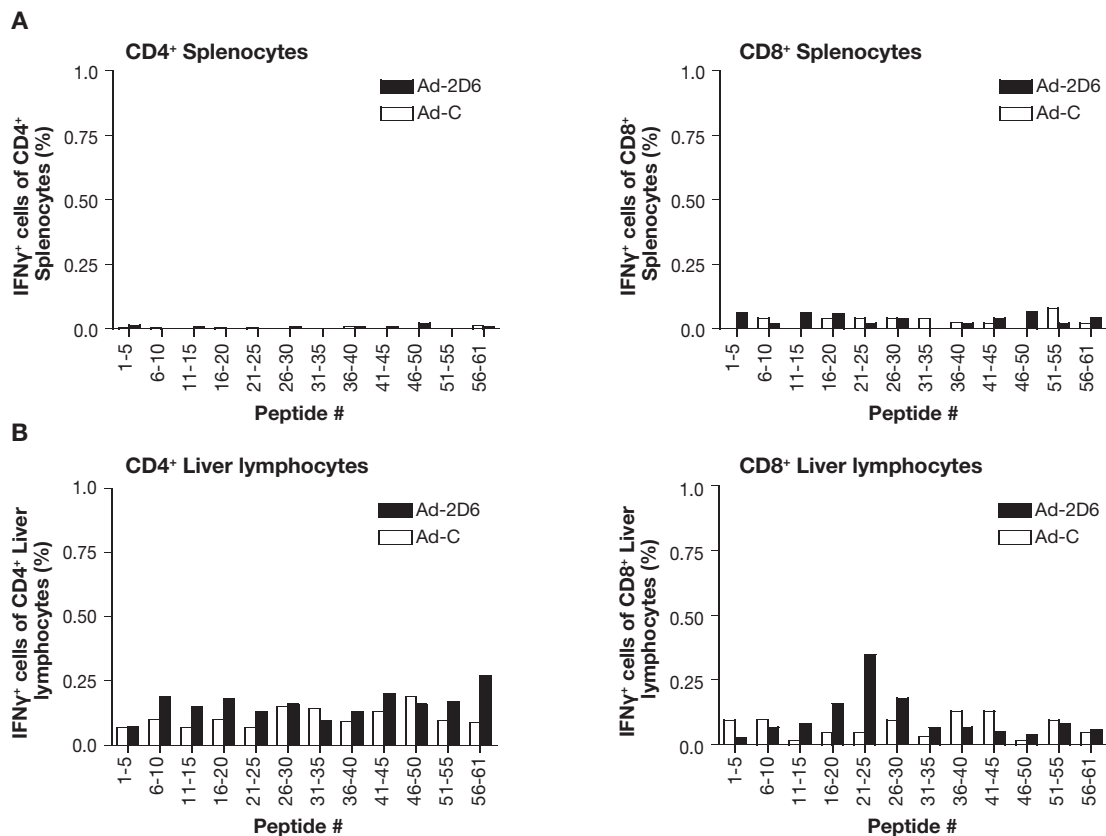


**Figure 21: Intracellular IFN- $\gamma$  staining after peptide pool stimulation in CYP2D6 mice**

(A) Surface CD4 (left side) or surface CD8 (right side) and intracellular IFN $\gamma$  staining of splenocytes of control virus (open bars) and Ad-2D6-infected (closed bars) CYP2D6 mice at week four post-infection after overnight stimulation with the corresponding peptide pool. (B) Surface CD4 (left side) or surface CD8 (right side) and intracellular IFN $\gamma$  staining of liver lymphocytes of control virus (open bars) and Ad-2D6-infected (closed bars) CYP2D6 mice at week four post-infection after overnight stimulation with the corresponding peptide.

To further investigate the CYP2D6-specific T cell response in Ad-2D6-infected CYP2D6 mice further ICCS with single peptide stimulation was performed (Figure 22). No significant difference in the frequency of IFN- $\gamma$  producing T cells isolated from the spleen was found between control virus and Ad-2D6-infected CYP2D6 mice. Only the peptide numbers 21, 22, 28

and 29 were able to induce above 0.2% IFN- $\gamma$  producing CD8<sup>+</sup> T cells in liver lymphocytes of Ad-2D6-infected CYP2D6 mice.

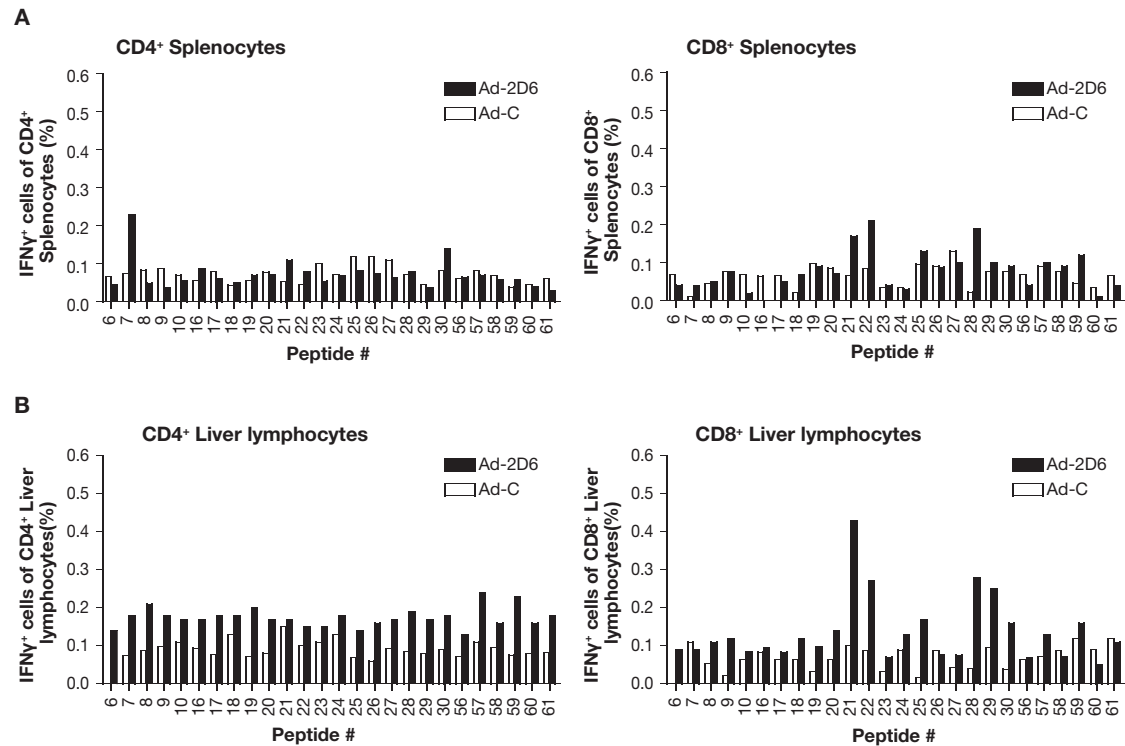


**Figure 22: Intracellular IFN- $\gamma$  staining after single peptide stimulation in CYP2D6 mice**

(A) Surface CD4 (left side) or surface CD8 (right side) and intracellular IFN $\gamma$  staining of splenocytes of control virus (open bars) and Ad-2D6-infected (closed bars) CYP2D6 mice at week four post-infection after overnight stimulation with the corresponding peptide. (B) Surface CD4 (left side) or surface CD8 (right side) and intracellular IFN $\gamma$  staining of liver lymphocytes of control virus (open bars) and Ad-2D6-infected (closed bars) CYP2D6 mice at week four post-infection after overnight stimulation with the corresponding peptide.

In summary, we could show that CD4<sup>+</sup> and CD8<sup>+</sup> T cells isolated from wild-type FVB/N mice infected with Ad-2D6, but not Ad-GFP, produced IFN- $\gamma$  after *ex vivo* stimulation with human CYP2D6 peptides. These data demonstrate that Ad-2D6-infection results in the breakdown of tolerance to human CYP2D6 on both the B cell and T cell level. In addition, we found that most CYP2D6-specific T cells were located in the liver of Ad-2D6-infected mice suggesting targeting and/or retention of CYP2D6-specific T cells. In accordance with our previous results indicating a partial tolerance in humanized CYP2D6 mice resulting in a less severe autoimmune liver damage we found that T cell tolerance seems to be more stringent in CYP2D6 mice than in FVB/N mice.

## **10 Discussion**

### **10.1 Breaking tolerance to the natural human liver autoantigen CYP2D6 by virus infection**

By infecting wild-type FVB/N and humanized CYP2D6 mice with an adenovirus vector expressing the natural human autoantigen CYP2D6, self-tolerance to CYP2D6 was broken, resulting in persistent autoimmune liver damage. For the first time we could show in an animal model the generation of autoantibodies with the same specificity as human LKM-1 occurring in AIH type 2 patients, combined with severe and persistent autoimmune-mediated hepatic damage, characterized by massive hepatocellular damage, strong cellular infiltration and the development of subcapsular fibrosis.

### **10.2 Mouse models for human autoimmune hepatitis**

Several, mostly transgenic, mouse model systems for AIH have been introduced in the past. The use of transgenic mice to study autoimmune-mediated diseases is well established and resulted in numerous theories and discoveries about the etiology and pathogenic mechanisms of other autoimmune diseases. The use of transgenic mice ensures the presence of a clearly defined antigen as a target for the aggressive immune response. Further, transgenic mice ensure a tissue-specific expression of the transgene that allows directing the autoimmune-mediated damage to the tissue of choice and it often enables specific tracking and monitoring of autoaggressive immune cells of interest. However, the expression of a transgenic target antigen often leads to a natural tolerance of the host against the transgene since it is considered a self-antigen. In order to break this natural tolerance several approaches that lead to specific or unspecific activation of autoreactive immune cells can be chosen. First, it is possible to overcome the natural tolerance by a massive unspecific activation of the immune system by administration of stimulators of the innate immune response. A second possibility is to directly transfer activated antigen-

specific lymphocytes in mice expressing the target antigen. A third possibility is the enhanced attraction of potential aggressive immune cells by infection with a virus that predominantly infects the organ of interest.

In an animal model of Frank Chisari's group transgenic mice expressing the HBsAg specifically in hepatocytes were generated and tolerance was broken by adoptively transferring activated T cells of HBsAg-primed donor mice. It was found that transferred HBsAg-specific CTL dominated the autoimmune response in HBsAg transgenic mice, released IFN- $\gamma$  upon antigen encounter and triggered apoptosis of HBsAg expressing hepatocytes. However, only a transient form of hepatic injury was observed which lasted less than three weeks following adoptive transfer (71). Nevertheless, this study indicates that T<sub>H</sub>1-mediated liver damage can be involved in autoimmune-mediated liver diseases.

In another model, the MHC class I molecule H-2K<sup>b</sup> was transgenically expressed in the liver of TCR transgenic mice whose T cells carried a H-2K<sup>b</sup>-specific TCR. However, those TCR transgenic T cells were tolerized against the MHC class I molecule H-2K<sup>b</sup> specifically expressed in the liver and tolerance could only be broken after additional transfer of cells expressing the target antigen H-2K<sup>b</sup> and IL-2. Nevertheless, no liver damage could be observed and additional infection with a liver-specific pathogen was necessary to induce transient hepatitis and liver damage reflected in elevated ALT indicating that breaking of peripheral tolerance as well as conditioning of the liver microenvironment is necessary to cause autoimmune tissue damage (72). In a follow up paper from the same group it was shown that injection of the immunostimulatory CpG-rich oligodeoxynucleotides (CpG-ODN) in H-2K<sup>b</sup>/TCR doubletransgenic mice was sufficient to initiate autoimmune-mediated liver damage caused by H-2K<sup>b</sup>-specific CD8<sup>+</sup> T cells. However, in order to maintain hepatic damage over a longer period of time (over eight weeks) CpG-ODN had to be repeatedly administered and termination of this inflammatory stimulus resulted in abrogation of disease. These findings indicated that additional factors are required for a self-perpetuation of autoimmunity (83).

In another animal model for AIH the immunodominant LCMV-GP expressed exclusively in the liver was used as transgene. These mice did not show any signs of autoimmunity under normal conditions and similar to the H-2K<sup>b</sup> transgenic mice, adoptive transfer of TCR transgenic T cells specific for the LCMV-GP expressed in the liver alone was not sufficient to induce disease. However, when these mice were infected with LCMV after adoptive transfer of TCR transgenic T cells specific for the LCMV-GP a transient form of hepatitis developed (73). As with the H-2K<sup>b</sup> mice it could be shown with this mouse model in a follow up paper that strong activation of the innate immune system is enough to initiate transient autoimmune-mediated liver damage caused by LCMV-GP-specific CD8<sup>+</sup> T cells (84). As the data obtained with H-2K<sup>b</sup> transgenic mice, these findings indicate that existence of autoreactive T cells specific for antigen within the liver is not sufficient to initiate autoimmune-mediated liver damage.

Another mouse model, which uses the well characterized LCMV proteins as targets is the TTR-LCMV mouse expressing LCMV-NP specifically in the liver. Tolerance to the LCMV-NP was broken by repeated vaccination with plasmids encoding the LCMV-NP and the T<sub>H</sub>1 stimulating cytokine IL-12 genes leading to a NP-specific CTL response, minor cellular infiltrates and elevated ALT (74). A related approach was used in another study, in which wild-type mice were xenoimmunized with a plasmid containing the human antigenic region of CYP2D6 (the target of LKM-1 antibodies) and FTCD (the target of LC1 antibodies). However, minor elevations in serum aminotransferase levels, a transient generation of anti-CYP2D6 and anti-LC1 antibodies and significant inflammation in the liver could only be found after co-expression of the T<sub>H</sub>1 stimulating cytokine IL-12 (75). Nevertheless, both of these studies support the data of Moriyama et al that T<sub>H</sub>1-mediated liver damage can play a role in autoimmune-mediated liver damage (71).

### **10.3 Lessons learned from animal models for AIH**

Autoimmune diseases are believed to be the result of genetic predisposition and environmental triggers such as bystander activation, molecular mimicry

or drug metabolism. Therefore, in theory, the liver should be a prime target for autoimmunity because it acts as a first line of defense against infectious, toxic, or carcinogenic agents arriving from the gut that could all eventually trigger activation of autoreactive immune cells either by molecular mimicry, bystander activation or neo-antigen formation. However, the frequency of autoimmune disease afflicting specifically the liver are relatively low when compared with other autoimmune diseases. One explanation for this is an overall bias of the liver to favor induction of tolerance rather than induction of immunity, which could already be demonstrated in the late 1960s by the spontaneous acceptance of liver allografts in many species (34). Several mechanisms have been proposed to be responsible for this bias towards tolerance induction in the liver including T cell inactivation by antigenic priming in the liver, tolerance induction via cross-presentation by LSEC, induction of regulatory T cells by LSEC and hepatic stellate cell-induced T cell apoptosis (32, 33, 37, 85, 86). Furthermore, it could be demonstrated that targeted expression of autoantigens in liver cells can induce autoantigen-specific  $T_{reg}$  cells that are able to suppress subsequent induction of an experimental autoimmune disease in animals (41). This preferred induction of tolerance against antigens encountered in the liver made the generation of a reliable animal model to study persistent autoimmune-mediated liver damage difficult. In most models, liver injury is only transient and can be achieved by rather complex intervention methods. Often, tolerance to a transgenic antigen expressed exclusively in the liver can only be broken by adoptive transfer of either previously primed T cells or transgenic T cells specific for the target antigen in combination with additional inflammatory triggers such as viral infection or overexpression of pro-inflammatory cytokines. In addition to the overall bias of the liver to induce tolerance, the complex methods used to trigger autoimmune liver damage itself could restrict the autoimmune response leading to only transient liver damage. For example in models that require the transfer of TCR transgenic T cells in mice that transgenically express the target antigen it might be possible that the relatively small number of TCR transgenic T cells

are confronted with an excess of antigen and therefore, after strong initial activation die by apoptosis. This process is called exhaustion or clonal deletion and can be seen for example after *i.v.* infection of wild-type C57BL/6 mice with a high dose of  $2 \times 10^6$  pfu of the fast replicating LCMV Docile (87). Another possibility how complex experimental methods may restrict the resulting autoimmune response in models that require the additional persistent expression of pro-inflammatory cytokines is that counteracting mechanism in the liver try to balance out the pro-inflammatory milieu in the liver. Nevertheless, those animal models were able to at least transiently break self-tolerance to specific liver antigens in an autoimmune-mediated fashion and could show that  $T_H1$ -mediated destruction of hepatocytes can play a role in autoimmune-mediated liver diseases. In addition, these models emphasized that not only breaking of tolerance but also conditioning of the liver microenvironment plays an important role for autoimmune-mediated liver damage.

#### **10.4 The CYP2D6 animal model for AIH**

As found by human studies, the use of animal models for AIH listed above and animal models for other autoimmune diseases it is known that genetic predisposition and breaking of tolerance are not sufficient to initiate a persistent autoimmune-mediated disease. Current opinion is that activation of the innate immune system, inflammatory processes as well as breaking of self-tolerance and down-regulation of possible regulatory mechanism might have to act in a synergistic fashion in order to initiate autoimmune-mediated damage. One possibility to induce such a complex scenario is molecular mimicry of host structures by pathogens and indeed, many autoimmune diseases have been associated with pathogen infections (15, 21-24, 47, 88). Therefore, our strategy was to build an animal model for AIH based on the initial concept of molecular mimicry as a possible cause for autoimmunity. In addition, instead of choosing an artificial model antigen to break tolerance we used the natural human autoantigen CYP2D6 which constitutes the major target autoantigen in human type 2 AIH (57). We used the wild-type FVB/N

mice as well as the humanized CYP2D6 mice that transgenically express the human CYP2D6 under the control of its own promotor predominantly in the liver (77). Natural tolerance to the human CYP2D6 autoantigen was broken by infection of mice with an adenovirus-vector expressing the human CYP2D6. Using both, the wild-type FVB/N mice that only express the mouse CYP2D6 homologues and the humanized CYP2D6 mice that express the transgenic CYP2D6 as well as endogenous CYP2Ds enabled us to have a model system for true molecular mimicry (wild-type FVB/N mice) and one for molecular identity (humanized CYP2D6 mice). Infecting wild-type FVB/N as well as humanized CYP2D6 mice with Ad-2D6 resulted in an initial acute hepatitis associated with hepatic adenovirus infection. This was followed by a persistent autoimmune-mediated hepatic damage, characterized by massive hepatocellular damage, strong subcapsular liver fibrosis as well as extensive subcapsular and peri-vascular infiltration by B cells, CD4<sup>+</sup> and CD8<sup>+</sup> T cells and macrophages. We could demonstrate that B cell tolerance was broken after infection with Ad-2D6 resulting in activation of CYP2D6-specific B cells and the generation of high titers of anti-CYP2D6 antibodies. For the first time generation of autoantibodies with the same specificity as human LKM-1 occurring in AIH type 2 patients could be generated in an animal model. In addition, we could show that the disease was less severe in humanized CYP2D6 compared to wild-type FVB/N mice, indicating that the presence of a self-antigen in the liver somewhat protects against autoimmune-mediated immune responses that targets the identical antigen present in the liver. Furthermore, we could demonstrate that virus infection was essential to induce persistent liver damage. In contrast, virus infection was not required for breaking of B cell tolerance and autoantibody production. In addition, T cell tolerance was broken after infection with Ad-2D6 resulting in the activation of CYP2D6-specific T cells that were able to produce IFN- $\gamma$  after *ex vivo* stimulation. The frequency of IFN- $\gamma$  producing T cells after overnight incubation with human CYP2D6 peptides was approximately ten times higher in Ad-2D6-infected wild-type FVB/N mice compared to transgenic CYP2D6 mice.

## 10.5 Advantages of the CYP2D6 mouse model

For an animal model to be relevant it needs to resemble the human disease and its consequences as much as possible. Autoimmune diseases however, are not induced by a single event alone but rather by the accumulation of several factors including genetic predisposition and environmental triggers that might have occurred years before the clinical signs for autoimmune tissue damage are detectable. Therefore very little is known so far about the etiology of autoimmune diseases and animal models that after an initial trigger lead to the manifestation of autoimmune-mediated tissue damage become valuable. Nevertheless, relevant animal models for autoimmune diseases should stay as close to potential trigger mechanisms for human autoimmune diseases as possible and reflect the clinical signs of the disease most accurately. Often proposed environmental triggers of autoimmune diseases in humans involve bystander activation, molecular mimicry or neo-antigen formation by for example drug metabolism (13). The clinical outcome of AIH that leads to chronic progressive liver damage and cirrhosis is characterized by the presence of persistent interface hepatitis and portal plasma cell infiltration on histologic examination and autoantibodies (51, 52). Some of the animal models discussed above served as experimental representation for transient autoimmune-mediated tissue damage. However, none of them could reproduce persistent liver damage in the presence of autoantibodies with the same specificity as human LKM-1 antibodies as occurring in AIH type 2 patients. In addition, most models used a rather artificial and unphysiological trigger mechanism to induce autoimmune-mediated tissue damage detected and only transient hepatitis and hepatocellular damage was observed. In contrast, the CYP2D6 mouse model based on the initial concept of molecular mimicry used a trigger for the induction of autoimmunity that is commonly accepted as one of the possible causes for human autoimmune-mediated diseases. The CYP2D6 mouse model resulted after an initial phase of acute hepatitis in persistent autoimmune-mediated liver damage. In this context, the CYP2D6 model is superior to others as it combines an acute anti-viral hepatitis phase with a

chronic and progressive autoimmune-mediated hepatitis. Therefore, the CYP2D6 model may offer a unique opportunity to study all mechanisms of virus-induced autoimmunity ranging from the initial activation of the innate immune system by viral infection to the autoimmune-mediated destruction of the liver.

## **10.6 The CYP2D6 mouse model and the etiology of AIH**

A common hypothesis to explain the etiology of autoimmune disease is genetic predisposition of the host paired with environmental triggers (13). Many autoimmune diseases such as T1D, MS, PBC, AIH and others have been linked to pathogen infections, however, no firm proof for environmental factors, such as viruses, as inducers of most human autoimmune diseases has been found as of yet. Nevertheless, for a few rare autoimmune-mediated diseases a temporal association between infection and autoimmune diseases could be proven, so for example for rheumatic fever in which antibodies found after bacterial infection cross-react with heart autoantigens and are postulated to lead to immune-mediated anti-heart autoimmunity (27) or in case of Guillain-Barré syndrome in which antibodies found after bacterial infection cross-react with peripheral nerve gangliosides (28). There are several possibilities that can make a direct link of autoimmunity to a single infection difficult even though the fact that infections have the possibility to induce strong activation of the innate as well as the adaptive immune system and the fact that there are many sequence homologies between pathogenic antigens and human autoantigens suggesting their involvement in the initiation of autoimmunity. First, it is likely that an acute infection that can activate autoreactive cells has already been cleared by the time of diagnosis of the resulting autoimmune disease making a causative association very hard to prove (also referred to as 'hit and run events'). Second, some virus infections are common and traces of these infections can not only be found in patients with autoimmune diseases but also in healthy individuals making it hard to link those infection to the initiation of the autoimmune disease. Third,

viruses might not directly induce autoimmunity but instead accelerate a preexisting autoimmune condition to progress to clinical disease and in addition, the exact time, location and magnitude of an infection might be important. In this context pathogenic infections or strong activators of the immune system in general are believed to induce a temporary immunological state (also referred to as 'fertile field') that can depending on genetic and environmental factors lead to autoimmune-mediated diseases (15, 16). In conjunction with the 'fertile field' hypothesis we could show in the CYP2D6 mouse that breaking of tolerance alone was not sufficient to induce an autoimmune liver disease. Infection with a liver-specific pathogen and therefore generation of a fertile field in the liver microenvironment was required to cause autoimmune-mediated tissue damage.

In human autoimmune hepatitis, several studies implicate viruses such as measles virus, hepatitis virus, cytomegalovirus and Epstein-Barr virus in its initiation (53, 89). For example it could be shown that HCV has the potential to induce autoreactive CD8<sup>+</sup> T cells which cross-reactively recognize the cytochrome P450 isoforms 2A6 and 2A7 that contain sequence homology to HCV (66). Further, it could be shown that antibodies against CYP2D6 in HCV and LKM-1 positive patients can cross-react with the HCV proteins NS3 and NS5a (56). In addition, a protein of HSV-1 has been reported to share sequence homology with the immunodominant CYP2D6 epitope suggesting a possibility of molecular mimicry as a mechanism involved in the etiology of AIH (57). Using the CYP2D6 mouse model we could demonstrate tolerance breakdown and triggering of persistent autoimmune-mediated hepatic damage not only in humanized CYP2D6 mice that confer molecular identity with the Ad-2D6 virus, but also in wild-type FVB/N mice that only express the mouse CYP2D isoenzymes. Mouse CYP2Ds confer high sequence homology to the human CYP2D6 and several mouse CYP2Ds, including the CYP2D22 that has been suggested to be the functional ortholog of human CYP2D6 (79) display up to 75% aa sequence homology to the human CYP2D6. Therefore, breaking of tolerance and persistent autoimmune-mediated liver damage in wild-type FVB/N mice was most likely induced because of true molecular

mimicry between the human CYP2D6 expressed by the adenovirus system and homologous mouse CYP2D sequences.

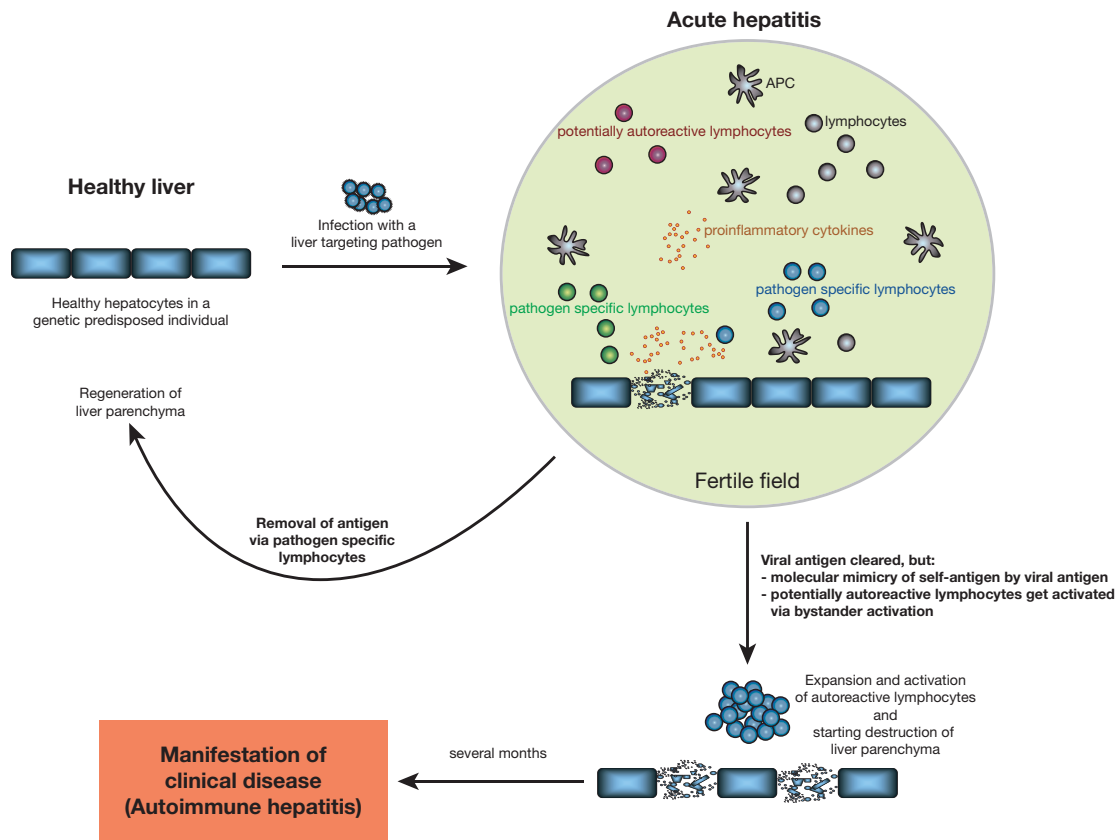


**Figure 23: Possible mechanism for induction of AIH**

Infection with a liver-tropic pathogen leads to the production of pro-inflammatory cytokines and chemokines that will then attract APCs and lymphocytes of all sorts. Lymphocytes specific for pathogen antigens (several possibilities) will expand and start to destroy the pathogen-infected hepatocytes leading to an acute hepatitis. The accumulation of specific as well as unspecific lymphocytes in combination with APCs and soluble chemokines/cytokines due to pathogen infection is also referred to as fertile field. Under normal circumstances the pathogen and pathogen-infected cells will be eliminated and the liver regenerates itself. However, especially in genetically predisposed individuals there is the possibility that autoreactive lymphocytes are being activated by either bystander activation or by pathogen antigens mimicking self-antigens. Those autoreactive lymphocytes will expand and target self-cells and start to destroy the liver parenchyma. Clinical signs of an autoimmune disease might only be detectable after several months.

Interestingly, we found that the disease was less severe in humanized CYP2D6 compared to wild-type FVB/N mice. These findings allow the speculation that similar yet not identical autoantigens might be better targets

for autoimmune reactions afflicting the liver due to less efficient central and peripheral tolerance mechanism.

Taken together we could demonstrate by the use of the CYP2D6 mouse model that persistent immune-mediated hepatitis can be triggered by molecular mimicry occurring in the context of a hepatotropic viral infection. These results support the evidence that molecular mimicry in combination with environmental factors such as viruses that can induce a 'fertile field' for the arrival of autoaggressive lymphocytes in the liver microenvironment is one of the possible mechanisms involved in the etiology of AIH (see Figure 23).

## **10.7 The CYP2D6 model and pathogenic mechanism of AIH**

The outcome of AIH is autoimmune-mediated persistent liver infiltration leading to progressive hepatocellular damage and the development of fibrosis. However, as of yet not much is known about the underlying pathogenic mechanisms that lead to destruction of hepatocytes in an autoimmune-mediated fashion. The presence of increased numbers of B and T lymphocytes, plasma cells and macrophages within the liver parenchyma (interface hepatitis) during an ongoing AIH in human patients as well as the presence of disease-specific autoantibodies indicates that several pathways may be contributing to the clinical manifestation of the disease.

Although there is relatively much known about the autoantibodies especially in AIH type 2 it is still not clear if they indeed play a role in the pathogenic mechanisms of AIH. It could be shown that LKM-1 autoantibodies, the hallmark of type 2 AIH, do recognize and bind to CYP2D6 exposed on the plasma membrane of hepatocytes (60) and that anti-LC1 antibodies, specific for AIH type 2 but only present in up to 50% of patients, seem to correlate with disease activity (61). In addition, residual plasma cells in the liver tissue of patients before withdrawal of immunosuppressive therapy are more frequently associated with relapse than with sustained remission (90).

However, the pathogenic role of autoantibodies in AIH is not yet resolved (91) and since autoantibodies related to AIH also appear in other chronic liver disease (LKM-1 antibodies in chronic HCV patients) and even in up to 15% of healthy individuals (in case of the ANA antibodies found predominantly in AIH type 1) it is unlikely that autoantibodies alone are responsible for the autoimmune-mediated tissue damage seen in AIH (53, 54). Supporting the theory that autoantibodies alone are not sufficient to induce autoimmune-mediated liver damage in human AIH, we found in our CYP2D6 animal model that treatment of mice with human recombinant CYP2D6 alone or in combination with Poly-IC, CpG, IFA or CFA resulted in breakdown of B cell tolerance but not autoimmune liver disease. Besides the strong association of MHC haplotypes with genetic susceptibility and a more severe form of AIH, several studies have proposed the involvement of T cell immunity in human AIH as well as in animal models for AIH (53). As described previously several animal models for AIH could show the involvement of  $T_H1$ -mediated hepatocellular destruction by  $CD8^+$  T cells in autoimmune-mediated liver damage (71, 74, 75). However, in those models either a  $T_H1$  promoting cytokine or already activated CTL were used to shift the immune response towards an aggressive  $CD8^+$  T cell response. Nevertheless, also in human AIH recent studies have identified CYP2D6-specific  $CD8^+$  T cells capable of secreting  $IFN-\gamma$  and of exerting cytotoxicity after recognition of CYP2D6 epitopic sequences in an HLA class I restricted fashion (92). In correlation with the data received for human AIH type 2 patients we could show in the CYP2D6 model that  $CD8^+$  T cells isolated during an ongoing autoimmune-mediated liver disease produce  $IFN-\gamma$  after *ex vivo* stimulation with specific peptide-epitopes of CYP2D6 further supporting the theory that MHC class I restricted killing of hepatocytes is involved in AIH.

$CD4^+$  T cells can influence immunity in several ways depending on the cytokine profile secreted. They can either skew the immune response towards a more aggressive  $T_H1$  response involving  $CD8^+$  T cells or towards the less aggressive  $T_H2$  response leading to the activation of B cells and production of antibodies. Already in the 1980's it could be shown that

patients with AIH have lower levels of circulating T cells expressing CD8 co-receptors (93) indicating a regulation towards the less aggressive  $T_H2$  response. Relatively newly described  $CD4^+$  T cell subsets,  $T_{reg}$  cells and  $T_H-17$  cells have been implemented to play an important role in autoimmune diseases.  $T_{reg}$  cells are described as a weakly self-reactive  $CD4^+$  T cells subset that is able to suppress either specifically or via bystander mechanisms autoreactive immune cells (5, 8) whereas the highly pro-inflammatory  $CD4^+$   $T_H-17$  cells are believed to play an important role during the initiation and propagation of an autoimmune disorder (4). So far nothing is known about  $T_H-17$  and their role in AIH, whereas it could be shown that in patients with AIH  $T_{regs}$  are defective both in number and function compared to normal controls and that these abnormalities related to the stage of the disease (4, 92, 94, 95). In a more classical approach, it could be shown that  $CD4^+$  T cells from AIH type 2 patients did proliferate and were able to produce IFN- $\gamma$ , IL-4 and IL-10 after *ex vivo* stimulation with overlapping peptides covering the whole CYP2D6 gene (63). In addition, they could correlate the number of epitopes recognized and the quantity of IFN- $\gamma$  (a typical  $T_H1$  cytokine) and IL-4 (a typical  $T_H2$  cytokine) produced with biochemical and histological markers of disease activity suggesting a pathogenic role of both  $T_H1$  and  $T_H2$  T cells in AIH type 2 (63). By the use of the exact same overlapping peptides spanning the whole CYP2D6 gene used in the study of Ma et al. we were able to show in the CYP2D6 model that  $CD4^+$  T cells isolated during an ongoing autoimmune-mediated liver disease were able to produce IFN- $\gamma$  after *ex vivo* stimulation. Since IFN- $\gamma$  is known to be a typical  $T_H1$  cytokine but also promotes antibody class switching to the mostly anti-viral isotype IgG2a (96) it is possible that  $T_H1$ - as well as  $T_H2$ -mediated pathogenic mechanism are involved in the detected autoimmune liver disease in the CYP2D6 mouse model. Interestingly, IgG2a binds with high affinity to Fc $\gamma$ RI expressed on macrophages, neutrophils, mast cells and natural killer cells (97, 98). In this context it is imaginable that opsonization of anti-CYP2D6 coated hepatocytes by Kupffer cells could play a pathogenic role in our model as well.

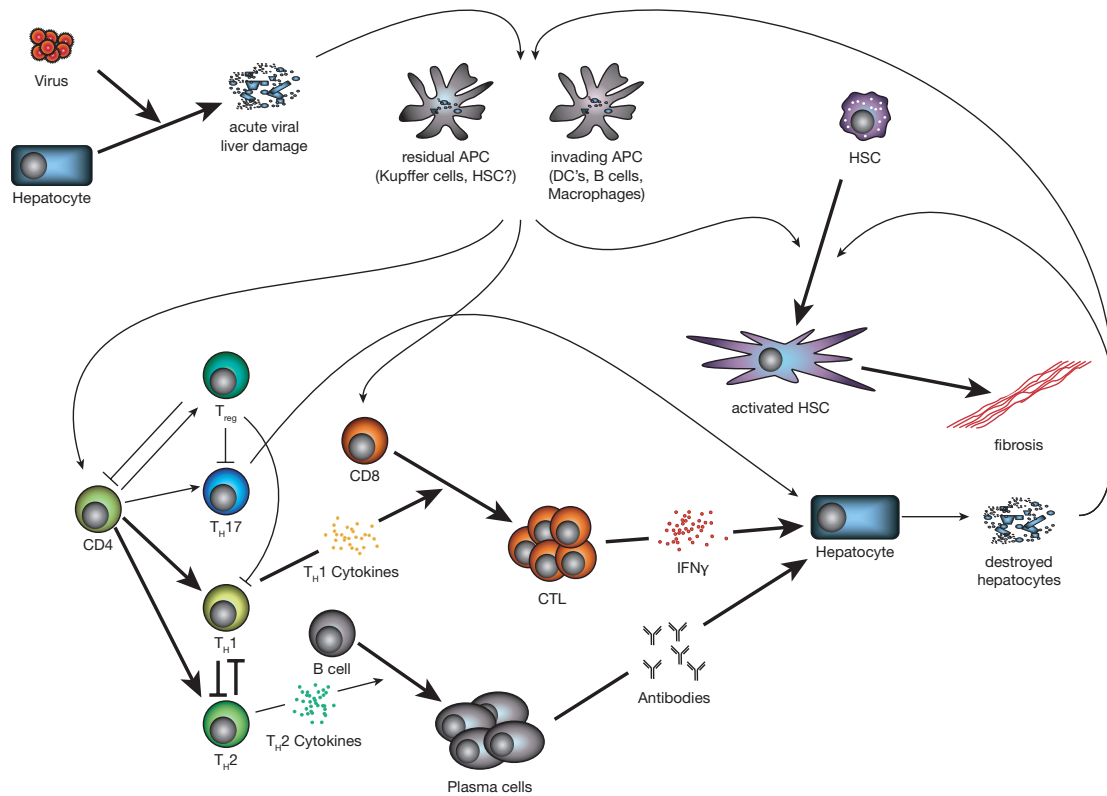


**Figure 24: Possible pathogenic mechanism in the CYP2D6 model**

Adenovirus infection leads to an initial acute hepatitis in combination with hepatocellular damage. Virus antigens as well as self-antigens can then be taken up by residual or invaded APCs, processed and presented to CD4<sup>+</sup> T helper cells or directly to CD8<sup>+</sup> T cell. The CD4<sup>+</sup> T helper cell becomes activated and according to the cytokine profile present and the nature of the antigen differentiates either in a T<sub>H</sub>1 type or T<sub>H</sub>2 type CD4<sup>+</sup> T helper cell. T<sub>H</sub>1 type CD4<sup>+</sup> T cells will activate CD8<sup>+</sup> T cells that then differentiate into IFN- $\gamma$  producing CTLs whereas T<sub>H</sub>2 type CD4<sup>+</sup> T cells will activate B cells that then differentiate into plasma cells and produce antibodies. One or both effector cells (CTL and plasmacells) respectively their products (IFN- $\gamma$  or antibodies) can target hepatocytes and cause the autoimmune-mediated hepatocellular damage seen during the persistent autoimmune phase in the CYP2D6 model. Besides the classical differentiation of CD4<sup>+</sup> T helper cells to T<sub>H</sub>1 type or T<sub>H</sub>2 type CD4<sup>+</sup> T helper cells it is possible that T<sub>H</sub>-17 and/or T<sub>reg</sub> cells are generated that can augment or abrogate the autoimmune process. However, the involvement of T<sub>H</sub>-17 and/or T<sub>reg</sub> cells in initiation and propagation or regulation of the autoimmune response still needs to be evaluated. HSC will get activated and produce collagen fibers leading to fibrosis. Thin arrows indicate assumptions that have not been tested by experiments yet while thick arrows indicate processes that have been confirmed by experimental testing in the CYP2D6 mouse model.

Comparing wild-type FVB/N and humanized CYP2D6 mice we found a less severe autoimmune liver damage in humanized CYP2D6 mice. Our data

showed only a minor decrease in the autoimmune B cell response measured by autoantibody production. In contrast, the autoimmune T cell response measured by IFN- $\gamma$  production after *ex vivo* CYP2D6 peptide stimulation was strongly decreased. Those findings confirm the theory that B cell tolerance is less stringent controlled than T cell tolerance (99, 100) and support the involvement of T<sub>H</sub>1- as well as T<sub>H</sub>2-mediated pathogenic mechanism in our mouse model for autoimmune mediated liver damage (summarized in Figure 24).

## **10.8 Possibilities of the CYP2D6 mouse model**

In summary we conclude that the CYP2D6 mouse model has the following advantages over other animal model systems described for AIH:

- It has a well-defined and feasible initiating event that constitutes one of the possible mechanisms leading to the initiation of human AIH (molecular mimicry).
- It uses the natural occurring autoantigen, the human CYP2D6 under its own promoter as a target antigen for the autoimmune response.
- It resembles the autoimmune response of human AIH type 2 by the production of LKM-1-like autoantibodies and the activation of T cells specific for CYP2D6 autoantigens
- It reflects the outcome of human AIH type 2 in persistent autoimmune-mediated hepatic damage, characterized by massive hepatocellular damage, strong cellular infiltration and the development of subcapsular fibrosis.

Being that close to the human autoimmune disease the CYP2D6 mouse model holds potential for the dissection of the mechanisms underlying human AIH. Following approaches might help to understand the complex processes involved:

- It will be necessary to further study the cellular immunity, involving the analysis of classical T cell subsets contributing to the autoimmune-mediated liver damage.

- Newly defined T cell subsets such as T<sub>reg</sub>, T<sub>H</sub>-17 and T<sub>H</sub>-9 cells and their contributions in abrogation/prevention or initiation of the disease have to be investigated.
- Adoptive transfer experiments, in which sorted cell populations and/or serum from diseased animals are transferred to healthy animals can be used to clarify whether cellular subsets or serum factors can induce or suppress an autoimmune-mediated liver disease.
- The CYP2D6 model crossed to several other transgenic or knockout mice could enable a better understanding of the potential contributions of humoral and cellular immunity to hepatic autoimmunity.

The CYP2D6 mouse model can not only be used to understand the mechanisms underlying human AIH but also serve as basis to investigate possible intervention strategies for autoimmune liver diseases. Possible therapies include administration of cytokines or neutralizing antibodies against them. It could be demonstrated in animal models for T1D that the effect of cytokines depends on the timing of administration, the dose and the route of administration (101-104). Further, depletion of lymphocyte subsets, such as CD3<sup>+</sup> T cells, as currently in use for T1D (105) could have positive effects on an ongoing autoimmune-mediated liver disease by deleting autoreactive T cells. Finally, oral/nasal administration of CYP2D6 could induce liver antigen-specific T<sub>reg</sub> cells as it could be shown in other animal models for autoimmune diseases (106, 107). However, most of these approaches depend on the right timing during the course of an autoimmune disease and a successful intervention might be bound to a certain time point during the development of the disease (also referred to as ‘window of opportunity’). Furthermore, a combination therapy might be the most successful approach as recently demonstrated in T1D (108, 109). In a combination therapy, the depletion of CD3<sup>+</sup> T cells is combined with the induction of T<sub>reg</sub> cells by administration of *intra nasal* autoantigen during the re-establishment of the immune homeostasis.

The use of an animal model that has a well-defined initiation of the disease such as the CYP2D6 model will allow the investigation of such intervention methods and the effects they have on the outcome of autoimmune-mediated liver damage.

# 11 Appendix

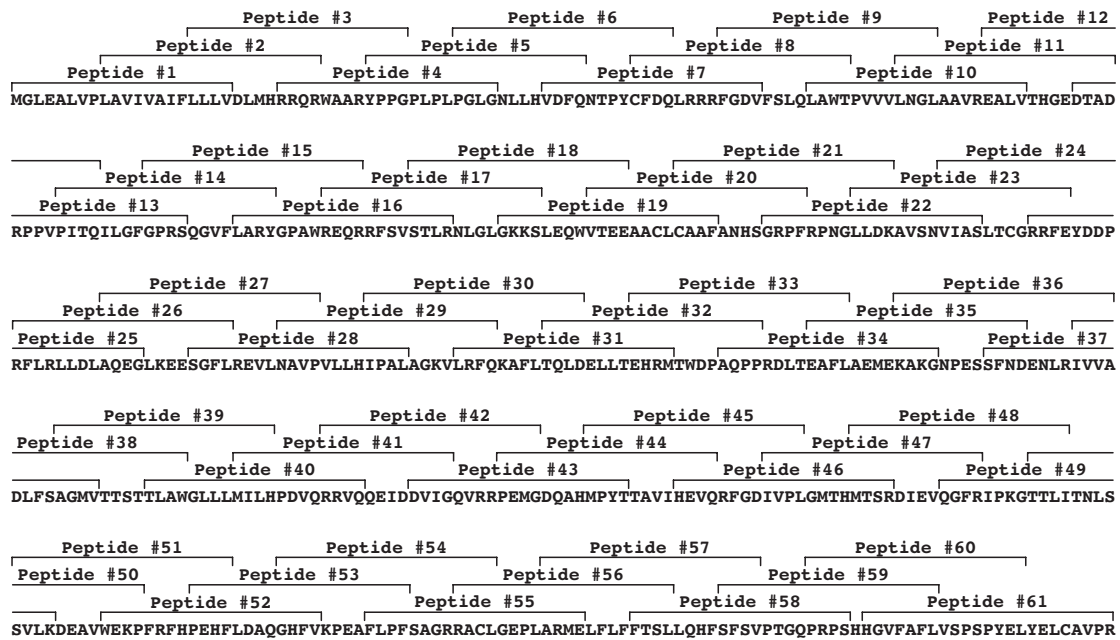


**Figure 25: 61 20mer sequences spanning the entire human CYP2D6**

Schematic overview of the 61 overlapping 20mer sequences spanning the entire human CYP2D6 gene received through collaboration with D. Bogdanos and D. Vergani from the King's College London School of Medicine at King's College Hospital

# 12 Material and Methods

## 12.1 Source of Materials

### 12.1.1 Plastic ware

70 µm nylon cell strainer	BD Falcon; 352350
96-well ELISA plates	Anicrin; 3911925
96-well V-bottom plates	Anicrin; 3911924
Cell culture flasks (25, 75, 175 cm <sup>2</sup> )	Cellstar
Coverslip	Menzel-gläser
Cryomolds	Electron Microscopy science; 62352-30
Cryotubes	Sarstedt; 72.379.002
Eppendorf tubes	Eppendorf
FACS-tubes	Biorad; 223-9390
FACS-tubes	BD Falcon; 352052
Falcon tubes (15, 50 ml)	Cellstar
Heparin coated capillary	Fisher scientific; 02-668-10
Needles (27G, 30 G)	BD Microlance
Plastic pipets (5, 10, 25, 50 ml)	Corning INC
Sialin coated slides	Menzel-gläser; J1800AMN/
Sterile Filter (500 ml)	Millipore; SCGPU05RE
Syringes (1 ml)	Terumo; BS-01T
Syringes (5, 10 ml)	Braun
Tissue culture dishes	Cellstar
Tissue culture plates (6, 12, 24, 48, 96 well)	Cellstar

### 12.1.2 Chemicals

Abnormal Control Assay Standard	Biotron Diagnostcs INC.; 01BTAbn
Acetic Acid	J.T. Baker; 6052
AEC (3-Amino-9-Ethylcarbazole)	MP Empowered Discovery; 195039
Agarose	Sigma; A9539
APS	Sigma; A3678
Aquamount	Merck; 1.08562.0050
Avidin Solution	Vector; T1115
Biotin Solution	Vector; T0821
Brefeldin A	Sigma; B6542

Bromophenol blue	Roth; 512.1
CFSE (5- (and 6-) carboxyfluorescein succinimidyl ester	Invitrogen; C1157
Chloroform	Riedel-de Haën; 32211
Complete freunds adjuvant	Sigma; F5881
Crystal violet	Sigma; C0775
DEPC (Diethylpyrocarbonate)	Sigma; D5758
DMSO (Dimethylsulfoxide)	Sigma; D5879
DTT (1,4-Dithiothreit)	Roth; 6908.1
ECF substrate	Amersham Bioscience; RPN 5785
EDTA	AppliChem; A1103.1000
Ethanol absolut	Riedel-de Haën; 24102
Ethidium bromide	Sigma; E8751
EZ-link sulfo-NHS-LC biotin	Pierce; 21336
Formaldehyde	Redel-de Haën; 33220
Glycerol	Roth; 3783.1
H <sub>2</sub> O <sub>2</sub>	Roth; 8070.1
HCl	Riedel-de Haën; 30721
Hematoxylin	AppliChem A4840.1000
HEPES	Gibco; 15630
Immunofluore mounting Medium	ICN; 622701
Incomplete freunds adjuvant	Sigma; F5506
Ionomycin	Sigma; I0634
Isofluran	Abbott; B506
Iso-Propanol	Prolabo; R11-36-67
Methanol	Fluka; 65543
Na <sub>2</sub> CO <sub>3</sub>	Sigma; S7795
NaCl	J.T. Baker; 0278
NaHCO <sub>3</sub>	Merck; 1.06329.0500
Na-N <sub>3</sub>	Roth; K305.1
NH <sub>4</sub> Cl	Merck; 1.01145.0500
Normal Control Assay Standard	Biotron Diagnostics INC.; 68665
Paraformaldehyde	Merck; 1.04005.1000
Pen/Strep	Gibco; 15140
Percoll	GE Healthcare; 17-0891-01
Peroxidase substrate	Vector; SK-4100
PMA (4 $\alpha$ -Phorbol-12-myristate 13-acetate)	Sigma; P148
Potassium acetate	Merck; 1.04820.1000

Rotiphorese Gel 30 (30% Acrylamide/0.8% bis-acrylamide)	Roth; 3029.1
Saponin	Sigma; S7900
SDS	Roth; 2326.2
Skim milk powder	Töpfer Allgäu; 60226
Sodium Pyruvate	Gibco; 11360
Syrius red solution (120 µl Sirius red in 0.1% saturated picric acid)	Electron Microscopy Sciences; 26357-02
TEMED	Roth; 2367.3
Tissue-Tek OCT	Sakura; 4583
Tri-Reagent	Sigma; T9424
Tris-HCl	Roth; 4855.2
Triton X-100	Sigma; T8787
Trypan blue	Sigma; T8154
Tween-20	Sigma; P7949
Xylene	Riedel-de Haën; 16446

### 12.1.3 Composition of buffers, solutions and culture media

0.1% Crystal violet	0.1% crystal violet 0.2% EtOH in ddH <sub>2</sub> O
0.5% Trypsin-EDTA	Gibco; 25300
2x Laemmli sample buffer	20% v/v Upper gel buffer 20% v/v Glycerol 4% SDS 1.54% DTT bromophenol blue
35% Percol buffer	35 ml Percol 4 ml 10x PBS and 60 ml PBS
ABC reagent solution (Peroxidase Substrate Kit DAB)	5 ml ddH <sub>2</sub> O 4 drops of DAB Stock solution 2 drops of Hydrogen Peroxide Solution
AEC-substrate	AEC diluted 1:50 with 50 mM Na-acetate buffer (pH 5) filtered through 0.2 µm filter 30% H <sub>2</sub> O <sub>2</sub> 1:2000
Biotinylation buffer	PBS 1 mM MgCl <sub>2</sub> 0.1 mM CaCl <sub>2</sub> pH 7.4 1 mg/ml freshly added biotin

Collagenase buffer	0.2 mg/ml collagenase IV 0.02 mg/ml DNase 5% FCS
DEPC H <sub>2</sub> O	1% DEPC in ddH <sub>2</sub> O stir over night and autoclave
DMEM + GlutaMax I	Gibco; 61965
ELISA blocking buffer	PBS 2% FCS
ELISA coating buffer	50 mM Na <sub>2</sub> CO <sub>3</sub> 50 mM NaHCO <sub>3</sub> pH 9.6
ELISA/ELISPOT washing buffer	PBS 0.05% Tween-20
FACS fixation buffer	PBS 0.1% PFA
FACS PBS/saponin buffer	PBS 1% FCS 0.1% NaN <sub>3</sub> 0.1% Saponin
FACS PBS/staining buffer	PBS 1% FCS 0.1% NaN <sub>3</sub>
FACS PFA/saponin buffer	PBS 0.1% Saponin 10 mM HEPES 4% PFA
FCS (Foetal calf serum)	Biochrom AG; S0115
IMDM	Gibco; 21980
Lower gel buffer	1.5 M Tris-HCl (pH 8.8) Autoclave
Medium 199 (10x)	Gibco; 21180-021
PBS	Gibco; 14190
Proteinase K	10 mg/ml Proteinase K 10 mM Tris-HCl (pH 7.5)
Proteinase K buffer	ddH <sub>2</sub> O 20% SDS 5 M NaCl 1 M Tris (pH 8) 0.5 M EDTA
Red blood cell lysis buffer	0.83% NH <sub>4</sub> Cl in ddH <sub>2</sub> O Sterile filtrated
RPMI 1640 + GlutaMax I	Gibco; 61870

Running buffer	25 mM Tris 192 mM Glycine 0.1% SDS pH 8.3
SPOT washing buffer	PBS 0.1% Tween-20
TAE buffer	40 mM Tris-Acetate 1 mM EDTA
Transfer buffer	1.44% Glycine 0.3% Tris 80% v/v ddH <sub>2</sub> O 20% v/v MeOH
Upper gel buffer	0.5 M Tris-HCl (pH 6.8) Autoclave

### 12.1.4 Enzymes and proteins

Collagenase IV	Sigma; C5138
DNase	Sigma; DN25
Human recombinant Cytochrome P450 2D6	Invitrogen; P2774
Human recombinant IL-2	Cell Concepts; C-20002-F
M-MLV-reverse transcriptase	Promega; M1705
Proteinase K	Carl Roth; 7528.1
RNase OUT	Invitrogen; 10777-019
RQ1 RNase-free DNase	Promega; M6101
Superscript II reverse transcriptase	Invitrogen; 18064-022
Taq-polymerase	Peqlab Biotechnologie GmbH; 01-1030

### 12.1.5 Nucleotides and nucleic acids

61x 20mer sequences of cytochrome P450 2D6	Ma et al. Gastroenterology 2006 (Figure 25)
CpG	IDT; ODN1826
CYP2D6 F Primer	5' AGA AGG GGA AGC AGG TTT G 3'
CYP2D6 R Primer	5' CGG CAC TCA GGA CTA ACT CAT C 3'
dNTP	Peqlab; 20-2011
Random Primers	Fermentas; S0142

## 12.1.6 Antibodies

### Antibodies used for FACS-staining

APC-anti-mouse CD8a/Lyt-2 (Clone 53-6.7)	Southern Biotech; 1550-11
FITC-anti-mouse CD4/L3T4 (Clone GK 1.5)	Southern Biotech; 1540-02
FITC-anti-mouse CD45R/B220 (RA3-6B2)	BD Pharmingen; 553088
FITC-anti-mouse CD8a/Lyt-2 (Clone 53-6.7)	Southern Biotech; 1550-02
PE-anti-mouse CD11c (p150/90)	eBioscience; 12-0114-82
PE-anti-mouse IFN- $\gamma$	BD Pharmingen; 5544412
PE-Cy5-anti-mouse CD8a/Lyt-2 (Clone 53-6.7)	Southern Biotech; 1550-16
Streptavidin-APC	Southern Biotech; 7100-11M

### Antibodies used for ELISA

AP-goat anti-mouse IgG	Southern Biotech; 1030-04
AP-goat anti-mouse IgM	Southern Biotech; 1020-04
AP-rat anti-mouse IgE	Southern Biotech; 1130-04

### Antibodies used for ELISPOT

Biotinylated-goat anti-mouse IgG ( $\gamma$ -chain-specific)	Southern Biotech; 1030-08
Biotinylated-goat anti-mouse IgM ( $\mu$ chain-specific)	Southern Biotech; 1020-08
Goat anti-mouse IgG+IgA+IgM (H+L)	Caltag Laboratories; M30900
HRPO-Avidin D	Vector Laboratories Inc.; A-2004

### Antibodies used for Western Blot

IRDye800-Donkey anti-mouse IgG (H+L)	Rockland; 610-732-124
IRDye800-Donkey anti-rabbit IgG (H+L)	Rockland; 611-732-127
Rabbit anti-Adenovirus type 5	Abcam; ab6982
Rabbit anti-Cytocrome P450 2D6	Abcam; ab4238-50

### Antibodies used for Histology

Anti-mouse CD4/L3T4 (Clone GK 1.5)	BD Pharmingen; 553043
Anti-mouse CD45R/B220 (RA3-6B2)	BD Pharmingen; 553084
Anti-mouse CD8a/Lyt-2 (Clone 53-6.7)	BD Pharmingen; 553027
Anti-mouse Collagen type I	Chemicon; AB765P
Anti-mouse F4/80	Serotec; MCAP497
Biotinylated anti-goat IgG (H+L)	Vector; BA-5000
Biotinylated anti-Guinea Pig IgG (H+L)	Vector; BA-7000
Biotinylated anti-hamster IgG (H+L)	Vector; BA-9100
Biotinylated anti-rabbit IgG (H+L)	Vector; BA-1000
Biotinylated anti-rat IgG (H+L)	Vector; BA-4001

### Antibodies used for B cell epitope mapping

IRDye800-Donkey anti-mouse IgG (H+L)	Rockland; 610-732-124
--------------------------------------	-----------------------

### 12.1.7 Kits

Alanine aminotransferase assay	Biotron Diagnostics INC.; 68-D
Asparate aminotransferase assay	Biotron Diagnostics INC.; 66-D
Avidin/Biotin blocking Kit	Vector; SP-2001
Cytotoxicity Detection Kit (LDH)	Roche; 11644793001
Mouse B cell enrichment Kit	EasySep; 19754
Mouse T cell enrichment Kit	EasySep; 19751
Peroxidase Substrate Kit DAB	Vector; SK-4100
Quantitec SYBR Green PCR	Qiagen; 204143
RNeasy Mini Kit	Quiagen; 74104
Roti-Histokitt	Roth; 6638.1
Roti-Quant Protein assay	Roth;
SlowFade Antifade Kit	Molecular Probs; S2828

### 12.1.8 Human Sera

All human sera, kindly provided by Prof. Dr. M. P. Manns, were from the human serum library of the Department of Gastroenterology, Hepatology and Endocrinology of the Medizinische Hochschule Hannover and have been previously tested for antigen-specificity by standardized immunofluorescence and competitive ELISA procedures. All patients have been clinically diagnosed with either type of AIH or PBC. The blood procurement protocol and analysis was approved by the Ethics Committee of the Medizinische Hochschule Hannover.

### 12.1.9 Cell lines

HEK-293 are adherent epithelial cells from human fetal kidney that contain left end sequences of the adenovirus 5 DNA (RF32764) and were originally provided by F.L. Graham. ATCC Nr: CRL-1573.

### 12.1.10 Viruses

Ad-2D6, obtained via Prof. Eric F. Johnson (The Scripps Research Institute, La Jolla, CA) was created by homologous recombination in *Escherichia coli* BJ5183 between a shuttle vector containing the cDNAs for CYP2D6 and pAdE1-E3 (82).

Ad-GFP was a gift from D.J. von Seggern (The Scripps Research Institute, La Jolla, CA).

### **12.1.11 Mice strains**

CYP2D6 humanized mice, generated by microinjection of the entire human CYP2D6 gene, including its promoter region, into the pronucleus of fertilized FVB/N mouse eggs to produce a transgenic mouse line (77), were provided by F.J. Gonzalez (National Cancer Institute, Bethesda, MD).

Wild-type FVB/NHsd mice were purchased from the breeding colony of Harlan Netherlands.

Wild-type C57BL/6 mice were purchased from the breeding colony of Harlan Netherlands.

Wild-type Balb/c mice were purchased from the breeding colony of Harlan Netherlands.

Experiments were carried out with age- and sex-matched animals kept under specific pathogen free (SPF) conditions and in accordance with German regulations. All animal experiments were approved by the local Ethics Animal Review Board (Darmstadt, Germany).

## **12.2 Methods**

### **12.2.1 Cell biological methods**

#### **12.2.1.1 Cultivation of cells**

Cells were cultured in plastic cell culture flasks (25, 75 or 175 cm<sup>2</sup>) at 37°C (5% CO<sub>2</sub>, relative humidity 95%) with appropriate medium.

Adherent cells were split when confluent. For this, medium was removed from the culture flask, the cellular monolayer was rinsed with 10 ml sterile PBS and the cells were incubated for 5–10 minutes at 37°C in 3 ml of trypsin-EDTA solution to detach the cells from the plastic. The detached cells were collected, resuspended in appropriate medium and split.

### **12.2.1.2 Freezing of cells**

A freezing container was pre-cooled for 30 minutes at 4°C. The freezing medium was prepared containing 90% FCS and 10% DMSO. Cells were trypsinized, washed with PBS and centrifuged at 1,500 rpm for five minutes. Cells were re-suspended in 1 ml of pre-cooled freezing medium and 1 ml aliquots were transferred into cryotubes. The aliquots were placed into the freezing container and transferred to -70°C. The freezing containers ensure that the cell samples are cooled down to -70°C at a rate of 1°C/min. After 48 hours, the cryotubes were transferred to the liquid nitrogen tank (-196°C).

### **12.2.1.3 Thawing of cells**

Cell aliquots were taken out of the liquid nitrogen tank and warmed immediately in a water bath to 37°C. Cells were transferred to a 50 ml Falcon tube and the appropriate medium was added slowly in the beginning until 20x the freezing volume was achieved. This procedure prevents cell damage due to osmotic shock. Cells were centrifuged and washed again with the medium. They were checked for their viability by trypan blue stain. Cells were cultured in appropriate conditions and the following day the cells were evaluated for viability and density.

### **12.2.1.4 Determining the density of a cell suspension**

The cellular density of a suspension was determined by mixing 10-20 µl of the cell suspension with an equal volume of Trypan blue solution. The cells in the resulting suspension were counted directly in a Neubauer chamber using a microscope. Dead cells were identified by cytoplasmic staining with Trypan blue. A grid at the bottom of the chamber was used to count the cells and the cell density (cells per ml) was calculated with the following formula:

$$\text{Cellular density (cells/ml)} = \text{number of cells on the grid} \times \text{dilution factor} \times 10^4 \text{ ml}^{-1}$$

### **12.2.1.5 Isolation of liver lymphocytes**

Liver cells were isolated by squeezing the liver through a 70 µm nylon cell strainer with a syringe plunger in 10 ml PBS. The cell suspension was

transferred to a 50 ml falcon tube and 10 ml collagenase buffer was added. After 45 – 60 minutes incubation at 37°C the cell suspension was centrifuged at 30 g for three minutes and the supernatant was transferred to a fresh 50 ml falcon tube. The supernatant was centrifuged at 650 g for 10 minutes and the pellet was resuspended in 20 ml percoll buffer and centrifuged again at 600 g for 20 minutes. The liver lymphocytes in the pellet were resuspended in RPMI 10% FCS and kept at 4°C until use.

#### **12.2.1.6 Isolation of splenocytes**

Spleen cells were isolated by squeezing the spleen through a 70 µm nylon cell strainer with a syringe plunger in 10 ml RPMI. With a pipette a single cell suspension was prepared in 10 ml RPMI. Residual tissue was removed by a quick spin at 1200 rpm for 10 seconds. The supernatant was centrifuged at 1500 rpm for five minutes at 4°C. To eliminate the red blood cells the pellet was resuspended in 5 ml 0.83% NH<sub>4</sub>Cl in PBS and incubated for one to two minutes at room temperature. To stop the reaction 5 ml RPMI 10% FCS was added and the cells were centrifuged at 1500 rpm for five minutes at 4°C. The cell pellet was resuspended in RPMI 10% FCS and the cells were kept at 4°C until use.

#### **12.2.1.7 Enzyme Linked Immunosorbent Assay (ELISA)**

To detect antibodies specific for human CYP2D6, 96-well microtiterplates were coated overnight at 4°C with 0.25 µg/ml recombinant human CYP2D6 in 100 µl of ELISA coating buffer and plates were blocked with 200 µl ELISA blocking buffer for 90 minutes at room temperature. Blocking buffer was removed and the plates were washed four times with 150 µl ELISA washing buffer. Sera were added in PBS containing 2% FCS and were incubated for 90 minutes at 37°C. The dilution series for each serum started at 1:300, followed by 1:3 dilution steps down to a final dilution of 1:656,100. After washing the plates four times with ELISA washing buffer 100 µl alkaline phosphatase labeled goat anti-mouse IgM or IgG antibody diluted 1:2000 in PBS containing 2% FCS was added for 90 minutes. After washing an

additional four times with ELISA washing buffer the reaction was developed by addition of 30 µl ECF substrate. Fluorescence intensity was determined using a Storm 560 (GE Healthcare Bio-Sciences). Sera dilutions with values of three standard deviations above the mean value of negative controls were considered positive.

#### **12.2.1.8 Detection of antibody-secreting cells (ELISPOT)**

To detect total or CYP2D6-specific antibody-secreting cells, 96-well filter plates were coated with 5 µg/ml of goat anti-mouse IgG+IgA+IgM or 0.25 µg/ml human CYP2D6 in PBS overnight at 4°C. After washing the plates once with 200 µl ELISPOT washing buffer and three times with 200 µl PBS the plates were blocked with 10% FCS in RPMI 1640 for two hours at room temperature. Total splenocytes diluted in DMEM containing 10% FCS were added in triplicates and incubated for five hours at 37°C in 5% CO<sub>2</sub>. The dilution series for each sample started at 1x10<sup>6</sup> cells in the first row and 5x10<sup>5</sup> cells in the 2<sup>nd</sup> row, followed by six 1:3 dilution steps. After washing the plates three times with 200 µl PBS and three times with ELISPOT washing buffer 50 µl biotinylated goat anti-mouse IgG diluted 1:1000 in PBS containing 0.05% Tween-20 and 1% FCS was added and plates were incubated overnight at 4°C. Plates were washed four times with 200 µl ELISPOT washing buffer. 50 µl 1:1000 diluted horseradish peroxidase-conjugated Avidin D in PBS containing 0.05% Tween-20 and 1% FCS was added for 60 minutes at room temperature. After washing the plates three times with 200 µl ELISA washing buffer and three times with PBS the reaction was developed by the addition of freshly prepared AEC substrate.

#### **12.2.1.9 Flow cytometry**

##### *FACS staining of blood, spleen and liver cells*

Cells were harvested and centrifuged at 1500 rpm for five minutes. Erythrocytes were lysed by resuspending the cell pellet with 5 ml 0.83% NH<sub>4</sub>Cl, wait for two minutes and adding 5 ml RPMI containing 10% FBS to stop the reaction. Around 10<sup>6</sup> cells were transferred to a V-bottom 96-well

plate. The cells were washed once by spinning the plate at 1600 rpm for five minutes at 4°C, resuspending with 150 µl FACS PBS/staining buffer and spinning again for five minutes. The cells were stained with fluorochrome labeled antibody of choice in 50 µl PBS/staining buffer for at least 20 minutes at 4°C in the dark. After two additional washes with 150 µl PBS/staining buffer the cells were resuspended in 200 µl PBS/staining buffer and transferred to FACS-tubes. Cells were fixed by addition of 100 µl FACS fixation buffer and analyzed by flow cytometry at a FACS Calibur (BD FACS Calibur).

### **12.2.1.10 Intracellular cytokine stain (ICCS)**

#### *Restimulation of lymphocytes*

Cytotoxic T lymphocytes (CTLs) produce Interferon  $\gamma$  (IFN $\gamma$ ) after stimulation; therefore intracellular staining for IFN $\gamma$  was used to quantify specific and functionally competent CTLs.

100 µl lymphocytes at 10<sup>7</sup> cells/ml in RPMI 10% FCS, 50 µl of the specific stimulant (8 µg/ml CYP2D6 20-mers) and 50 µl RPMI 10% FCS containing 4 µg/ml Brefeldin A (to block secretion of IFN $\gamma$ ) were added per well of a flat-bottom 96 well plate. Negative and positive controls were included adding 50µl of medium or 50µl of 20 ng/ml Phorbol 12-myristate 13-acetate (PMA, T cell activator) and 2 mg/ml Ionomycin respectively. The plate was incubated for six hours or overnight at 37°C, 5% CO<sub>2</sub>. The cells were resuspended and transferred to a 96-well V-bottom plate and ready for staining.

#### *Staining*

After the cells were washed twice by resuspending with 150 µl PBS/staining buffer and spinning at 1600 rpm for five minutes at 4°C the cells were stained with fluorochrome labeled anti-CD8 and/or anti-CD4 antibody in 50 µl PBS/staining buffer for at least 20 minutes at 4°C in the dark. After two additional washes with 150 µl PBS/staining buffer the cells were fixed and permeabilised with 100 µl of PFA/saponin solution for 10 minutes at room temperature. After the cells were washed twice by resuspending with 150 µl

PBS/saponin buffer and spinning at 1600 rpm for seven minutes at 4°C the cells were stained with PE-conjugated anti-mouse-IFN $\gamma$  antibody in 50  $\mu$ l PBS/saponin buffer for 30 minutes at 4°C in the dark. After washing the cells two times with PBS/saponin buffer and once with PBS/staining buffer the cells were resuspended in 200  $\mu$ l PBS/staining buffer and transferred to FACS-tubes. Cells were fixed by addition of 100  $\mu$ l FACS fixation buffer and analyzed by flow cytometry.

### **12.2.1.11 Adenovirus production**

HEK-293 cells were cultivated in 175 cm<sup>2</sup> flasks in 293-medium (DMEM + Glutamax containing 10% FCS, 1% penicillin, 1% streptomycin, 1% HEPES and 1% non-essential aa). Medium was removed from the confluent flasks and cells were infected with either Ad-GFP or Ad-2D6 with a MOI of 50 in a total volume of 15 ml 293-medium. After four hours incubation at 37°C, 5% CO<sub>2</sub> 15 ml pre-warmed 293-medium was added and the cells were incubated at 37°C, 5% CO<sub>2</sub> for three days or until most cells were detached as clusters. The content of all flasks was transferred to 50 ml falcon tubes and centrifuged at 1100 rpm for five minutes at 4°C. After centrifugation the supernatant was discarded and three pellets were combined in 1 ml 293-medium. The cells were transferred to cryotubes, snap-frozen in liquid nitrogen and stored for later purification at -80°C.

### **12.2.1.12 Adenovirus purification**

Cryotubes containing adenovirus-infected cells were put through four rapid thaw/freeze cycles by thawing them at 37°C, vortexing and refreeze in liquid nitrogen. The resulting cell lysate was pooled in a 15 ml falcon tube and centrifuged at 1500 g for 10 minutes at 4°C. The supernatant was transferred to a 50 ml falcon tube and mixed with 18 ml 293-medium. Very slowly 3 ml of the cleared cell lysate was transferred onto a CsCl gradient previously prepared by overlaying 4 ml 40% CsCl in PBS with 4.5 ml 15% CsCl in PBS in an ultracentrifuge tube. The cell lysate was centrifuged at 25'400 rpm for 17 hours at 4°C resulting in an upper (immature virus) and lower (mature

virus) virus band. To collect the mature virus a 23G needle connected to a 2 ml syringe was carefully inserted into the ultracentrifuge tube directly under the lower virus band and the virus was slowly aspirated. The virus was transferred to a slide-a-lyzer cassette (10 kDa) and dialyzed against 2 liter cold PBS for six hours and then over night after a PBS change. In the morning the virus was collected and transferred to a 15 ml falcon tube. After the virus particle concentration was determined by a protein assay the virus was diluted in PBS and glycerol was added to a 10% final concentration. The virus was then transferred to cryotubes, snap-frozen in liquid nitrogen and stored at -80°C.

#### **12.2.1.13 Cytopathic effect assay**

A cytopathic effect assay was performed to determine Adenovirus titers (110). The assay was performed in tissue culture grade 96-well plates.

90 µl of DMEM 3% FCS was added to each well of a 96-well plate. Virus was diluted 1:100 in DMEM 3% FCS and 10 µl were added in triplicates to wells of the first column. Dilutions were made with a multi-channel pipette by taking 10 µl from the first column, adding to the next column, mixing, carrying over 10 µl etc, which corresponded to a stepwise dilution of 1:10. Tips were changed after each dilution step.

To each well of the 96-well plates,  $3-5 \times 10^4$  HEK-293 cells were added starting from the side with the highest virus dilution and the plates were put into a 5% CO<sub>2</sub> incubator at 37°C for 5-10 days or until a confluent cell-monolayer has formed. After incubation 90 µl of medium were carefully removed from each well and cells were fixed by addition of 150 µl 10% formaldehyde in PBS for 10 minutes at room temperature. After staining for five minutes with 0.1% crystal violet the plates were washed with water and dried inverted on absorbent paper. The viral titer is defined as the titer, which causes lysis of the cells in 50% of the wells in a given dilution and is defined as tissue culture infectious dosis 50% (TCID<sub>50</sub> units). TCID<sub>50</sub> are calculated by the Reed-Muench method as follows:

$$\text{Proportionate distance} = \frac{(\% \text{ positive above } 50\%) - 50\%}{(\% \text{ positive above } 50\%) - (\% \text{ positive below } 50\%)}$$

$$\log ID_{50} = (\log \text{ dilution above } 50\%) + (\text{proportionate distance} \times \log \text{ dilution factor})$$

$$\text{TCID}_{50} \text{ per unit volume} = \frac{1}{ID_{50}} \times \frac{1}{\text{virus volume inoculation}}$$

#### **12.2.1.14 Immunohistological stainings**

##### *Immunohistochemical stainings*

Livers were harvested at the times indicated, immersed in Tissue-Tek OCT, and quick-frozen on dry ice. 6 µm tissue sections were cut using a cryomicrotome and mounted on sialin-coated slides. After fixing the sections in 90% ethanol at -20°C for 15 minutes, the sections were put on a paper towel to dry for 10 minutes and circles were drawn around the specimen with a wax pencil. The sections were washed two times in PBS for two minutes and incubated in 0.3% H<sub>2</sub>O<sub>2</sub>/0.1% Na-azid in PBS for 15 minutes at room temperature. After washing two times in PBS for two minutes one drop of avidin was placed on each specimen and incubated for 10 minutes at room temperature. The sections were washed again and one drop of biotin was placed on each specimen and incubated for 10 minutes at room temperature. After an additional washing step, a few drops of 10% FBS in PBS was added and incubated for 15 minutes at room temperature. The 10% FBS in PBS was tapped off, the sections were washed quickly in PBS and 100 µl of the first antibody diluted 1:200 in 10% FBS in PBS was added on each specimen and incubated for one hour at room temperature in a humidified chamber. After tapping off the first antibody solution, the sections were washed two times in PBS for four minutes and 100 µl of biotinylated secondary antibody diluted 1:200 in 10% FBS in PBS was added on each specimen and incubated for 45 minutes at room temperature in a humidified chamber. The secondary antibody solution was tapped off and sections were washed two times for four minutes in PBS. One drop of ABC reagent solution was added on each specimen and incubated for 30 minutes at room temperature. After tapping off the remaining ABC reagent and two washes in

PBS for four minutes 100  $\mu$ l peroxidase substrate was added on each specimen and incubated for five minutes at room temperature. The reaction was stopped by washing in PBS and the sections were counterstained in hematoxylin solution for five minutes at room temperature and washed two times in PBS. After adding two drops of aquamount onto each section a coverslip was placed onto each slide. The sections were then incubated at room temperature for more than two hours and pictures were made at a Microscope (Biozero BZ-8000, Keyence).

### *Sirius red staining of collagen fibers*

Livers were harvested at the times indicated, immersed in Tissue-Tek OCT, and quick-frozen on dry ice. 6- $\mu$ m tissue sections were cut using a cryomicrotome and mounted on sialin-coated slides. After fixing the sections in 90% ethanol at -20°C for 15 minutes, the sections were put on a paper towel to dry for 10 minutes and circles were drawn around the specimen with a wax pencil. 120  $\mu$ l Sirius red solution was added on each specimen and incubated for one hour at room temperature. After washing two times in 0.01 N HCl for two minutes, the sections were rinsed in H<sub>2</sub>O and dehydrated in three changes of absolute ethanol for one minute each. The sections were incubated two times in xylene for two minutes and a few drops of Roti-Histokit I was placed onto each slide and covered with a coverslip.

### *Immunofluorescence stainings*

Livers were harvested at the times indicated, immersed in Tissue-Tek OCT, and quick-frozen on dry ice. 6- $\mu$ m tissue sections were cut using a cryomicrotome and mounted on sialin-coated slides. After fixing the sections in 90% ethanol at -20°C for 15 minutes, the sections were put on a paper towel to dry for 10 minutes and circles were drawn around the specimen with a wax pencil. The sections were washed two times in PBS for two minutes and incubated for 30 minutes with PBS containing 10% FBS. After tapping off the PBS/FCS blocking solution the sections were washed in PBS and the first antibody diluted 1:200 in PBS containing 10% FBS was added to the

sections and incubated for two hours at room temperature in the dark. After washing three times in PBS for four minutes the fluorescent-labeled secondary antibody diluted 1:200 in 10% FBS PBS was added and the sections were incubated for one hour at room temperature in a humidified chamber. The secondary antibody solution was tapped off and the sections were washed three times in PBS for four minutes and then mounted in immunofluore mounting medium.

#### **12.2.1.15 Serum values for liver damage**

##### *Alanine aminotransferase (ALT) and aspartate aminotransferase (AST)*

ALT and AST were determined by using serum aminotransferase enzyme activity assays (BioTron Diagnostics Inc.). In brief, 37.5 µl of serum glutamate-pyruvate transaminase (SGPT) reagent or serum glutamate-oxalacetate transaminase (SGOT) reagent respectively, were added to 96-well flat bottom microtiterplates. After addition of 7.5 µl sera and standards, plates were incubated for 40 minutes at 37°C. After incubation 37.5 µl of ALT or AST color developer A were added and plates were incubated for further 15 minutes at 37°C. In the end 150 µl ALT or AST color developer B was added and after 5 minutes incubation at room temperature the OD was read at 540 nm using a microplate reader (Sunrise, Tecan). ALT and AST Serum levels (Units/l) were calculated using the normal and abnormal standards.

##### *Alkaline Phosphatase (AP) and Gamma Glutamyl Transpeptidase (GGT)*

AP and GGT were measured by the central laboratory of the Clinic of the Johann Wolfgang Goethe University in Frankfurt am Main. The sera were diluted 1:4 prior to measurement.

#### **12.2.1.16 Preparation of microsomes from liver homogenates**

Livers were harvested and homogenized with a tissue homogenizer in 20 ml PBS. To get rid of the large cell debris and nuclei the liver homogenate was centrifuged at 3'000 g for 15 minutes and the supernatant was transferred to a new tube. The supernatant was then centrifuged at 20'000 g for 15 minutes

to pellet the mitochondria and larger membrane fractions. After the supernatant was transferred to a new tube it was centrifuged at 100'000 g for one hour. After the supernatant containing the cytoplasm was discarded the pellet containing the microsomes was resuspended in 5 ml PBS and the protein concentration was measured.

#### **12.2.1.17 MACS purification of B cells and T cells**

Lymphocytes were harvested either from the spleen or liver and resuspended at a concentration of  $1 \times 10^8$  cells/ml in PBS containing 2% FCS and 5% normal rat serum in a FACS tube. A small sample was collected for FACS analysis of pre-separated cells. EasySep negative selection mouse enrichment cocktail was added at a concentration of 50  $\mu$ l/ml of cells and the suspension was incubated for 15 minutes at 4°C. After incubation EasySep biotin selection cocktail was added at a concentration of 100  $\mu$ l/ml of cells and after 15 minutes incubation at 4°C magnetic nanoparticles at a concentration of 50  $\mu$ l/ml of cells were added and the cell suspension was mixed by pipetting. After 15 minutes incubation at 4°C the cell suspension was filled up to 2.5 ml with PBS containing 2% FCS and mixed. The cells were then placed for five minutes in an EasySep magnet at room temperature and after incubation the EasySep magnet was inverted in one continuous motion and the cell suspension collected in a FACS tube. This separation process was repeated two more times. A small sample was collected for FACS analysis of separated cells and cells were used for further experiments.

### **12.2.2 Molecular biological methods**

#### **12.2.2.1 Mouse tail DNA isolation**

Tail biopsies (0.3 cm) were digested overnight with 5  $\mu$ l of proteinase K (10 mg/ml) in 500  $\mu$ l of proteinase K buffer at 55°C. 75  $\mu$ l of 8M KOAc and 500  $\mu$ l chloroform were added and the tubes were inverted several times, incubated at -70°C for 15 minutes and centrifuged for five minutes at 14'000 rpm in a micro-centrifuge. Then the supernatant was transferred to new tubes, 1 ml of

ethanol was added and the tubes were inverted several times. After centrifugation at 14'000 rpm for 10 minutes the supernatant was removed and the DNA pellet was washed with 1 ml of 70% ethanol. DNA was air dried for 10 to 30 minutes and then re-dissolved in 100 µl TE buffer and stored at 4°C.

### **12.2.2.2 RNA extraction from tissues**

Tissues were harvested and homogenized in 1 ml TRI reagent per 50-100 mg tissue with a tissue homogenizer. Per 50-100 mg tissue 0.2 ml chloroform was added and the homogenate was vortexed for 15-20 seconds. After 2-15 minutes incubation at room temperature the homogenate was centrifuged at 12'000 g for 15 minutes at 4°C. After centrifugation the upper aqueous phase was transferred into a new tube and 0.5 ml isopropanol was added. The tubes were inverted several times and after an incubation of 5-10 minutes centrifuged at 12'000 g for eight minutes. The supernatant was removed and the RNA pellet was washed with 1 ml 75% ethanol. After centrifugation at 7'500 g for five minutes the RNA pellet was air dried for 5-10 minutes and then re-dissolved in an appropriate volume of H<sub>2</sub>O<sub>DEPC</sub> and incubated at 56°C for 10 minutes. The RNA concentration was determined on a Nano-drop (ND-1000 Spectrometer) and the RNA was stored at -80°C for further usage.

### **12.2.2.3 Polymerase chain reaction (PCR)**

PCR was used to amplify the transgenic insert of the CYP2D6 mice for screening (77).

*The components of the PCR reaction:*

ddH <sub>2</sub> O	19.9 µl
10x PCR buffer	2.5 µl
10 mM dNTP-Mix	0.5 µl
10 µM CYP2D6 R Primer	0.5 µl
10 µM CYP2D6 F Primer	0.5 µl
TAQ-Polymerase	0.1 µl
DNA	1 µl

### *Cycling:*

5 minutes initial denaturation at 94°C

35 cycles:

30 seconds denaturation at 94°C

30 seconds primer annealing at 56°C

1 minute elongation at 72°C

3 minute additional elongation at 72°C

Cool to 4°C

For all reactions a water sample was included as negative control to confirm the viability of the PCR result. PCR products were analyzed by agarose gel electrophoresis.

#### **12.2.2.4 DNA agarose gel electrophoresis**

Separation of DNA fragments of different sizes was achieved by agarose gel electrophoresis. A 1% agarose gel was routinely used as the expected size of the fragments was between 0.5 and 10 kb. Agarose was dissolved in TAE buffer by boiling. After cooling to hand temperature 1 µg/ml Ethidium bromide was added while stirring. The solution was poured into an appropriate gel tray with inserted combs. Following cooling and solidification the combs were removed and the gel was placed into an electrophoresis container containing 1x TAE as running buffer. The slots were loaded with DNA samples to which 16% of 6x DNA loading dye was added. An appropriate DNA molecular weight marker was run in parallel in order to evaluate molecular weights of the DNA fragments. The voltage applied for the separation was 5V per cm space between the two electrodes. The gels were run for 20-120 minutes and the separated DNA bands were visualized and pictures were taken under UV irradiation (300 nm).

#### **12.2.2.5 Quantification of DNA, RNA and proteins**

DNA and RNA concentrations were measured on a Nano-drop (ND-1000 Spectrometer).

Protein concentrations were measured with a Bio-rad Protein assay and the standard protocol was followed. In brief, 50  $\mu$ l PBS and 50  $\mu$ l protein sample were mixed and 2-fold serial diluted with PBS over 11 steps of a 96-well flat bottom plate. The standard solution (2 mg/ml) was serial diluted 2-fold with PBS in duplicates and two wells were filled with 100  $\mu$ l PBS as blank controls. Color developer was diluted 1:5 in PBS, 200  $\mu$ l were added to all wells and the plate was measured at 595 nm with an ELISA microplate reader (Sunrise, Tecan).

#### **12.2.2.6 B cell epitope mapping**

Arrays of 162 staggered 12mer synthetic peptides covering the entire human CYP2D6 sequence were covalently linked to nylon membranes (custom SPOTs service; Sigma-Aldrich). The N-terminal aa of the 12mer peptides were shifted within the human CYP2D6 by three aa residues. Membranes were blocked for six hours at room temperature in 2% dry milk/PBS before they were incubated overnight at 4°C with serum diluted 1:200 in SPOT washing buffer. Membranes were washed four times in SPOT washing buffer and were then incubated at room temperature for two hours with IRDye800 labeled secondary antibody diluted 1:20'000 in SPOT washing buffer. After two washes in SPOT washing buffer and three washes in PBS, fluorescence intensity was analyzed using an infrared imaging system (Odyssey; LI-COR Bioscience GmbH).

#### **12.2.2.7 SDS PAGE**

For the separation of proteins, first an appropriate separating gel (10% for cytochrome P450 2D6 and 12% for adenovirus type 5 separation) was prepared using a 0.75 mm spacer:

	10%	12%
Acrylamide	3.33 ml	4 ml
Lower gel buffer	2.5 ml	2.5 ml
Distilled water	4.07 ml	3.4 ml

SDS (20% w/v)	50 $\mu$ l	50 $\mu$ l
TEMED	5 $\mu$ l	5 $\mu$ l
APS (10% w/v)	50 $\mu$ l	50 $\mu$ l

Just after adding the TEMED and APS, the acrylamide solution was poured to about 5.3 cm from the bottom. During polymerisation an isopropanol or water overlay was added. After more than one hour of polymerisation the overlay was removed and a 3% stacking gel was prepared:

	10%
Acrylamide	0.5 ml
Upper gel buffer	1.25 ml
Distilled water	3.25 ml
SDS (20% w/v)	25 $\mu$ l
TEMED	5 $\mu$ l
APS (10% w/v)	25 $\mu$ l

Immediately after pouring, the comb was added. Samples were heated for 5 minutes to 95°C in 1x Laemmli sample buffer. After polymerization, the comb was removed and the wells were washed with 1x Running buffer to remove any unpolymerised acrylamide. The gels were mounted in the electrophoresis apparatus and the inner chamber was filled with 1x Running buffer. The samples were loaded and the outer chamber was also filled with Running buffer. Electrophoresis was performed at 125–140 V until the front reached the bottom of the gel (about one hour).

### **12.2.2.8 Western blotting**

A PVDF membrane (5.2 x 8.5 cm) was prepared and put into methanol for five seconds. The membrane and four pieces of Whatman paper (6 x 9 cm) were equilibrated in transfer buffer for five minutes. The gel and the membrane were put into the blotting apparatus together with the Whatman paper in the following order: 2 Whatman paper – membrane – gel – 2 Whatman paper. Air bubbles in between were removed by rolling a glass

pipette over the stock. The proteins were blotted onto the membrane at constant 125 mA for one and a half hours.

For blocking, the membrane was incubated for two hours at room temperature in PBS 5% milk containing 0.1% Tween-20 on a shaker. The primary antibody was diluted 1:2'000 (anti-Cytochrome P450 2D6) or 1:4'000 (anti-Adenovirus type 5) in PBS 5% milk containing 0.1% Tween-20. The membrane was incubated over night at 4°C together with 10 ml of the antibody solution. After washing six times with PBS 5% milk containing 0.1% Tween-20 for 5 minutes, the second stage antibody, an IRDye conjugated monoclonal anti-rabbit IgG was added at a dilution of 1:20'000 in 10ml PBS 5% milk containing 0.1% Tween-20. The membrane was incubated together with this solution at room temperature for two hours, washed three times with PBS 5% milk containing 0.1% Tween-20 and another three times with PBS for 5 minutes. The separated protein bands were visualized and pictures were taken on a Pharos (Pharos FX Plus Molecular Imager, Bio Rad)

### **12.2.3 Experiments with mice**

#### **12.2.3.1 Serum collection**

Mice were anesthetized with isofluran and blood samples were taken retro-orbitally with a heparin coated capillary and collected in an eppendorf tube. The blood was then centrifuged for 10 minutes at 6'000 rpm in a microcentrifuge and serum was transferred to a new eppendorf tube and stored at -80°C. Serum was collected at various time points as indicated.

#### **12.2.3.2 Injections**

Unless described otherwise, mice were injected with a total of  $2 \times 10^{10}$  particles of Ad-2D6 or Ad-GFP (*i.p.* and *i.v.*).

##### *Intravenous injections (i.v.)*

Mice were anesthetized with isofluran and 100 µl virus, human recombinant CYP2D6 alone or in combination with CpG or pIC were injected with a syringe retro-orbitally at the time points indicated.

### *Intraperitoneal injections (i.p.)*

Mice were held in one hand and 100 µl virus were injected with a syringe intra peritoneal.

### *Subcutaneous injections (s.c.)*

Mice were anesthetized with isofluran and 100 µl CFA or IFA emulsified using two glass syringes were injected with a syringe under the skin at several locations on the back of the mouse.

### **12.2.3.3 Liver perfusions**

Mice were anesthetized with isofluran and killed by cervical dislocation. After the abdomen had been opened the hepatic vein and hepatic artery were cut and the liver was perfused with ~5 ml PBS through the hepatic portal vein. The liver was removed and appropriately stored for further processing.

## 13References:

1. Goldsby, R. 2000. *Kuby Immunology*. New York: W.H. Freeman and Company.
2. Murphy, K. 2008. *Janeway's immunobiology*. New York: Garland Science, Taylor & Francis Group, LLC.
3. Zinkernagel, R.M., and Doherty, P.C. 1974. Restriction of in vitro T cell-mediated cytotoxicity in lymphocytic choriomeningitis within a syngeneic or semiallogeneic system. *Nature* 248:701-702.
4. Bettelli, E., Oukka, M., and Kuchroo, V.K. 2007. T(H)-17 cells in the circle of immunity and autoimmunity. *Nat Immunol* 8:345-350.
5. Schwartz, R.H. 2005. Natural regulatory T cells and self-tolerance. *Nat Immunol* 6:327-330.
6. Limmer, A., Ohl, J., Kurts, C., Ljunggren, H.G., Reiss, Y., Groettrup, M., Momburg, F., Arnold, B., and Knolle, P.A. 2000. Efficient presentation of exogenous antigen by liver endothelial cells to CD8+ T cells results in antigen-specific T-cell tolerance. *Nat Med* 6:1348-1354.
7. Goodnow, C.C. 1996. Balancing immunity and tolerance: deleting and tuning lymphocyte repertoires. *Proc Natl Acad Sci U S A* 93:2264-2271.
8. von Herrath, M., and Homann, D. 2004. Tolerance tag team. *Nat Med* 10:585-587.
9. Gonzalez, A., Katz, J.D., Mattei, M.G., Kikutani, H., Benoist, C., and Mathis, D. 1997. Genetic control of diabetes progression. *Immunity* 7:873-883.
10. Pociot, F., and McDermott, M.F. 2002. Genetics of type 1 diabetes mellitus. *Genes Immun* 3:235-249.
11. Semana, G., Allanic, H., Quillivic, F., Vallejo, M.T., Simon, J.P., Genetet, B., and Fauchet, R. 1990. Implication of the HLA-DRB3 gene in Graves' disease: predominance of allele Dw24. *Hum Immunol* 29:143-149.
12. Djilali-Saiah, I., Renous, R., Caillat-Zucman, S., Debray, D., and Alvarez, F. 2004. Linkage disequilibrium between HLA class II region and autoimmune hepatitis in pediatric patients. *J Hepatol* 40:904-909.
13. Christen, U., and von Herrath, M.G. 2004. Initiation of autoimmunity. *Curr Opin Immunol* 16:759-767.
14. Anderson, M.S., Venanzi, E.S., Klein, L., Chen, Z., Berzins, S.P., Turley, S.J., von Boehmer, H., Bronson, R., Dierich, A., Benoist, C., et al. 2002. Projection of an immunological self shadow within the thymus by the aire protein. *Science* 298:1395-1401.
15. Christen, U., and von Herrath, M.G. 2005. Infections and autoimmunity--good or bad? *J Immunol* 174:7481-7486.

16. von Herrath, M.G., Fujinami, R.S., and Whitton, J.L. 2003. Microorganisms and autoimmunity: making the barren field fertile? *Nat Rev Microbiol* 1:151-157.
17. Mena, I., Fischer, C., Gebhard, J.R., Perry, C.M., Harkins, S., and Whitton, J.L. 2000. Coxsackievirus infection of the pancreas: evaluation of receptor expression, pathogenesis, and immunopathology. *Virology* 271:276-288.
18. Oldstone, M.B. 1987. Molecular mimicry and autoimmune disease. *Cell* 50:819-820.
19. Oldstone, M.B. 1998. Molecular mimicry and immune-mediated diseases. *Faseb J* 12:1255-1265.
20. Ohashi, P.S., Oehen, S., Buerki, K., Pircher, H., Ohashi, C.T., Odermatt, B., Malissen, B., Zinkernagel, R.M., and Hengartner, H. 1991. Ablation of "tolerance" and induction of diabetes by virus infection in viral antigen transgenic mice. *Cell* 65:305-317.
21. Oldstone, M.B., Nerenberg, M., Southern, P., Price, J., and Lewicki, H. 1991. Virus infection triggers insulin-dependent diabetes mellitus in a transgenic model: role of anti-self (virus) immune response. *Cell* 65:319-331.
22. Benoist, C., and Mathis, D. 2001. Autoimmunity provoked by infection: how good is the case for T cell epitope mimicry? *Nat Immunol* 2:797-801.
23. Croxford, J.L., Anger, H.A., and Miller, S.D. 2005. Viral delivery of an epitope from *Haemophilus influenzae* induces central nervous system autoimmune disease by molecular mimicry. *J Immunol* 174:907-917.
24. Olson, J.K., Croxford, J.L., Calenoff, M.A., Dal Canto, M.C., and Miller, S.D. 2001. A virus-induced molecular mimicry model of multiple sclerosis. *J Clin Invest* 108:311-318.
25. Bach, J.F. 2005. Infections and autoimmune diseases. *J Autoimmun* 25 Suppl:74-80.
26. Rose, N.R., and Mackay, I.R. 2000. Molecular mimicry: a critical look at exemplary instances in human diseases. *Cell Mol Life Sci* 57:542-551.
27. Kirvan, C.A., Swedo, S.E., Heuser, J.S., and Cunningham, M.W. 2003. Mimicry and autoantibody-mediated neuronal cell signaling in Sydenham chorea. *Nat Med* 9:914-920.
28. Ang, C.W., Jacobs, B.C., and Laman, J.D. 2004. The Guillain-Barre syndrome: a true case of molecular mimicry. *Trends Immunol* 25:61-66.
29. Gut, J. 1998. Molecular basis of halothane hepatitis. *Arch Toxicol Suppl* 20:3-17.
30. Kretz-Rommel, A., and Rubin, R.L. 2000. Disruption of positive selection of thymocytes causes autoimmunity. *Nat Med* 6:298-305.

31. Yoshida, S., and Gershwin, M.E. 1993. Autoimmunity and selected environmental factors of disease induction. *Semin Arthritis Rheum* 22:399-419.
32. Bertolino, P., Klimpel, G., and Lemon, S.M. 2000. Hepatic inflammation and immunity: a summary of a conference on the function of the immune system within the liver. *Hepatology* 31:1374-1378.
33. Crispe, I.N. 2003. Hepatic T cells and liver tolerance. *Nat Rev Immunol* 3:51-62.
34. Calne, R.Y., Sells, R.A., Pena, J.R., Davis, D.R., Millard, P.R., Herbertson, B.M., Binns, R.M., and Davies, D.A. 1969. Induction of immunological tolerance by porcine liver allografts. *Nature* 223:472-476.
35. Guebre-Xabier, M., Schwenk, R., and Krzych, U. 1999. Memory phenotype CD8(+) T cells persist in livers of mice protected against malaria by immunization with attenuated *Plasmodium berghei* sporozoites. *Eur J Immunol* 29:3978-3986.
36. Guidotti, L.G., and Chisari, F.V. 2006. Immunobiology and pathogenesis of viral hepatitis. *Annu Rev Pathol* 1:23-61.
37. Knolle, P.A., and Gerken, G. 2000. Local control of the immune response in the liver. *Immunol Rev* 174:21-34.
38. Roland, C.R., Mangino, M.J., Duffy, B.F., and Flye, M.W. 1993. Lymphocyte suppression by Kupffer cells prevents portal venous tolerance induction: a study of macrophage function after intravenous gadolinium. *Transplantation* 55:1151-1158.
39. Yu, S., Nakafusa, Y., and Flye, M.W. 1994. Portal vein administration of donor cells promotes peripheral allospecific hyporesponsiveness and graft tolerance. *Surgery* 116:229-234; discussion 234-225.
40. Bertolino, P., Trescol-Biemont, M.C., and Rouboudin-Combe, C. 1998. Hepatocytes induce functional activation of naive CD8+ T lymphocytes but fail to promote survival. *Eur J Immunol* 28:221-236.
41. Luth, S., Huber, S., Schramm, C., Buch, T., Zander, S., Stadelmann, C., Bruck, W., Wraith, D.C., Herkel, J., and Lohse, A.W. 2008. Ectopic expression of neural autoantigen in mouse liver suppresses experimental autoimmune neuroinflammation by inducing antigen-specific Tregs. *J Clin Invest* 118:3403-3410.
42. Kisseleva, T., and Brenner, D.A. 2006. Hepatic stellate cells and the reversal of fibrosis. *J Gastroenterol Hepatol* 21 Suppl 3:S84-87.
43. Bogdanos, D.P., Invernizzi, P., Mackay, I.R., and Vergani, D. 2008. Autoimmune liver serology: Current diagnostic and clinical challenges. *World J Gastroenterol* 14:3374-3387.
44. Moritoki, Y., Lian, Z.X., Ohsugi, Y., Ueno, Y., and Gershwin, M.E. 2006. B cells and autoimmune liver diseases. *Autoimmun Rev* 5:449-457.

45. Muratori, P., Granito, A., Pappas, G., Muratori, L., Lenzi, M., and Bianchi, F.B. 2008. Autoimmune liver disease 2007. *Mol Aspects Med* 29:96-102.
46. Gershwin, M.E., and Mackay, I.R. 2008. The causes of primary biliary cirrhosis: Convenient and inconvenient truths. *Hepatology* 47:737-745.
47. Selmi, C., and Gershwin, M.E. 2004. Bacteria and human autoimmunity: the case of primary biliary cirrhosis. *Curr Opin Rheumatol* 16:406-410.
48. Selmi, C., Invernizzi, P., Keeffe, E.B., Coppel, R.L., Podda, M., Rossaro, L., Ansari, A.A., and Gershwin, M.E. 2004. Epidemiology and pathogenesis of primary biliary cirrhosis. *J Clin Gastroenterol* 38:264-271.
49. Czaja, A.J., and Norman, G.L. 2003. Autoantibodies in the diagnosis and management of liver disease. *J Clin Gastroenterol* 37:315-329.
50. Alvarez, F., Berg, P.A., Bianchi, F.B., Bianchi, L., Burroughs, A.K., Cancado, E.L., Chapman, R.W., Cooksley, W.G., Czaja, A.J., Desmet, V.J., et al. 1999. International Autoimmune Hepatitis Group Report: review of criteria for diagnosis of autoimmune hepatitis. *J Hepatol* 31:929-938.
51. Czaja, A.J., and Freese, D.K. 2002. Diagnosis and treatment of autoimmune hepatitis. *Hepatology* 36:479-497.
52. Manns, M.P., and Vogel, A. 2006. Autoimmune hepatitis, from mechanisms to therapy. *Hepatology* 43:S132-144.
53. Krawitt, E.L. 2006. Autoimmune hepatitis. *N Engl J Med* 354:54-66.
54. Zachou, K., Rigopoulou, E., and Dalekos, G.N. 2004. Autoantibodies and autoantigens in autoimmune hepatitis: important tools in clinical practice and to study pathogenesis of the disease. *J Autoimmune Dis* 1:2.
55. Gueguen, M., Boniface, O., Bernard, O., Clerc, F., Cartwright, T., and Alvarez, F. 1991. Identification of the main epitope on human cytochrome P450 IID6 recognized by anti-liver kidney microsome antibody. *J Autoimmun* 4:607-615.
56. Kerkar, N., Choudhuri, K., Ma, Y., Mahmoud, A., Bogdanos, D.P., Muratori, L., Bianchi, F., Williams, R., Mieli-Vergani, G., and Vergani, D. 2003. Cytochrome P4502D6(193-212): a new immunodominant epitope and target of virus/self cross-reactivity in liver kidney microsomal autoantibody type 1-positive liver disease. *J Immunol* 170:1481-1489.
57. Manns, M.P., Griffin, K.J., Sullivan, K.F., and Johnson, E.F. 1991. LKM-1 autoantibodies recognize a short linear sequence in P450IID6, a cytochrome P-450 monooxygenase. *J Clin Invest* 88:1370-1378.
58. Yamamoto, A.M., Mura, C., De Lemos-Chiarandini, C., Krishnamoorthy, R., and Alvarez, F. 1993. Cytochrome P450IID6 recognized by LKM1 antibody is not exposed on the surface of hepatocytes. *Clin Exp Immunol* 92:381-390.

59. Djilali-Saiah, I., Fakhfakh, A., Louafi, H., Caillat-Zucman, S., Debray, D., and Alvarez, F. 2006. HLA class II influences humoral autoimmunity in patients with type 2 autoimmune hepatitis. *J Hepatol* 45:844-850.
60. Muratori, L., Parola, M., Ripalti, A., Robino, G., Muratori, P., Bellomo, G., Carini, R., Lenzi, M., Landini, M.P., Albano, E., et al. 2000. Liver/kidney microsomal antibody type 1 targets CYP2D6 on hepatocyte plasma membrane. *Gut* 46:553-561.
61. Muratori, L., Cataleta, M., Muratori, P., Lenzi, M., and Bianchi, F.B. 1998. Liver/kidney microsomal antibody type 1 and liver cytosol antibody type 1 concentrations in type 2 autoimmune hepatitis. *Gut* 42:721-726.
62. Longhi, M.S., Hussain, M.J., Bogdanos, D.P., Quaglia, A., Mieli-Vergani, G., Ma, Y., and Vergani, D. 2007. Cytochrome P450IID6-specific CD8 T cell immune responses mirror disease activity in autoimmune hepatitis type 2. *Hepatology* 46:472-484.
63. Ma, Y., Bogdanos, D.P., Hussain, M.J., Underhill, J., Bansal, S., Longhi, M.S., Cheeseman, P., Mieli-Vergani, G., and Vergani, D. 2006. Polyclonal T-cell responses to cytochrome P450IID6 are associated with disease activity in autoimmune hepatitis type 2. *Gastroenterology* 130:868-882.
64. Lenzi, M., Ballardini, G., Fusconi, M., Cassani, F., Selleri, L., Volta, U., Zauli, D., and Bianchi, F.B. 1990. Type 2 autoimmune hepatitis and hepatitis C virus infection. *Lancet* 335:258-259.
65. Miyakawa, H., Kitazawa, E., Kikuchi, K., Fujikawa, H., Kawaguchi, N., Abe, K., Matsushita, M., Matsushima, H., Igarashi, T., Hankins, R.W., et al. 2000. Immunoreactivity to various human cytochrome P450 proteins of sera from patients with autoimmune hepatitis, chronic hepatitis B, and chronic hepatitis C. *Autoimmunity* 33:23-32.
66. Kammer, A.R., van der Burg, S.H., Grabscheid, B., Hunziker, I.P., Kwappenberg, K.M., Reichen, J., Melief, C.J., and Cerny, A. 1999. Molecular mimicry of human cytochrome P450 by hepatitis C virus at the level of cytotoxic T cell recognition. *J Exp Med* 190:169-176.
67. Dalekos, G.N., Obermayer-Straub, P., Bartels, M., Maeda, T., Kayser, A., Braun, S., Loges, S., Schmidt, E., Gershwin, M.E., and Manns, M.P. 2003. Cytochrome P450 2A6: a new hepatic autoantigen in patients with chronic hepatitis C virus infection. *J Hepatol* 39:800-806.
68. Czaja, A.J. 2006. Overlap syndrome of primary biliary cirrhosis and autoimmune hepatitis: a foray across diagnostic boundaries. *J Hepatol* 44:251-252.
69. Bowen, D.G. 2008. Of mice and molecular mimicry: modeling autoimmune hepatitis. *Hepatology* 48:1013-1015.
70. Christen, U., Holdener, M., and Hintermann, E. 2007. Animal models for autoimmune hepatitis. *Autoimmun Rev* 6:306-311.
71. Moriyama, T., Guilhot, S., Klopchin, K., Moss, B., Pinkert, C.A., Palmiter, R.D., Brinster, R.L., Kanagawa, O., and Chisari, F.V. 1990.

- Immunobiology and pathogenesis of hepatocellular injury in hepatitis B virus transgenic mice. *Science* 248:361-364.
72. Limmer, A., Sacher, T., Alferink, J., Kretschmar, M., Schonrich, G., Nichterlein, T., Arnold, B., and Hammerling, G.J. 1998. Failure to induce organ-specific autoimmunity by breaking of tolerance: importance of the microenvironment. *Eur J Immunol* 28:2395-2406.
  73. Voehringer, D., Blaser, C., Grawitz, A.B., Chisari, F.V., Buerki, K., and Pircher, H. 2000. Break of T cell ignorance to a viral antigen in the liver induces hepatitis. *J Immunol* 165:2415-2422.
  74. Djilali-Saiah, I., Lapierre, P., Vittozi, S., and Alvarez, F. 2002. DNA vaccination breaks tolerance for a neo-self antigen in liver: a transgenic murine model of autoimmune hepatitis. *J Immunol* 169:4889-4896.
  75. Lapierre, P., Djilali-Saiah, I., Vitozzi, S., and Alvarez, F. 2004. A murine model of type 2 autoimmune hepatitis: Xenoinmunization with human antigens. *Hepatology* 39:1066-1074.
  76. Christen, U., and von Herrath, M.G. 2004. Induction, acceleration or prevention of autoimmunity by molecular mimicry. *Mol Immunol* 40:1113-1120.
  77. Corchero, J., Granvil, C.P., Akiyama, T.E., Hayhurst, G.P., Pimprale, S., Feigenbaum, L., Idle, J.R., and Gonzalez, F.J. 2001. The CYP2D6 humanized mouse: effect of the human CYP2D6 transgene and HNF4alpha on the disposition of debrisoquine in the mouse. *Mol Pharmacol* 60:1260-1267.
  78. Miksys, S.L., Cheung, C., Gonzalez, F.J., and Tyndale, R.F. 2005. Human CYP2D6 and mouse CYP2Ds: organ distribution in a humanized mouse model. *Drug Metab Dispos* 33:1495-1502.
  79. Blume, N., Leonard, J., Xu, Z.J., Watanabe, O., Remotti, H., and Fishman, J. 2000. Characterization of Cyp2d22, a novel cytochrome P450 expressed in mouse mammary cells. *Arch Biochem Biophys* 381:191-204.
  80. Holdener, M., Hintermann, E., Bayer, M., Rhode, A., Rodrigo, E., Hintereder, G., Johnson, E.F., Gonzalez, F.J., Pfeilschifter, J., Manns, M.P., et al. 2008. Breaking tolerance to the natural human liver autoantigen cytochrome P450 2D6 by virus infection. *J Exp Med* 205:1409-1422.
  81. Russell, W.C. 2000. Update on adenovirus and its vectors. *J Gen Virol* 81:2573-2604.
  82. Chartier, C., Degryse, E., Gantzer, M., Dieterle, A., Pavirani, A., and Mehtali, M. 1996. Efficient generation of recombinant adenovirus vectors by homologous recombination in *Escherichia coli*. *J Virol* 70:4805-4810.
  83. Sacher, T., Knolle, P., Nichterlein, T., Arnold, B., Hammerling, G.J., and Limmer, A. 2002. CpG-ODN-induced inflammation is sufficient to cause T-cell-mediated autoaggression against hepatocytes. *Eur J Immunol* 32:3628-3637.

84. Lang, K.S., Georgiev, P., Recher, M., Navarini, A.A., Bergthaler, A., Heikenwalder, M., Harris, N.L., Junt, T., Odermatt, B., Clavien, P.A., et al. 2006. Immunoprivileged status of the liver is controlled by Toll-like receptor 3 signaling. *J Clin Invest* 116:2456-2463.
85. Bowen, D.G., Zen, M., Holz, L., Davis, T., McCaughan, G.W., and Bertolino, P. 2004. The site of primary T cell activation is a determinant of the balance between intrahepatic tolerance and immunity. *J Clin Invest* 114:701-712.
86. Chen, C.H., Kuo, L.M., Chang, Y., Wu, W., Goldbach, C., Ross, M.A., Stolz, D.B., Chen, L., Fung, J.J., Lu, L., et al. 2006. In vivo immune modulatory activity of hepatic stellate cells in mice. *Hepatology* 44:1171-1181.
87. Moskophidis, D., Lechner, F., Pircher, H., and Zinkernagel, R.M. 1993. Virus persistence in acutely infected immunocompetent mice by exhaustion of antiviral cytotoxic effector T cells. *Nature* 362:758-761.
88. Christen, U., Edelmann, K.H., McGavern, D.B., Wolfe, T., Coon, B., Teague, M.K., Miller, S.D., Oldstone, M.B., and von Herrath, M.G. 2004. A viral epitope that mimics a self antigen can accelerate but not initiate autoimmune diabetes. *J Clin Invest* 114:1290-1298.
89. Czaja, A.J. 2004. Autoimmune liver disease. *Curr Opin Gastroenterol* 20:231-240.
90. Czaja, A.J., and Carpenter, H.A. 2003. Histological features associated with relapse after corticosteroid withdrawal in type 1 autoimmune hepatitis. *Liver Int* 23:116-123.
91. Strassburg, C.P., and Manns, M.P. 2002. Autoantibodies and autoantigens in autoimmune hepatitis. *Semin Liver Dis* 22:339-352.
92. Longhi, M.S., Ma, Y., Bogdanos, D.P., Cheeseman, P., Mieli-Vergani, G., and Vergani, D. 2004. Impairment of CD4(+)CD25(+) regulatory T-cells in autoimmune liver disease. *J Hepatol* 41:31-37.
93. Lobo-Yeo, A., Alviggi, L., Mieli-Vergani, G., Portmann, B., Mowat, A.P., and Vergani, D. 1987. Preferential activation of helper/inducer T lymphocytes in autoimmune chronic active hepatitis. *Clin Exp Immunol* 67:95-104.
94. Longhi, M.S., Hussain, M.J., Mitry, R.R., Arora, S.K., Mieli-Vergani, G., Vergani, D., and Ma, Y. 2006. Functional study of CD4+CD25+ regulatory T cells in health and autoimmune hepatitis. *J Immunol* 176:4484-4491.
95. Longhi, M.S., Ma, Y., Mitry, R.R., Bogdanos, D.P., Heneghan, M., Cheeseman, P., Mieli-Vergani, G., and Vergani, D. 2005. Effect of CD4+ CD25+ regulatory T-cells on CD8 T-cell function in patients with autoimmune hepatitis. *J Autoimmun* 25:63-71.
96. Coutelier, J.P., van der Logt, J.T., Heessen, F.W., Vink, A., and van Snick, J. 1988. Virally induced modulation of murine IgG antibody subclasses. *J Exp Med* 168:2373-2378.

97. Unkeless, J.C. 1977. The presence of two Fc receptors on mouse macrophages: evidence from a variant cell line and differential trypsin sensitivity. *J Exp Med* 145:931-945.
98. Unkeless, J.C., Scigliano, E., and Freedman, V.H. 1988. Structure and function of human and murine receptors for IgG. *Annu Rev Immunol* 6:251-281.
99. Mamula, M.J., Lin, R.H., Janeway, C.A., Jr., and Hardin, J.A. 1992. Breaking T cell tolerance with foreign and self co-immunogens. A study of autoimmune B and T cell epitopes of cytochrome c. *J Immunol* 149:789-795.
100. Zinkernagel, R.M., Pircher, H.P., Ohashi, P., Oehen, S., Odermatt, B., Mak, T., Arnheiter, H., Burki, K., and Hengartner, H. 1991. T and B cell tolerance and responses to viral antigens in transgenic mice: implications for the pathogenesis of autoimmune versus immunopathological disease. *Immunol Rev* 122:133-171.
101. Christen, U., Benke, D., Wolfe, T., Rodrigo, E., Rhode, A., Hughes, A.C., Oldstone, M.B., and von Herrath, M.G. 2004. Cure of prediabetic mice by viral infections involves lymphocyte recruitment along an IP-10 gradient. *J Clin Invest* 113:74-84.
102. Christen, U., and Von Herrath, M.G. 2004. IP-10 and type 1 diabetes: a question of time and location. *Autoimmunity* 37:273-282.
103. Christen, U., Wolfe, T., Mohrle, U., Hughes, A.C., Rodrigo, E., Green, E.A., Flavell, R.A., and von Herrath, M.G. 2001. A dual role for TNF-alpha in type 1 diabetes: islet-specific expression abrogates the ongoing autoimmune process when induced late but not early during pathogenesis. *J Immunol* 166:7023-7032.
104. Oikawa, Y., Shimada, A., Kasuga, A., Morimoto, J., Osaki, T., Tahara, H., Miyazaki, T., Tashiro, F., Yamato, E., Miyazaki, J., et al. 2003. Systemic administration of IL-18 promotes diabetes development in young nonobese diabetic mice. *J Immunol* 171:5865-5875.
105. Chatenoud, L., and Bluestone, J.A. 2007. CD3-specific antibodies: a portal to the treatment of autoimmunity. *Nat Rev Immunol* 7:622-632.
106. Homann, D., Dyrberg, T., Petersen, J., Oldstone, M.B., and von Herrath, M.G. 1999. Insulin in oral immune "tolerance": a one-amino acid change in the B chain makes the difference. *J Immunol* 163:1833-1838.
107. von Herrath, M.G., Dyrberg, T., and Oldstone, M.B. 1996. Oral insulin treatment suppresses virus-induced antigen-specific destruction of beta cells and prevents autoimmune diabetes in transgenic mice. *J Clin Invest* 98:1324-1331.
108. Bresson, D., Togher, L., Rodrigo, E., Chen, Y., Bluestone, J.A., Herold, K.C., and von Herrath, M. 2006. Anti-CD3 and nasal proinsulin combination therapy enhances remission from recent-onset autoimmune diabetes by inducing Tregs. *J Clin Invest* 116:1371-1381.

109. Bresson, D., and von Herrath, M. 2007. Moving towards efficient therapies in type 1 diabetes: to combine or not to combine? *Autoimmun Rev* 6:315-322.
110. Krebs, P., Scandella, E., Odermatt, B., and Ludewig, B. 2005. Rapid functional exhaustion and deletion of CTL following immunization with recombinant adenovirus. *J Immunol* 174:4559-4566.

## 14 Acknowledgments

First of all I thank Urs Christen for the great support, the competent supervising throughout my doctoral thesis and for all the interesting discussions about science and other topics. I thank him for giving me the freedom to make my own experiences and to bring in my own thoughts, but always giving helpful advice when it was needed as well as the opportunity to work on such an interesting topic.

I thank Prof. Dr. Theo Dingermann who agreed to be my doctoral thesis supervisor and for the appraisal of this work.

I thank Prof. Dr. Heinfried H. Radeke for agreeing to supervise my doctoral thesis and for his excellent questions after my talks.

I am thankful to Prof. Dr. Josef Pfeilschifter for his support during the time I was working in this institute.

I thank Prof. Dr. M.G. Von Herrath who allowed me to work for two years in his laboratory in La Jolla, which was an exciting time that led to the start of my doctoral thesis.

Special thank belongs to Edith Hintermann for all her help that contributed a lot to my thesis, all the helpful tips she shared and all the organizing she did for our whole lab.

I thank Monika and Kerstin for the good times we had during our lunch times in Frankfurt and the whole DI-3 Lab for the great times we had in La Jolla.

In addition, very special thank belongs to Selina for all the discussions and wonderful times we spent together in as well as outside the lab.

Finally I would like to express my deepest gratitude to my parents and my brother for supporting me in every respect during my studies.

# 15 Curriculum vitae

## Personal data:

Martin Holdener

Born 23.05.1978 in Luzern, Switzerland

## Education:

1985-1991	Primarschule Luzern
1991-1994	Sekundarschule Luzern/Uttenberg
1994-1999	Kantonsschule Luzern/Typus Wirtschaft

Certificate: Maturität

## University:

10/1999-04/2004	Swiss Federal Institute of Technology Zurich Compartment of biology Certificate: Diplom als Naturwissenschaftler
10/2000	1. Vordiplom
10/2001	2. Vordiplom
07/2002-06/2003	Semester- and diploma-thesis at the Institute of Experimental Immunology, University Hospital Zurich
03/2004	Schlussdiplom

## Post-graduate experience:

03/2004-12/2004	Graduate scientist at the Institute of Experimental Immunology, University Hospital Zurich
12/2004-11/2005	Graduate scientist at the La Jolla Institute for allergy and immunology, La Jolla, California, USA

## Doctoral degree:

11/2005-2009	J.W. Goethe - University Frankfurt/Main, supervised by PD Dr. phil. nat. Dr. med. habil. U. Christen
11/2005-09/2006	La Jolla Institute for allergy and immunology, La Jolla, California, USA
09/2006-2009	Institute für allgemeine Pharmakologie und Toxikologie, Klinikum der J.W. Goethe - Universität Frankfurt/Main

**Academic teacher:**

Prof. Dr. R.M. Zinkernagel, Prof. Dr. H. Hengartner, Dr. B.M. Senn, Dr. K. Fink, Dr. L. Hangartner, Dr. M. Geuking, Prof. Dr. M.G. von Herrath, PD Dr. U. Christen, Dr. E. Hintermann, Prof. Dr. H. H. Radeke, Prof. Dr. Th. Dingermann, Prof. Dr. J. Pfeilschifter

## 16 Publications

### Paper:

**Holdener, M.**, Bogdanos, D.P., Christen, S., Bayer, M., Pfeilschifter, J., Hintermann, E., Christen, U. 2009. The CYP2D6 model for autoimmune hepatitis: Characterization of the CD4 and CD8 T cell response. (*manuscript in preparation*).

**Holdener, M.**, Hintermann, E., Bayer, M., Rhode, A., Rodrigo, E., Hintereder, G., Johnson, E.F., Gonzalez, F.J., Pfeilschifter, J., Manns, M.P., Von Herrath, M.G., Christen, U. 2008. Breaking tolerance to the natural human liver autoantigen cytochrome P450 2D6 by virus infection. *J Exp Med* 205:1409-1422.

Fink, K., Zellweger, R., Weber, J., Manjarrez-Orduno, N., **Holdener, M.**, Senn, B.M., Hengartner, H., Zinkernagel, R.M., and Macpherson, A.J. 2008. Long-term maternal imprinting of the specific B cell repertoire by maternal antibodies. *Eur J Immunol* 38:90-101.

Christen, U., **Holdener, M.**, and Hintermann, E. 2007. Animal models for autoimmune hepatitis. *Autoimmun Rev* 6:306-311.

Fink, K., Lang, K.S., Manjarrez-Orduno, N., Junt, T., Senn, B.M., **Holdener, M.**, Akira, S., Zinkernagel, R.M., and Hengartner, H. 2006. Early type I interferon-mediated signals on B cells specifically enhance antiviral humoral responses. *Eur J Immunol* 36:2094-2105.

## Poster presentation/Talks:

**Holdener, M.**, Hintermann, E., Rhode, A., Johnson, E.F., Manns, M.P., Von Herrath, M.G., Christen, U. A novel model for virus-induced autoimmune hepatitis. – 2006 poster presentation at the Keystone symposia: Tolerance, Autoimmunity and Immune Regulation, Beaver Run Resort, Breckenridge, Colorado, USA.

**Holdener, M.**, Hintermann, E., Johnson, E.F., Manns, M.P., Von Herrath, M.G., Christen, U. The CYP450 mouse model for autoimmune hepatitis: Breaking of self-tolerance in transgenic CYP2D6 and wild-type FVB mice by viral infection.

2006 poster presentation at the Falk Symposium 157: Chronic Hepatitis: Metabolic, Cholestatic, Viral and Autoimmune, Freiburg, Germany.

2007 poster presentation at the 37<sup>th</sup> Annual Meeting of the German Society for Immunology, Heidelberg, Germany.

2007 poster presentation at the Annual Meeting of the Swiss Society of Pharmacology and Toxicology, Bern, Switzerland.

2008 poster presentation at the 49<sup>th</sup> Annual Meeting of the DGPT, Mainz, Germany.

**Holdener, M.**, Hintermann, E., Bayer, M., Manns, M.P., Von Herrath, M.G., Christen, U. The CYP2D6 mouse model for autoimmune liver disease: Mapping of cytochrome P450 2D6 T cell epitopes in mice with autoimmune hepatitis. - 2009 oral presentation at the 50. Annual Meeting of the DGPT, Mainz, Germany.